A STUDY OF THE ADSORPTION/DESORPTION OF METHANE/CARBON DIOXIDE ON THE SURFACE OF DIFFERENT RESERVOIR ROCKS

BY

MOHAMMED ALTAHIR ELIEBID ELNAEEM

A Thesis Presented to the
DEANSHIP OF GRADUATE STUDIES

KING FAHD UNIVERSITY OF PETROLEUM & MINERALS

DHAHRAN, SAUDI ARABIA

In Partial Fulfillment of the
Requirements for the Degree of

MASTER OF SCIENCE

In

PETROLEUM ENGINEERING

December, 2016

KING FAHD UNIVERSITY OF PETROLEUM & MINERALS

DHAHRAN- 31261, SAUDI ARABIA

DEANSHIP OF GRADUATE STUDIES

This thesis, written by **MOHAMMED ALTAHIR ELIEBID ELNAEEM** under the direction his thesis advisor and approved by his thesis committee, has been presented and accepted by the Dean of Graduate Studies, in partial fulfillment of the requirements for the degree of **MASTER OF SCIENCE IN PETROLEUM ENGINEERING.**

Mohamed Mahmoud

Dr. Mohamed A. Mahmoud
(Advisor)

Dr. Abdullah S. Sultan
Department Chairman

Shawabkeh

Dr. Reyad A. Shawabkeh
(Co-Advisor)

Dr. Salam A. Zummo
Dean of Graduate Studies

Dr. Abdullah S. Sultan
(Member)

19/1/17

Date

Dhafer A. Al-Shehri

Dr. Dhafer A. Al-Shehri
(Member)

Salaheldin Elkatatny

Dr. Salaheldin A. Elkatatny
(Member)

To my family, especially my mom Awatif may Allah grant her health, happiness and heaven in the afterlife, everything that I do will come short compared to what you are giving me and I will never take your love for granted. To my dad Altahir may Allah grant him mercy and forgiveness.

For my brother and sisters for their support and prayers, and for my nieces and nephews. For my aunts and uncles and my cousins.

For my friends and my teachers and educators through the years.

ACKNOWLEDGMENTS

All praise and gratitude to Allah lord of the worlds for blessing me with the intellect, strength and patience to attain this level of education.

I acknowledge King Fahd University of Petroleum & Minerals and Ministry of Higher Education in Saudi Arabia for providing me with the opportunity to acquire this Master degree. I extend my appreciation to my advisor Dr. Mohammed Mahmoud for his great efforts, guidance, patience and support. My sincere thanks and gratitude to my Co-advisor Dr. Reyad Shawabkeh who has been working with me day and night, for his extraordinary support, guidance and efforts without him I could never finish this work. Also, special thanks to my thesis committee members Dr. Abdallah Sultan, Dr. Dhafer Al-Shehri and Dr. Salaheldin Elkatatny for their assistance and valuable comments.

My appreciations also extend to the Petroleum Engineering Department for their support and for Dr. Mohammed Omar for his help. Special thanks and gratefulness to my family and friends for being there for me through all these years I am forever grateful.

TABLE OF CONTENTS

LIST OF TABLES

LIST OF FIGURES

LIST OF ABBREVIATIONS

EDX	:	Energy Dispersive X-ray analysis
EGR	:	Enhanced Gas Recovery
SEM	:	Scanning Electron Microscope
SSE	:	Sum of Squared Errors
TOC	:	Total Organic Carbon
XRD	:	X-ray Diffraction
$\mathbf{k_l}$	:	Langmuir constant = $1/P_L$
$\mathbf{Q_l}$	:	Langmuir maximum uptake, mg/g
P	:	Pressure, bar or psi
Q,q	:	Gas uptake, mg/g
$\mathbf{k_f, k_c, n}$	:	Freundlich constants
$\mathbf{Q_m}$	:	BET maximum uptake, mg/g
$\mathbf{P_s}$	:	Saturation pressure, bar or psi
$\mathbf{k_b}$	:	BET constant.
$\mathbf{\Delta H_{ads}}$	:	Heat of adsorption, kJ/mol
$\mathbf{\Delta G_{ads}}$	:	Standard free energy of Gibbs, kJ/mol
$\mathbf{\Delta S_{ads}}$	:	Standard entropy, J/mol. K
R	:	Universal gas constant (8.314J/mol K)

$\mathbf{R^2}$	:	Regression coefficient of determination
$\mathbf{G_P}$	:	Cumulative produced gas, Scf
G	:	Initial Gas In Place, Scf
$\mathbf{B_g}$	:	Gas formation volume factor
$\mathbf{S_{gi}}$	:	Initial gas saturation, fraction
$\boldsymbol{\varphi}$	:	Porosity, fraction
$\boldsymbol{\rho_B}$**, VB**	:	Density and bulk volume of the reservoir rock

ABSTRACT

Full Name : Mohammed Altahir Eliebid Elnaeem

Thesis Title : A study of the adsorption/desorption of methane/carbon dioxide on the surface of different reservoir rocks

Major Field : Petroleum Engineering

Date of Degree : December, 2016

The natural gas production, optimum enhanced gas recovery and sequestration processes are significantly dependent on the adsorption/desorption behavior of CH_4 and CO_2 on the reservoir rock. Most studies in natural gas engineering apply Langmuir isotherm as an adsorption model. Also, most mathematical and empirical correlations used Langmuir isotherm to model adsorption on shale are developed from coal-bed methane which may has very different characteristics and adsorption behavior than other rock types. Instead of analyzing the real behavior of natural gas production from these reservoirs, in literature continuum flow models such as Darcy's law are integrated with alteration in rock permeability to compensate for the excess flow from molecular flow and gas slippage which Darcy's equation fails to capture. These modifications do not accurately explain the mechanism of the flow and rather provide a compensated correction to a specific case ever changing from rock to another and for different gas mixtures.

In this study, the adsorption of CH_4 and CO_2 on carbonate, tight sandstone and shale gas reservoir rocks was investigated. Pink Desert carbonate, Kentucky tight sandstone and two shale gas rocks are used in this study. Adsorption isotherms were studied for the gases at different temperatures on the three rock types. In all experiments, intact rock samples cubes were used to preserve the reservoir rock integrity and obtain more representative results.

In all testing temperatures CO_2 adsorption on carbonate was considerably higher than CH_4, Although the adsorption decreased tremendously as the temperature increased from 50°C to 100°C and 150°C. Also, the study of competitive adsorption showed increasing CO_2 percentage increases gas adsorption amount at all temperatures. However, Kentucky tight sandstone exhibited a different behavior with temperature; the adsorption decreased after increasing the temperature from 50°C to 100°C but at 150°C the adsorption increased significantly more than in 50°C due to the changes in water bearing clay minerals at high temperature. On the other hand, shale rocks had various behaviors because of the kerogen (TOC) and mineralogical composition. Adsorption isotherms analysis concluded that Langmuir isotherm does not represent the adsorption behavior of the studied rocks at different temperatures and using Freundlich or BET is more representative.

ملخص الرسالة

الاسم الكامل: محمد الطاهر العبيد النعيم

عنوان الرسالة: دراسة إدمصاص/نضح الميثان/ثاني أكسيد الكربون على أسطح صخور مكامن مختلفة

التخصص: هندسة البترول

تاريخ الدرجة العلمية: ديسمبر ٢٠١٦

إنّ طبيعة إدمصاص الغاز الطبيعي على الصخور المكمنية لها تأثير كبير على انتاج الغاز واختيار عمليات تحسين استخراج الغاز وتخزين ثاني أكسيد الكربون. في هذا البحث تمت دراسة امتزاز غاز الميثان النقي، غاز ثاني أكسيد الكربون ومزيج من الغازين على صخور مكامن كربوناتية، رملية وطينية زيتية. تم استخدام صخر الصحراء الوردي للكربونات وصخر كنتاكي قليل النفاذية للصخور الرملية وعدة صخور زيتية طينية. تم كذلك دراسة ايزوثيرمات الادمصاص لكل الغازات على درجات حرارة مختلفة لكل الصخور. في هذه الدراسة تم استخدام عينات صخور سليمة لحفظ تركيب الصخور والحصول على نتائج تمثل واقع تواجد هذه الصخور في المكامن. أظهرت النتائج ان ادمصاص ثاني اكيد الكربون اعلى بكثير من امتزاز الميثان في الصخور الكربوناتية في كل درجات الحرارة بالرغم من ان الادمصاص قل كثيرا عند زيادة درجة الحرارة من ٥٠ درجة مئوية الي ١٠٠ درجة مئوية و١٥٠ درجة مئوية. كما أوضحت الدراسة ان زيادة نسبة ثاني الكسيد الكربون في مزيج الغاز تزيد من الامتصاص الكلي للغاز. ادمصاص صخر كنتاكي كان له تأثرا مغايرا مع درجة الحرارة حيث ان الادمصاص قل عند ١٠٠ درجة مئوية كما في حالة الكربونات ولكنه عند ١٥٠ درجة مئوية زاد عن الادمصاص عند ٥٠ درجة مئوية بسبب التغيرات التي حدثت للمعادن الصلصالية الحاملة للماء في الصخر مع ارتفاع الحرارة. اما في حالة الصخور الزيتية الطينية فقد أظهرت تغيرات عديدة مع تكوين الصخر ونسبة الكيروجين (الكربون العضوي الكلي) في تلك الصخور. دراسة ايثوثيرمات الادمصاص أوضحت ان ايزوثيرم -لانقومير- لا يمثل ادمصاص الغازات المدروسة على مختلف الصخور وان ايزوثيرم -فرايندولخ- و-بي إي تي- يمثلان الامتزاز على مختلف درجات الحرارة.

CHAPTER 1

INTRODUCTION

The gas flow mechanisms research in reservoir formations has grown significantly through the past decades. The beginning was by modifying Darcy's equation to consider the gas molecular effect as an increase in the permeability. The studies by Ertiken et al., (1986) adopted Klinkenberg's slippage effect to increase the predicted production from unconventional reservoirs [1],[2]. Clarkson et al., (2011) then used Ertekin concept in the rate transient analysis [3]. Jones et al., (1980) found a formula for diffusivity constant at 24°C and 500 psi using air and their data then used by Ozkan at al., (2010) to add concentration driven diffusion which modeled as slippage permeability to Darcy's flow [4],[5]. But due to the limitation of Jones test conditions, the need for more broad test conditions was necessary. Javadpour et al., (2009) found expression stating that in addition to slippage Knudson diffusion -which is a result of collisions of gas molecules with the pore wall- are important in tight pores [6].

Furthermore, Chalmers (2007), Ross (2009) and Clarkson (2011) added the adsorbed gas on the surface to the dissolved gas in organic matter (Kerogen) which can be in substantial amount specially in Coal Bed Methane (CBM) formations [7]–[9]. However, a lot of researchers ignored the solution gas, focusing only on the adsorption incorporating Langmuir monolayer isotherm or Brunauer-Emmet-Teller (BET) isotherm [10],[11].

While Swami et al., (2012) showed that the gas diffusion from kerogen is very significant and should not be excluded [12].

1.1 Adsorption of gases on rock surface

The adsorption phenomenon exists when the gas is attached to the surface of the substance and held into its pores physically or chemically. The physical adsorption is due to Vander Walls forces and electrostatic forces, and the chemical adsorption is caused by strong chemical bonds [13]. This adsorption process is directly proportional to the pressure of the free gas; increasing the pressure increases the adsorption process. On the other hand, decreasing the pressure in the desorption process decreases the adsorbed gas [14]. Furthermore, the maximum volume of adsorbed gas is usually determined by the adsorption isotherm which represents the equilibrium volume of the gas adsorbed on substance surface at isothermal conditions [15].

The models of isotherm include Langmuir, Potential Theory, and Gibbs [16]. The Gibbs model uses the equation of state in two-dimensional films to define the sorption process, and it has been used by Saunders (1985) and Stevenson (1991) to model the gas adsorption [17],[18]. Moreover, the potential theory describes the adsorbed gas volume as thermodynamic sorption potential. Langmuir Isotherm [10] is explained as the equilibrium between the absorption and desorption. The Langmuir model includes three different types of isotherms; the Langmuir, the Freundlich, and the mixture of both Langmuir and Freundlich isotherms [16]. Langmuir isotherm is being widely used in the literature to define the adsorption and competitive adsorption processes [19],[20].

Unlike conventional gas reservoirs in which gas is mainly amassed as free particles in the pore space of the rock, gas is stored in shale gas reservoirs as both free gas in the pores and

fractures, and the adsorbed gas adhered to the mineral and organic surface [21]. But since shale formations has very low permeability lowering the pressure to produce the adsorbed gas is impractical. Therefore, horizontal and multi-lateral multi-stage fracturing is used to free enormous amounts of gas. In these ultra-low permeability shale reservoirs, the gas is produced mainly in two stages. Firstly, from the fractures and the production rate declined quickly as gas produced depending on the reservoir properties. In the second stage gas desorption and in which is characterized by less decline rate. However, this effect on the production decline is yet to be studied. Furthermore, in the early stages of production from hydraulically fractured horizontal shale gas wells gas desorption had insignificant effect [22]. While Nelson (2014) investigated long term Marcellus shale gas production performance [23].

Wu (2014) derived analytical solution for the gas flow with adsorption/desorption assuming isothermal system, ideal gas and neglecting the gravity, to get the equation for radial and linear coordinates [24]:

$$\nabla.\left(\beta\frac{k}{\mu}\mathrm{P}\nabla P\right)=\phi\beta\frac{\partial P}{\partial t}+\alpha\frac{\partial\left(\frac{P}{P+P_L}\right)}{\partial t} \tag{1}$$

In radial coordinates:

$$\frac{1}{r}\frac{\partial}{\partial r}\left(r\frac{\partial P^2}{\partial r}\right)=\left[\frac{\phi\mu}{Pk}+\frac{\alpha\mu}{P\beta k}\frac{P_L}{(P+P_L)}\right]\frac{\partial P^2}{\partial t} \tag{2}$$

1.2 Adsorption isotherms classifications

Adsorption isotherms are used to describe adsorption characteristics of gases on the rock surface and as input parameters to model the gas flow and transport in porous media. The approximately isothermal reservoir conditions allow monitoring the adsorption/desorption

behavior with the change in reservoir pressure. Lacking the appropriate expression of the adsorption data can lead to severe errors in the transport modeling process [25]. Simple models such as Langmuir and Freundlich isotherms are widely used to fit and define the adsorption data, but they frequently lack the accuracy and more sophisticated complex models are applied [26]. Giles (1974) categorized the adsorption isotherms based on observation and depending on their gradients and curvature to four main modules (S (sigmoidal-shape), L (Langmuir), H (high affinity), C (Linear)) and five subcategories to incorporate the variation and maximum points (Table 1.1) [27].

Class	Subgroup	S Vs C	K_d Vs S	Log K_d Vs Log s
S	1	concave	positive slope	positive slope
L	1	convex	negative slope, line	negative slope
H	1	convex	negative slope, curve	negative slope
C	1	line	zero slope	zero slope
S,L,H	2	plateau	neg. slope, line or curve	$s_T = s$ at low K_d
S,L,H	3	plateau, inflection	minimum	minimum
S,L,H	4	plateau, infl, plateau		

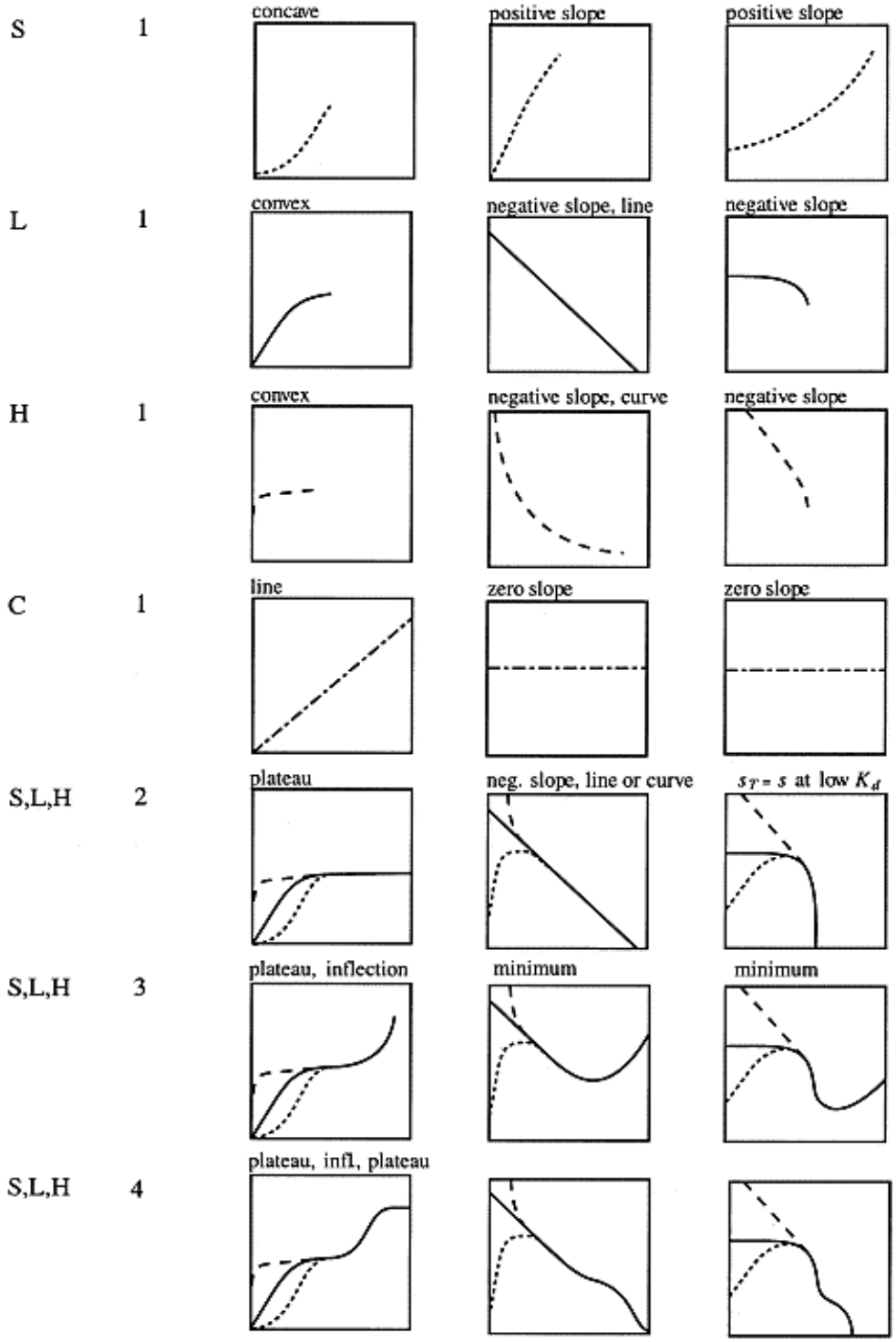

Figure 1.1 Giles Isotherm categorizations

Table 1.1 Adsorption isotherms categorization and their equations.

Author	Formula
Langmuir [10]	$q_T \frac{kP}{1+kP}$
Two-site Langmuir	$q_T\left(\frac{f_1k_1P}{1+f_1k_1P}+\frac{f_2k_2P}{1+f_2k_2P}\right)$
Modified Langmuir	$q_T\left(\frac{k_1P}{1+k_1P}+\frac{k_2P}{1+k_2P}\right)$
BET [11]	$\left(\frac{k_1P}{1+k_2P}\right)\left(\frac{1}{1-k_3P}\right)$
Farley–Dzombak–Morel [28]	$\frac{q_Tk_1P}{1+k_1P}+\left(\frac{X-q_T}{1+k_1P}+\frac{k_1X_c}{1+k_1P}\right)\times\left(\frac{k_2P}{1-k_2P}\right)-\frac{k_2}{k_3}P$
Freundlich [29]	K_FP^{α}
General Langmuir Freundlich	$s_T\frac{(kP)^{\alpha}}{1+(kP)^{\alpha}}$
General Freundlich	$s_T\left(\frac{kP}{1+kP}\right)^{\alpha}$
Redlich–Peterson	$s_T\frac{kP}{1+(kP)^{\alpha}}$
Toth [30]	$s_T\frac{kP}{(1+(kP)^{\alpha})^{1/\alpha}}$
Aranovich–Donohue [31]	$\left(\frac{k_1P}{1+k_2P}\right)\left(\frac{1}{1-k_3P}\right)^{\alpha}$
Temkin [32]	$k_1\ln P+k_2$
Fowler–Guggenheim [33]	$\frac{q/q_T}{1-q/q_T}=k_1\exp(k_2q/q_T)\mathrm{P}$

For α >1 Freundlich equation follows S1 with zero slope at C = 0.

1.3 Research Motivation

Most of the studies in gas reservoir engineering flow modeling applied Langmuir isotherm [10] as an adsorption model, which assumes total equilibrium between the adsorbed and free gas at isobaric – constant pore pressure - and isothermal – constant temperature - processes. Furthermore, sometimes authors add Langmuir isotherm in the adsorption term in the material balance equation when modeling gas production even when the adsorption models do not follow Langmuir isotherm [34], [35] (see Figure 1.2-Figure 1.3). It should also be noted that most of the mathematical and empirical correlations for shale are developed from coal bed methane which has high TOC content and has very different characteristics and adsorption behavior than other rock types [36]–[39]. But in reality the gas adsorption isotherm shape is directly related to the gas, rock properties, pore-space geometry and specific surface area [40]. These investigations failed to develop a general model to describe the adsorption behavior of natural gas through different rock types and consider the wide spectrum of minerals that constitute and cover the surfaces of these rocks. For example, carbonate rocks have wide different Calcite to dolomite ratios, and even when they have the same percentage of Calcite the facies - grain shapes, cementation and depositional environment of these rocks are completely different [41] (see Figure 1.4). Sandstones also exhibit a very diverse mineral components and mixtures of carbonate, silicate and clay minerals which are very sensitive to temperature changes. on the other hand, shale rocks cover even a wider and more complex range of chemical composition, physical properties, and hence adsorption behaviors.

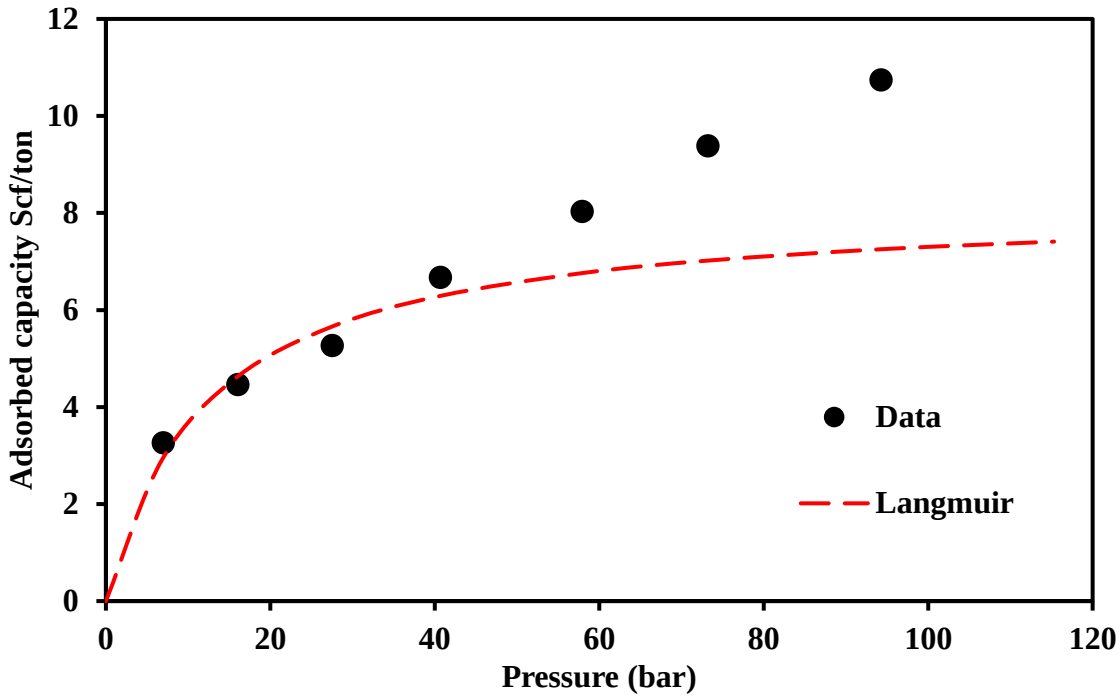

Figure 1.2 Weak fitting of Langmuir isotherm to shale experimental data [42].

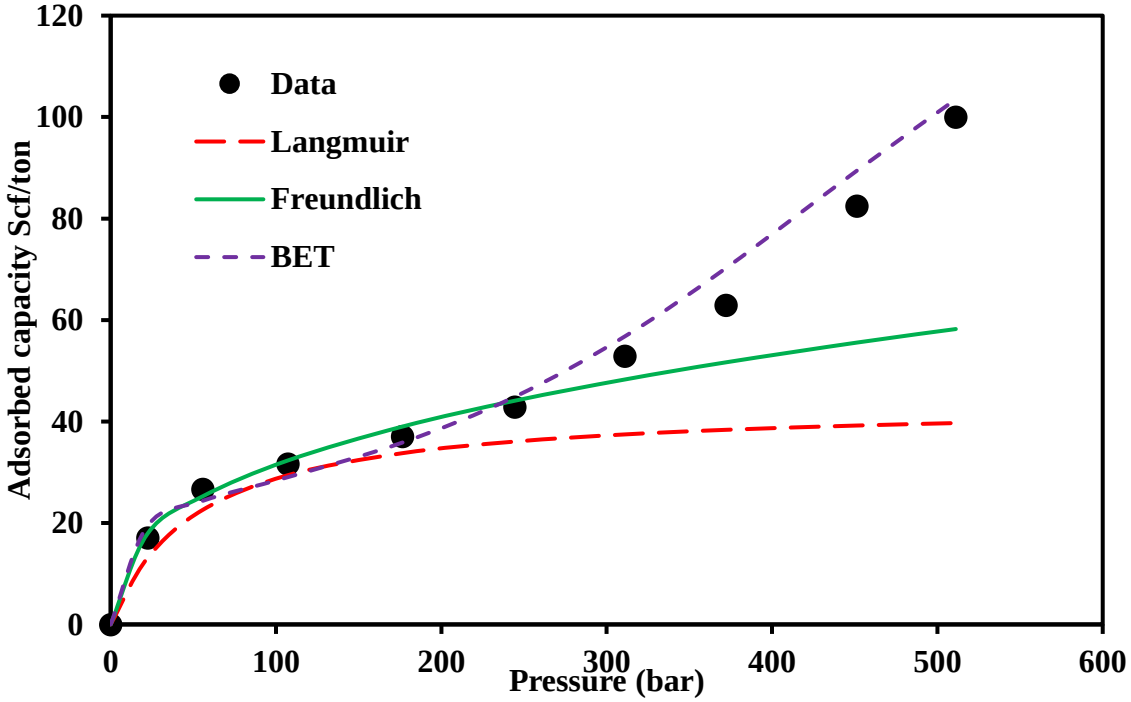

Figure 1.3 Adsorption isotherms fitting comparison for shale sample, Langmuir isotherm is only fitting at low pressure [43].

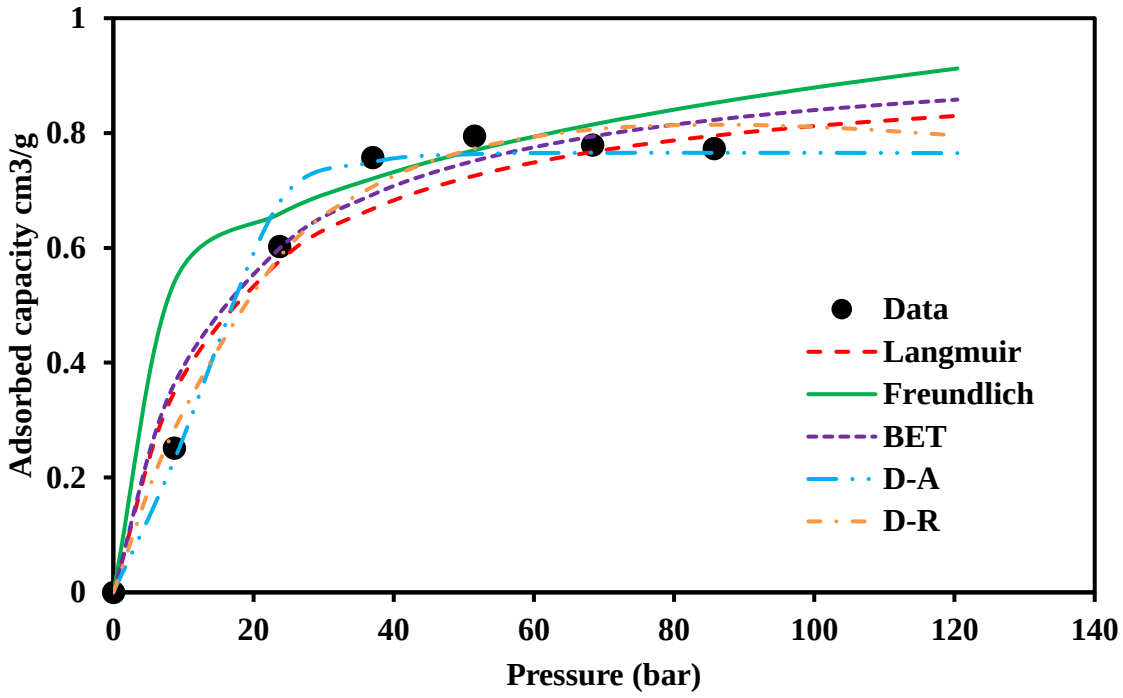

Figure 1.4 Adsorption isotherms fitting comparison for marine rich shale sample, Langmuir isotherm is not the best fit [37].

Instead of analyzing the real behavior of natural gas production from these reservoirs researchers integrated continuum flow models such as Darcy's law with alternation in the permeability to compensate the excess flow form molecular flow and gas slippage which Darcy's equation fails to capture. These modifications were led by Klinkenberg[2] by proposing a corrected apparent gas permeability. Several authors [6], [12], [44]–[47] had followed the same approach ignoring the desorption mechanism, pore-geometry changes induced by pressure and stress by just modifying the slippage parameter which resulted in different results indicating more flow at nanoscale than the one Darcy's model predicted [48]. These modifications do not explain the mechanism of the flow and rather provide a compensated correction to a specific case ever changing from rock to another and for different gas mixtures.

Adding to that most the adsorption studies do not consider the difference between Chemisorption and Physisorption for different lithology types which leads to misleading analysis and interpretation of the reservoir rock adsorption behavior.

One of the important aspects of gas reservoir engineering practices is quantifying the original gas in place (G) for gas reservoirs and material balance equation (MBE) with its simple formulation in the famous (P/Z) arrangement has been widely used to determine the (G) based on the cumulative gas production (G_P) and check other reserve estimation methods [49]. Although the early forms of MBE were developed to capture only the volumetric relationship between (G) and (G_P) at constant pore volume considering only the gas expansion energy, it has been modified to comprise other driving mechanism indices including over pressured reservoirs residual gas expansion[50], water encroachment, formation compressibility and gas adsorption for coal bed methane or shale reservoirs[51].

All these drive mechanism provide a total compressibility expression which is very important in production data rate transient analysis[52].

Volumetric reservoirs Material balance without considering the gas desorption is given by:

$$GB_{gi} = (G - G_p)B_g \tag{3}$$

Where G quantifies the initial gas in place, G_P is the cumulative produced gas and B_{gi} and B_g are the gas formation volume factor at initial pressure and current pressure respectively. For Langmuir isotherm, the amount of gas a per unit mass of the rock is expressed by specific gas content in scf/ton:

$$V = \frac{V_l k_l p}{1 + k_l p} \tag{4}$$

Where V_L is gas content in scf/rcf and K_L is the reciprocal of Langmuir pressure parameter P_L at which half of V_L is desorbed. Usually the specific gas content is expressed in (scf/ton).

Then the total volume of adsorbed gas is calculated using:

$$G_a = \rho_B V_B \frac{V_l k_l p}{1 + k_l p} \tag{5}$$

Where ρ_B and V_B are the density and bulk volume of the reservoir rock, respectively, on dry and clean conditions. Then the reservoir cubic feet due to the desorption:

$$\Delta V_d = \rho_B B_g \frac{GB_{gi}}{\varphi S_{gi}} \left(\frac{V_l k_l p_i}{1 + k_l p_i} - \frac{V_l k_l p}{1 + k_l p} \right) \tag{6}$$

Then the MBE after considering the gas desorption is expressed by:

$$GB_{gi} = (G - G_p) B_g + \rho_B B_g \frac{GB_{gi}}{\varphi S_{gi}} \left(\frac{V_l k_l p_i}{1 + k_l p_i} - \frac{V_l k_l p}{1 + k_l p} \right) \tag{7}$$

Where S_{gi} is the initial gas saturation and φ is the porosity. The same approach can be used to include other isotherms which they are determined from adsorption experiment in the laboratory. Lacking the adequate accurate expression can lead to either an over or under estimation which affect the whole development plan for the gas fields [53].

Desorption correction is also necessary in conventional gas reservoirs since one of the primary assumption of MBE is there is no interaction between the gas and reservoir rock[35], which is not entirely true. In most of the conventional gas reservoirs on contrary to the common assumption that the initial gas in place (G) is equal to the free gas in the pores[52], but there is considerable amount of adsorbed gas should be added to the free gas volume especially in low pressure reservoirs[54]. In the past decades, the researchers

investigated this adsorption/desorption phenomenon. However, they did not provide an accurate procedure that fits the wide spectrum of gas reservoirs rock compositions.

The same approach can be applied for reservoirs that follow other isotherms. Freundlich is direct since q is the maximum amount adsorbed and for BET Q_m is equivalent to Q_L. Furthermore, when testing materials that has great micropores capacity it is tremendously important to differentiate between the micropore filling and the gas adsorption on the surface of the material. Usually, rocks with large micropore volume are very adsorptive and failing to distinguish between the two mechanisms can lead to great errors in calculations or describing the pore structure of the tested material [55].

To accurately describe the adsorption behaviors of these complex rocks this study covers a wide range of reservoir rocks and focuses on shale rocks hence they represent a huge challenge in natural gas production engineering. Also, investigates various parameters that may affect the adsorption isotherm including; temperature, facies, natural gas composition, chemical adsorption -if exists-, and TOC (Total Organic Carbon) effect in shale rocks.

1.4 Research Objectives

The literature survey highlighted the significance of adsorption to accurately describe gas and reservoir rock interaction, and its important role in reserve estimation, production, enhanced oil and gas recovery, sequestration, production decline analysis, simulation and history matching. The main objectives of this study are:

1. Study methane adsorption isotherm for different reservoir rock types at different temperatures to obtain a comprehensive understanding of how the rock system behaves at different conditions.

2. Study the competitive adsorption between CO_2 and CH_4 with different mixture of CO_2 and CH_4 and at different temperatures.

The applications that can be drawn from this study will give:

1. Better quantification of natural gas production mechanisms and production decline due to adsorption/desorption mechanisms.
2. Accurate estimation of adsorption isotherms for better simulation and history matching.
3. Accurate estimation of Initial Gas in Place (IGIP).
4. Enhanced Gas Recovery (EGR) by CO_2 injection.
5. Effect of natural gas CO_2 content on the gas production.
6. Selecting the proper CO_2 storage conditions.

CHAPTER 1

METHODOLOGY

2.1 Samples Preparation

A cubic sample of different rocks is prepared in the dimension of 0.5 cm^3 from 6" cores with approximate weight of 1.3 g. The Limestone samples (Figure 1.1) were cleaned with distilled water and dried in the oven at 150^oC for 24 hours, while Sandstone samples (Figure 1.2) were cleaned using compressed air and dried for 48 hours in the oven at 40^oC and Shale samples (Figure 1.3) were cleaned using compressed air.

Figure 1.1 Pink Desert Limestone sample cube 0.5cm^3.

Figure 1.2 Kentucky sample cube 0.5cm^3.

Figure 1.3 SH1 Shale sample cube 0.5cm^3.

2.2 Samples Characterization

The rock samples were analyzed using XRD to determine their mineralogical composition using Bruker D8 Advanced X-ray Diffractometer (Figure 1.4). The rock sample surface characterization was carried out using a Scanning Electron Microscopes - Energy Dispersive X-ray analyzer (SEM-EDS) using (JEOL, Japan) JSM-6610 Scanning Electron Microscope with high voltage mode resolution of 3.0nm (30kV), 8nm (3kV) and 15nm (1kV) and maximum magnification of 300,000 with simultaneous elemental analysis employing attached (Oxford, United Kingdom) X-Max SDD X-ray detector through high count rates with 125eV energy resolution (Figure 1.5).

2.3 Experimental procedures

The sample's measured weight was calibrated by heating the sample to 50^{o}C under vacuum for 1 hour, followed by a buoyancy calibration experiment on the sample in Helium at constant 50^{o}C through 8 stages and maximum pressure of 45-50 bars using (Rubotherm^{TM}) magnetic suspension balance (Figure 1.6-Figure 1.7) which is the backbone of the experiment system.

Unlike conventional weight measuring instruments the magnetic suspension balance is based on the principle of contact free weight measurement system between the weighting apparatus and the experiment cell to obtain high precision results even at high pressure high temperature conditions. The balance utilizes a suspended permanent magnet connected to sample, measuring load decoupling device and a sensor core. The system is weight is then contactless is transmitted without any restrictions to an electric magnet

attached to the bottom of microbalance in atmospheric conditions outside the measuring vessel. The balance can work with pressure up to 200 bar and temperature range from -40 to 200^{o}C and sample mass range from 0 to 25g with resolution of 1µg.

The gas is dosed into the system using FLEXIDOSE system (±0.05 bar) through two mass flow controllers at the gas inlets, two shut-off valves after the gas inlets and two pressure sensors 200 bar and 40 bar combined with four shut-off valves two for diverting the gas to ventilation or vacuum and the other two to shut-off the pressure controller depending the pressure of the reaction cell.

The temperature is controlled by high efficiency heating system ±0.1^{o}C consists of electric heater (+50°C to +400°C) surrounding the reaction chamber and a liquid thermostat (-20°C to +150°C) which automatically maintain the temperature through the experiment. All the measuring parameters are calibrated at preset zero point intervals (every 4 minutes) to adjust any deflection from the required settings.

Then the adsorption isotherm is measured at various pressure set points with maximum pressure of 50 bar and at constant temperature i.e. 50^{o}C. The adsorption isotherm data is recorded through measuring the sample weight in response to the various pressure set points.

Figure 1.4 X-ray diffraction instrument.

The setup is used to measure Pure CO_2 and CH_4 isotherms. Furthermore, the competitive adsorption between CH_4 and CO_2 is investigated using a mixture of CO_2 and CH_4 covering 5%, 10%, 20%, and 50% CO_2 respectively using the same 50^oC temperature and exact pressure set points. Lastly, the effect of temperature is studied on the competitive adsorption using a constant mixture of 10%CO_2 – 90%CH_4 at 100^oC, 150^oC respectively with a Helium buoyancy measurement at these temperatures. Also, the effect of the temperature on pure CH_4 and pure CO_2 has also will be measured at 100^oC and 150^oC.

Figure 1.5 SEM instrument.

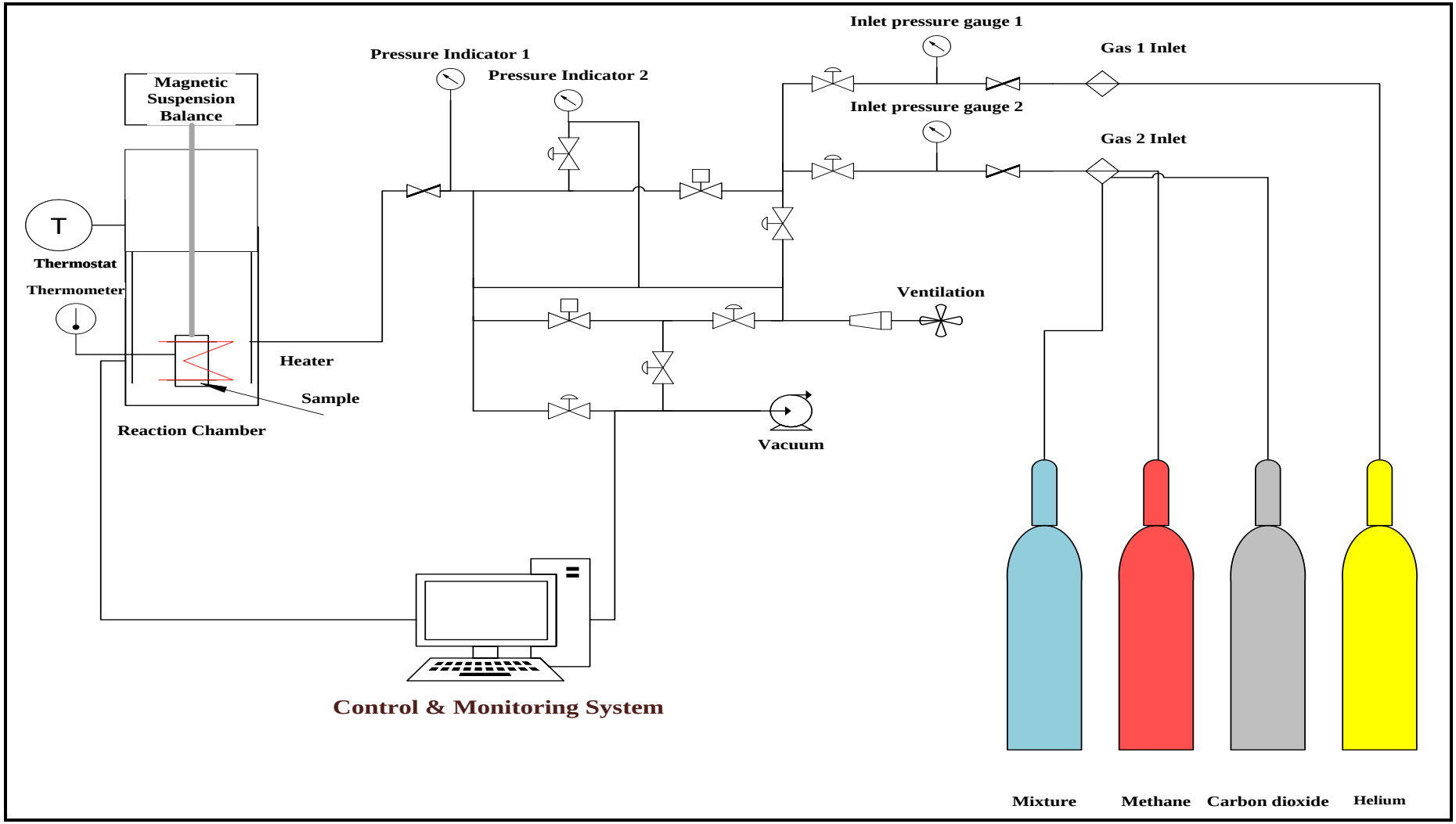

Figure 1.6 Schematic diagram of Rubotherm Magnetic Suspension Balance.

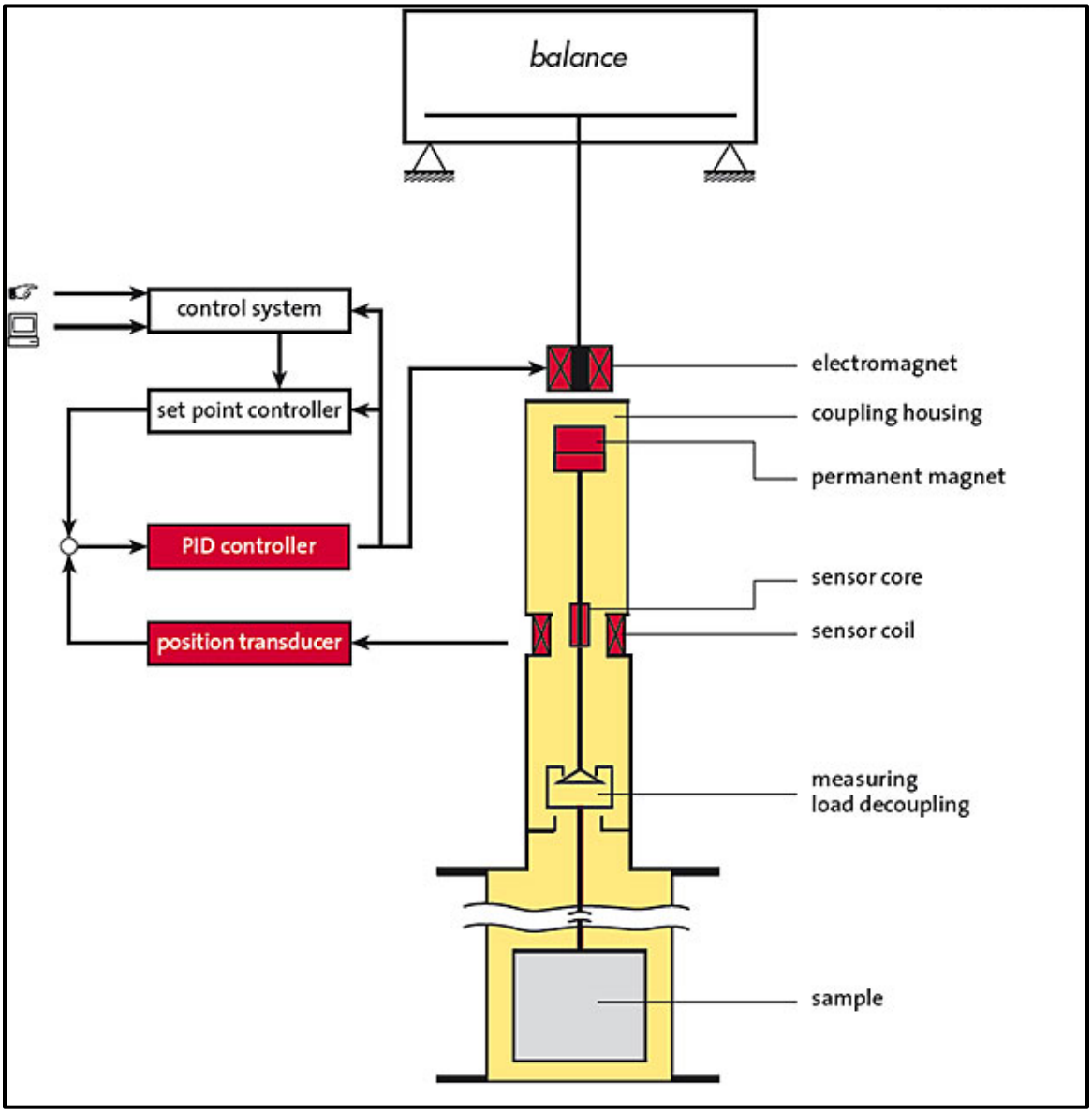

Figure 1.7 Rubotherm Magnetic Suspension Balance Operating Principle.

CHAPTER 2

ADSORPTION/DESORPTION OF CO_2/CH_4 BY CARBONATE ROCKS

3.1 Summary

In this Chapter, CO_2 injection for Enhanced Gas Recovery (EGR) and sequestration after primary recovery is investigated. Also, competitive adsorption of CH_4 and CO_2 is studied in the temperature range 50°C-150°C using a mixture of CO_2 and CH_4. Methane adsorption on the surface of the carbonate rock reduced from 50 mg/g at 50°C to 12.4 mg/g at 150°C. Addition of 10% CO_2 to methane has enhanced the adsorption from 23 for the pure methane to 30 mg/g for the 10% CO_2 gas mixture at 100°C. The adsorption experiments have shown that the adsorption of CO_2 on Pink Desert limestone is four times higher than that of CH_4 at the same pressure and temperature due to the high affinity of CO_2 to the carbonate rocks. The thermodynamic analysis confirmed the high natural selectivity of carbonate toward CO_2 with lower heat of adsorption for CO_2 and the adsorption is spontaneous at low temperatures. The adsorption-desorption experiments showed that CO_2 content of injected gas has a strong influence on natural gas desorption from the rocks. The CO_2 content and rock minerology influence the desorption isotherm model. The potential of using CO_2 in EGR and sequestration applications especially in low temperature reservoirs is discussed.

A model that explains the contribution of the desorption of natural gas to the total gas production is proposed.

3.2 Introduction

The International Energy Agency, EIA[56] forecast showed that the energy consumption will double and reach 5.7 trillion cubic meters in the next three decades. These demands are fixated in Europe and North America while more than two thirds of the production will come from the Middle East and Africa. The Middle East alone has more than 40% of the proven global gas reserves approximately 90% of it is in carbonate reservoirs [2–4]. However, carbonate reservoirs pose a great challenge due to its high heterogeneity and complexity. Most of oil and gas resources are trapped in carbonate reservoirs and because of that they have got the attention of industry and experts to improve the characterization, formation evaluation, and sweep efficiency and ultimately improving the hydrocarbon recovery.

Implementation of carbon capture and sequestration in Enhanced Gas Recovery (EGR) has recently gained great momentum in terms of recovery cost, feasibility, and environmental remediation [60]. This emerging technology has dual advantages of reducing the emission of CO_2 into atmosphere and recovering the residual gas that is left in the reservoir after primary recovery [61]. The potential of using CO_2 for EGR and sequestration purposes has recently been addressed as dual benefit solution to balance CO_2 sequestration cost[7–10]and several projects adopted this technique for conventional carbonate reservoirs in Western Canada[66] and Algeria [67].

The gas recovery efficiency depends on many factors such as the type of rock formation, competitive adsorption-desorption of CO_2 and natural gas on the formation, and the

reservoir temperature and pressure [68].Adsorption-desorption and diffusion processes are the main characteristics controlling EGR and CO_2 sequestration [69]. Many studies reported the interaction of CO_2 with different reservoir rocks, nevertheless the focus was unconventional reservoirs[15–22].Yet, little efforts have been made to study the adsorption-desorption of CO_2on the different types of carbonate rocks and assess its impact on the natural gas recovery process[78].

The previous experimental studies showed that CO_2 content in natural gas has a major influence on natural gas desorption from carbonate rocks. In addition, the selection of the desorption isotherm model is influenced by the CO_2 content of natural gas. The carbonate mineralogy is another factor that affects the desorption behavior of natural gas[79].

Most of the adsorption studies on rocks used powdered samples which do not represent the actual reservoir rock [25–28].

Intact rock cubes were used to accurately measure rock real adsorption-desorption responses. Adsorption-desorption experiments are carried out at high pressure and high temperature to study CO_2 and methane adsorption behavior on carbonate surface. The effect of injecting pure CO_2 and a mixture of CO_2 (10 vol%) and CH_4 on natural gas adsorption on carbonate rocks are studied. Adsorption isotherm are developed based on the rock type and gas composition to explain the contribution of natural gas desorption to the total gas production. In addition, this study provides tools for predicting methane production due to CO_2 injection.

3.3 Experimental setup and procedure

Measuring the gas adsorption/desorption on the surface of rocks is often conducted using volumetric based or gravimetric approaches [83]. In general, gravimetric methods which

are adopted here involve using a sensitive microbalance to quantify the variation in the sample weight related to the adsorption under controlled pressure and temperature[84]. These gravimetric methods are extremely accurate and can be conducted using small size samples [85]. Whereas volumetric methods are conducted by allowing the pressure to expand from a reference cell to a measuring cell and record the change in pressure which will be related to gas adsorption. Although they are faster and permit the use of large sample volumes, but they lack the accuracy of gravimetric methods [55].

A cubic sample of Pink Desert Limestone was prepared in the dimension of 0.5 cm^3 from 6" core with approximate weight of 1 gram. The sample was cleaned, soaked in distilled water for 24 hours, and dried in the oven at 150^oC for 24 hours. Then, the sample's measured weight has been calibrated by heating the sample to 100^oC under vacuum for 1 hour, followed by buoyancy measurement with Helium at constant 100^oC through 8 stages and a maximum pressure of 45 bars using (Rubotherm^{TM}) magnetic suspension balance. The apparent sample weight, accounting for the impact of gas density, is corrected by blank and buoyancy experiments at each temperature using Helium. Helium is considered as an inert gas, and it can reach all the permeable pores of the sample without being adsorbed [30, 32, 33]. These corrections are used to obtain the absolute adsorption isotherm as function of pressure and temperature q (P, T) only. In addition, the corrections will help in offsetting the effect of sample holder and the loss of weight due to the buoyancy of the solid adsorbent which causes apparent weight loss [87].After that, the adsorption isotherm for pure CO_2 was measured at different pressures with a maximum pressure of 50 bar and at constant temperature of 100^oC.

The adsorption isotherm is recorded through measuring the weight of the sample at different pressures. In all experiments, an electric heating system and high efficiency thermostat were used to control the temperature within the accuracy of ± 0.1^{o}C. The same setup was used to measure pure CH_4 isotherm. Furthermore, the competitive adsorption of CH_4 and CO_2 was investigated using a mixture of CO_2 and CH_4 (10% CO_2).

Finally, the effect of temperature on the competitive adsorption was investigated using a constant mixture of 10% CO_2 and 90% CH_4 at 50^{o}C and 150^{o}C, respectively with Helium buoyancy measurement at these temperatures. Furthermore, the effect of temperature on pure CH_4 and pure CO_2 was also examined at 50^{o}C and 150^{o}C.

3.4 Results and discussion

3.4.1 Characterization of Pink Desert Limestone

The SEM image of the rock sample given in (Figure 2.1) demonstrates that the sample is a fine-grained, moderately sorted, sub rounded and the bio clasts include micritized peloids, echinoderms, interparticle porosities with minor amounts of moldic and intraparticle porosities that show the heterogeneity of the Pink Desert carbonate. The pores are reduced by syntaxial calcite overgrowths and blocky calcite cement. The porosity is 25%, and the average pore size is 50-300 microns (up to 700-micron pore). XRD results showed it is mainly composed of calcite (95%), and dolomite (5%).

3.4.2 Adsorption of CH_4 and CO_2

Determining the actual adsorption capacity of methane and carbon dioxide for different rocks is extremely important for comprehending the CO_2 storage and methane desorption processes [88]. The sorption phenomenon is manifested when the gas molecules are

attached to the surface of the substance and held into its pores by physical or chemical means. The physical sorption is due to van der Walls forces and electrostatic forces, and the chemical sorption is caused by strong chemical bonds [13].

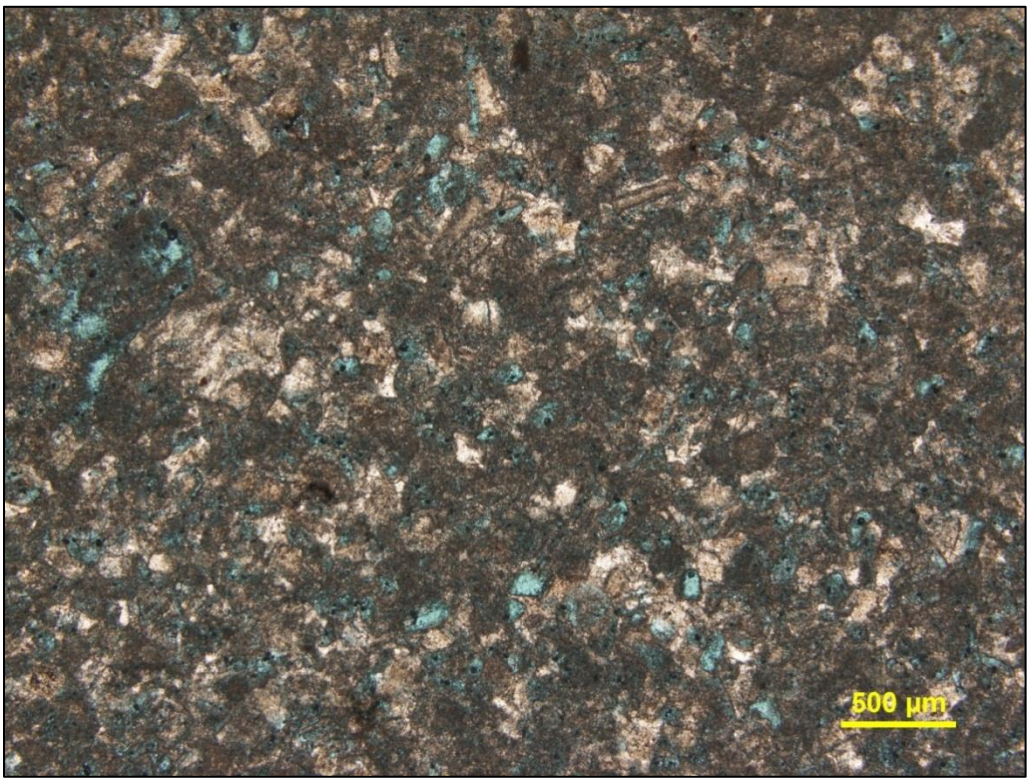

Figure 2.1 SEM section of Pink Deseret limestone.

This adsorption process is directly proportional to the pressure of the free gas; increasing the pressure increases the adsorption process. On the other hand, decreasing the pressure in the desorption process decreases the adsorbed gas [14]. Furthermore, the maximum volume of adsorbed gas is usually determined by the sorption isotherm which represents the equilibrium volume of the gas adsorbed on substance surface at isothermal conditions [15].

Adsorption isotherms are utilized to describe adsorption characteristics of gases on the rock surface and as input parameters to model the gas flow and transport in porous media. Lacking the appropriate expression of the adsorption data can lead to severe errors in the

transport modeling process [25]. Simple models such as Langmuir and Freundlich isotherms are widely used to fit and define the adsorption data, but they frequently lack the accuracy and more sophisticated complex models are applied [26]. Because the isotherm models are based on the idea of adsorption behavior at constant temperature (reservoir temperature) with different pressures (average reservoir pressure) which is the case in gas reservoirs since they often stay in the same temperature during the depletion phase for most of the reservoir life.

Langmuir is a monolayer model that describes the adsorption equilibrium on the surface of the rock by[10]:

$$q = \frac{Q_l k_l p}{1 + k_l p} \tag{8}$$

where Q_l (mg/g) is the maximum mass of gas adsorbed per unit mass to cover the complete monolayer and k_l is the Langmuir constant of equilibrium (1/mg).The Freundlich isotherm is given by[29]:

$$q = k_f p^n \tag{9}$$

where k_f and n are constants. The BET isotherm describes the multilayer adsorption on the surface of the rock[11]:

$$q = \frac{Q_m k_b p}{(p_s - p)[1 + (k_b - 1)\frac{p}{p_s}} \tag{10}$$

The Langmuir model includes three different types of isotherms; the Langmuir, the Freundlich, and the mixture of both Langmuir and Freundlich isotherms [16]. Langmuir isotherm is widely used in the literature to define the adsorption [19] and the competitive adsorption processes[20].

Figure 2.2-Figure 2.4 show isotherms fitting using non-linear regression with MATLAB 2016a and confirmed using Excel 2016 for pure CO_2, CO_2/CH_4 (10/90%) and pure CH_4

at100^{o}C. Langmuir mono-layer isotherm poorly fit the experimental data since it assumes a homogenous surface and rock surface is widely heterogeneous in our case. The high R^2 and low SSE values are obtained only at extremely low pressures. The adsorption isotherms are used as input parameters for simulation of gas flow, gas in-place assessment and production decline curve analysis to predict the behavior of the reservoir during depletion. When Langmuir model is used for modeling CO_2/CH_4 adsorption in carbonate, it yields inaccurate predictions and estimation for the gas in place and gas flow in porous media. However, Freundlich empirical isotherm, which accounts for surface heterogeneity[89] and BET multilayer isotherm, showed an excellent fit with lower SSE and high R^2. The fitting parameters are listed in Table 2.1.

The maximum CO_2 amount adsorbed by Pink Desert carbonate was 190 mg/g obtained at 50^{o}C and 50 bar. Further increase in sample temperature decreased this amount to 97.9 mg/g at 100^{o}C and 60.2 mg/g at 150^{o}C. On the contrary, the amount of methane adsorbed at these temperatures were 48 mg/g, 23.06 mg/g and 12.43 mg/g at 50^{o}C, 100^{o}C and 150^{o}C, respectively. For the 10% CO_2/CH_4 mixture, the total gas uptake increased to 52.7 mg/g, 29.74 mg/g and 18.3 mg/g at 50^{o}C, 100^{o}C and 150^{o}C accordingly. This is due to calcite and dolomite high affinity toward CO_2 and strong selectivity over methane [90].

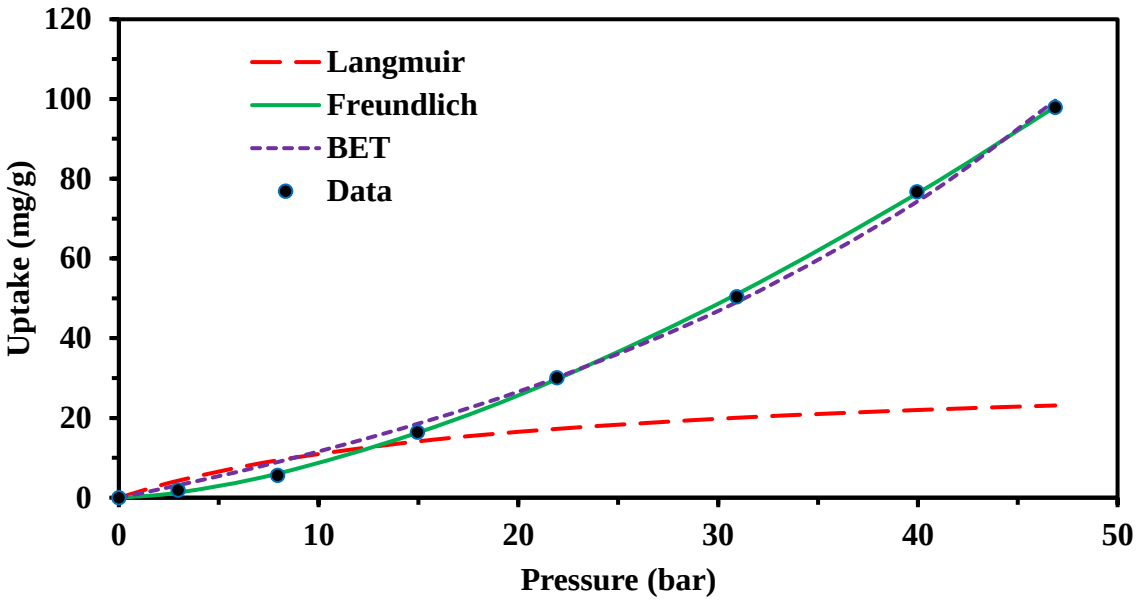

Figure 2.2 Fitting of CO_2 adsorption on Pink Desert limestone at 100°C with Langmuir, Freundlich and BET.

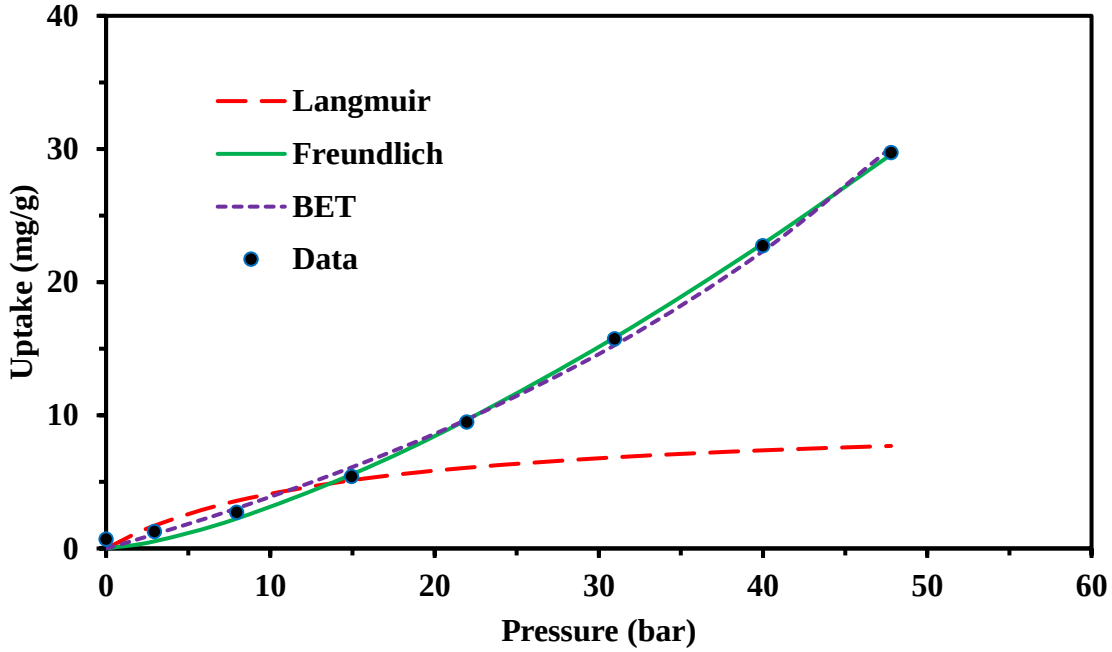

Figure 2.3 Fitting of 10%CO_2 adsorption on Pink Desert limestone at 100°C with Langmuir, Freundlich and BET.

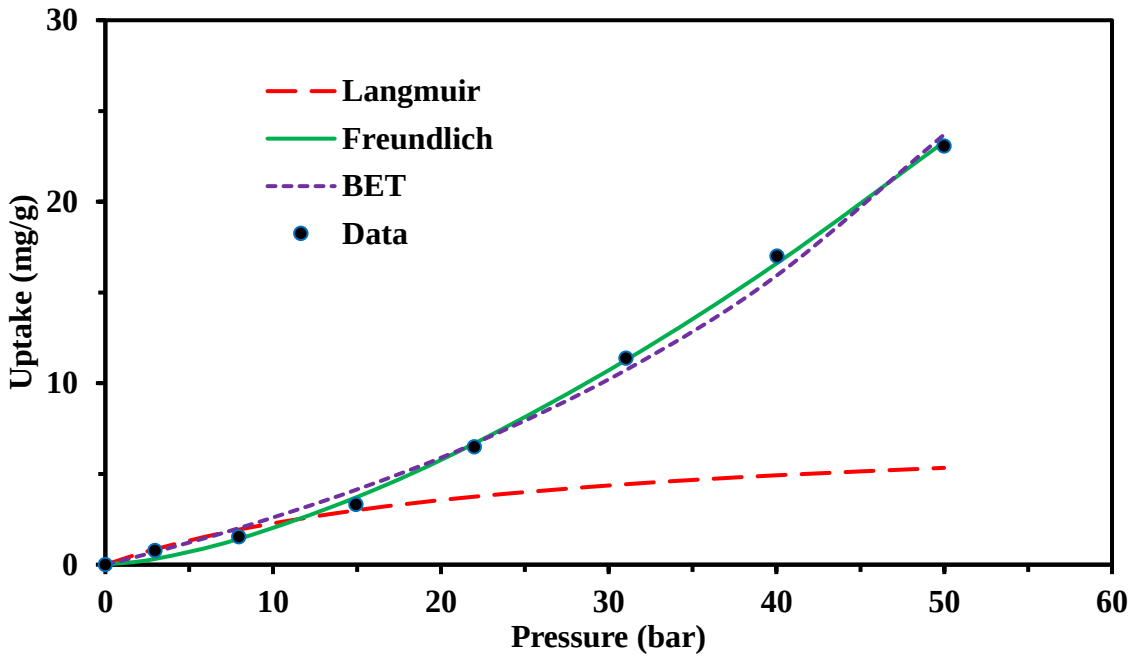

Figure 2.4 Fitting of CH_4 adsorption on Pink Desert limestone at 100°C with Langmuir, Freundlich and BET.

Adsorption/desorption reversibility of CO_2 on carbonate surface at 50°C, 100°C and 150°C is shown in Figure 2.5 indicating only physical sorption took place in the process which is anticipated at medium temperature ranges [91]. However, increasing the temperature resulted in exponential decrease in the maximum uptake which can be attributed to the exothermic nature of CO_2 adsorption [92], [93].

Pure methane and CO_2/CH_4 mixture (Figure 2.6,Figure 2.7) also exhibit the same behavior. The hysteresis between adsorption-desorption curves in CO_2/CH_4 mixture (Figure 2.7) show that less gas was desorbed than that adsorbed at the same pressure at low and high temperatures. This is likely due to insufficient waiting time [94], narrow and non-uniform carbonate pores [95]. Also, this can be attributed to the reversible interaction between CO_2 and limestone [96] at low pressure which is good for long time underground CO_2 storage. Hence, methane will be desorbed first at the same pressure which is favorable in EGR

process [97]. These results emphasize that storing CO_2 is preferable in shallow and low temperature reservoirs [98], [99].

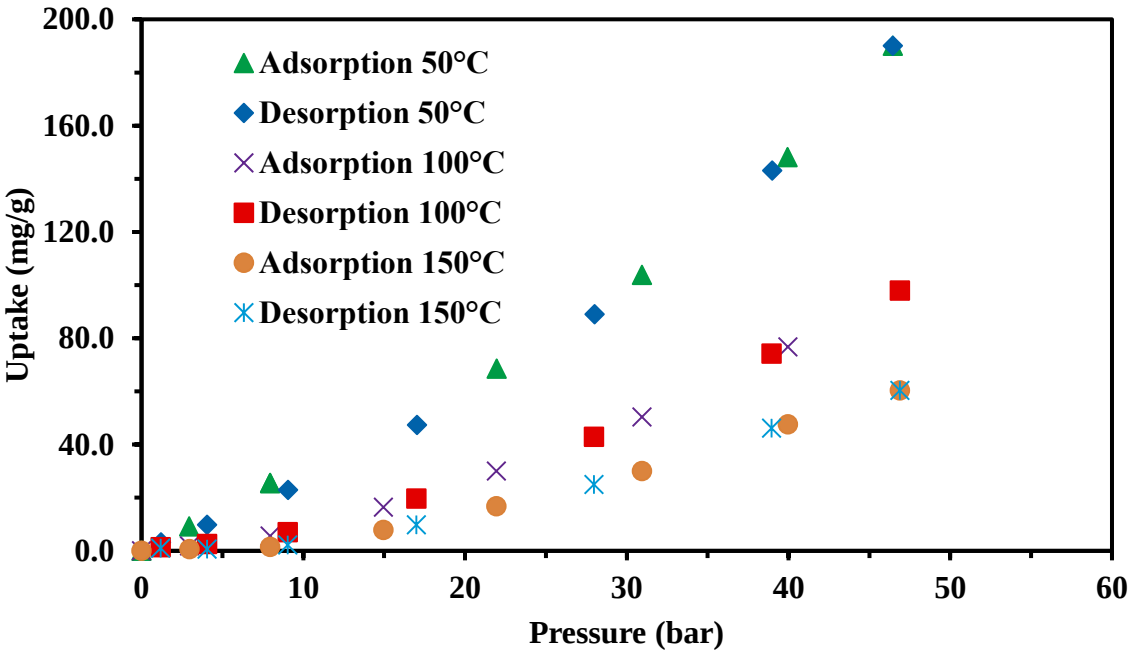

Figure 2.5 Effect of temperature on adsorption/desorption of CO_2 on Pink Desert limestone.

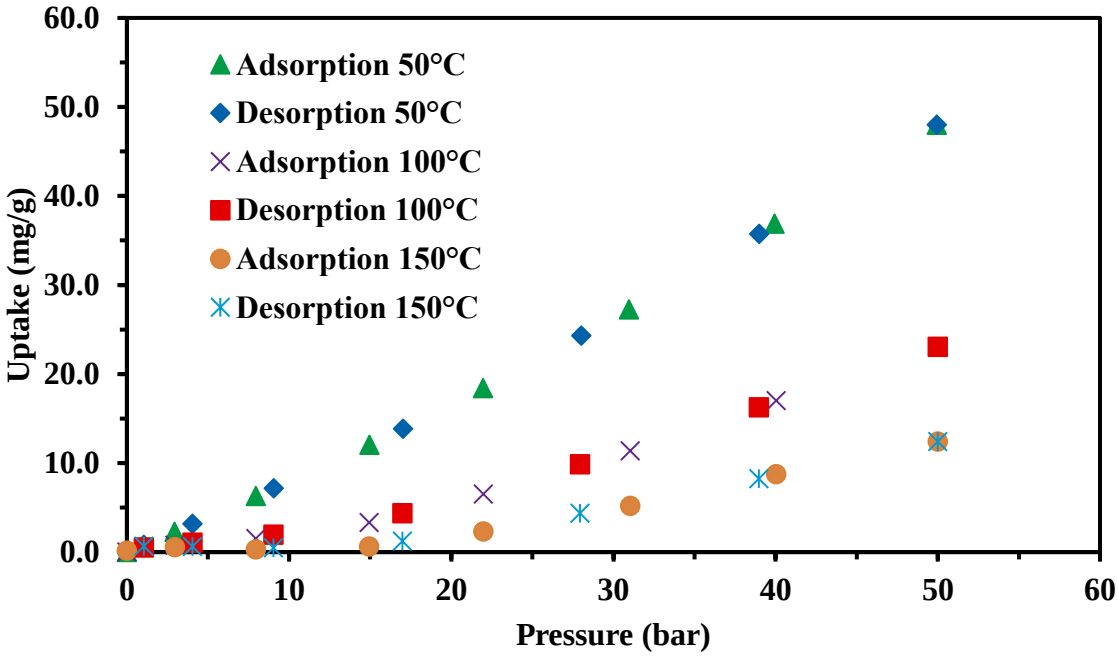

Figure 2.6 Effect of temperature on adsorption/desorption of CH_4 on Pink Desert limestone

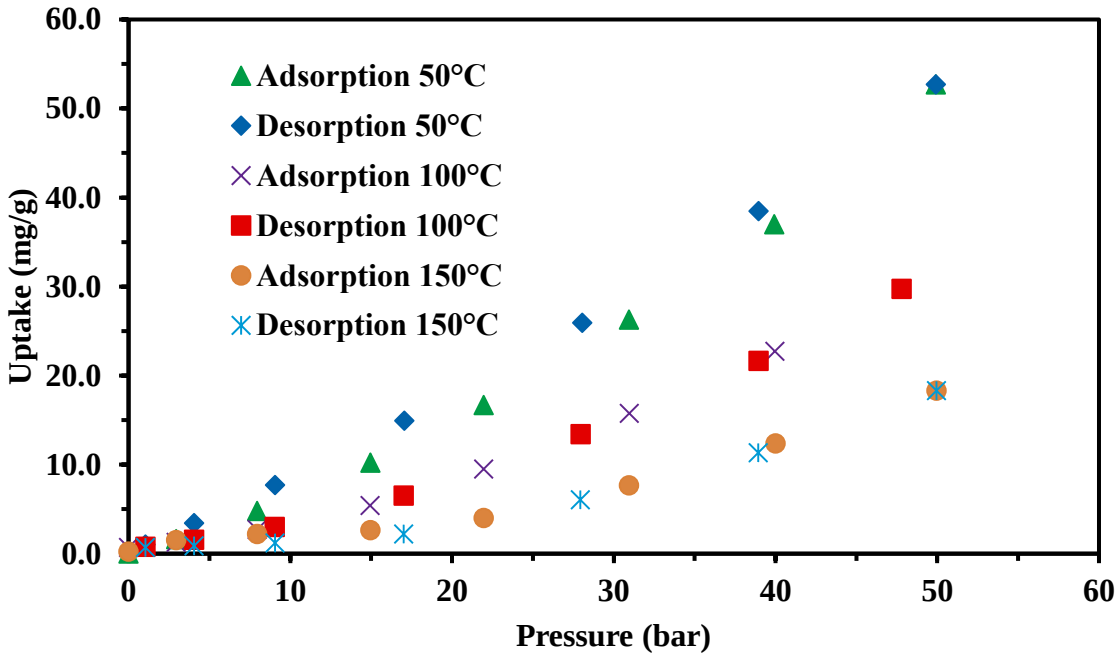

Figure 2.7 Effect of temperature on adsorption/desorption of 10% $CO_2$and 90% CH_4 mixture on Pink Desert limestone

Table 2.1 Langmuir, Freundlich and BET isotherms fitting constants for CH_4, CO_2 and 10% CO_2 at different temperatures

Gas		Langmuir				Freundlich				BET				
	Temperature (^oC)	Q_l	k_l	R^2	SSE	k_f	n	R^2	SSE	Q_m	k_b	P_s	R^2	SSE
100% CH_4	50	23	0.05	0.98	5.315	0.540	1.146	1	0.33	72.7	1.41	141	1	2.85
	100	8	0.04	0.98	0.268	0.061	1.52	0.99	0.62	42	0.64	117	0.99	2.86
	150	2.5	0.07	0.87	0.83	0.006	1.96	0.99	1.018	33	0.32	111	0.98	3.05
10% CO_2/CH_4	50	27	0.035	0.94	2.86	0.23	1.39	0.99	3.13	98	0.79	129	0.98	0.79
	100	10	0.07	0.95	1.51	0.113	1.44	0.99	1.35	58.5	0.68	120	0.99	1.72
	150	3.5	0.2	0.91	0.101	0.025	1.69	0.98	4.37	51	0.4	124	0.99	2.77
100% CO_2	50	80	0.06	0.96	8.53	1.4	1.27	1	17.6	230	1.3	111	1	41.69
	100	33	0.05	0.92	25.11	0.23	1.57	1	1.32	176.585	0.625	108.848	0.99	27.49
	150	14	0.04	0.97	11.57	0.08	1.73	0.999	4.63	120	0.45	102	0.99	32.24

3.4.3 Thermodynamics of adsorption on Carbonate

Heat of adsorption, standard entropy and Gibbs free energy are estimated from the isotherm data at different temperatures (50°, 100° and 150°C). The values of these parameters provide information about the spontaneous nature and randomness of the process [57, 59]. Equations (11) to (13) are used to quantify the thermodynamic variables including free energy of adsorption, heat of adsorption and standard heat of adsorption [102]:

$$\Delta G^0_{ads} = -RT \ln K_c \tag{11}$$

$$\ln K_c = \frac{\Delta S^0_{ads}}{R} - \frac{\Delta H^0_{ads}}{RT} \tag{12}$$

$$K_c = \frac{q_e}{P_e^n} \tag{13}$$

where R is the universal gas constant (8.314J/mol K); K_c is Freundlich constant; ΔG^0_{ads} is the standard free energy of Gibbs, ΔS^0_{ads} is the standard entropy and ΔH^0_{ads} is the heat of adsorption. All parameters are computed from Freundlich model by plotting $\ln K_c$ vs. 1/T (K) and $\Delta H^0_{ads}$is calculated from the slope while ΔS^0_{ads} is obtained from the intercept, and q_e and P_e^n are the equilibrium values of gas adsorption (see Table 2.2 and Appendix A).

Table 2.2 Pure CH_4, pure CO_2 and 10% CO_2 heat of adsorption Arrhenius plot fitting parameters between 50°C, 100°C and 150°C.

	100% CH_4	10% CO_2 / 90% CH_4	100% CO_2
Slope	6102.7	2966	3927.2
Intercept	-19.398	-10.501	-11.869
Regression Coefficient, R^2	0.992	0.919	0.995

The values of ΔG_{ads}, ΔH_{ads} and ΔS_{ads} are computed in Table 2.3. The negative values of ΔH_{ads} confirms the exothermic nature of CH_4 and CO_2 adsorption [103][104]. At 50°C the value of ΔG_{ads} for pure carbon dioxide is negative emphasizing the CO_2 spontaneous nature

of adsorption onto the Pink Desert limestone [105]. As the temperature increases up to 100°C

and 150°C the positive values of ΔG_{ads} for the three gas systems (CO_2, CH_4 and 10% CO_2) increases demonstrating the un-favored spontaneity at high temperatures hence the adsorption energy becomes less than the thermal energy. Also, these results indicate that at most reservoir temperatures, the Pink Desert adsorption of carbon dioxide is much more preferred to methane, which is a consequence of the high selectivity of calcite and dolomite towards capturing carbon dioxide [106], [107].

The low range negative of ΔH_{ads} is due to the exothermic nature of the physical adsorption of CO_2 and CH_4 hence the adsorption is taking place due to van der Waals interaction between the surface of the rock and the two gases [108], [109]. Furthermore, the reversibility of the physisorption process is very useful in EGR where it is required to displace and extract all the adsorbed methane by injecting carbon dioxide [110].

Table 2.3 Thermodynamic parameters for pure CO_2, pure CH_4 and 10% CO_2 mixture at different adsorption temperatures.

	100% CO_2		100% CH_4		10% CO_2 / 90% CH_4	
Temperature (°C)	K_c	ΔG_{ads} (kJ/mol)	K_c	ΔG_{ads} (kJ/mol)	K_c	ΔG_{ads} (kJ/mol)
50	1.395	-0.894	0.540	1.657	0.227	3.986
100	0.233	4.525	0.061	8.703	0.113	6.765
150	0.080	8.880	0.006	17.984	0.025	13.027
ΔH_{ads}(kJ/mol)	-32.653		-50.741		-24.661	
ΔS_{ads} (J/mol. K)	-98.684		-161.284		-87.310	

3.4.4 Enhanced Gas Recovery

Figure 2.6 shows that methane adsorption on the surface of the carbonate rock reduced from 50 mg/g at 50^{o}C to 12.4 mg/g at 150^{o}C. The increase in rock temperature from 50^{o} to 150^{o}C has reduced methane adsorption by ~ 4 times. The reduction in the adsorption can be translated to increase in methane desorption by 400%. For a calcite reservoir rock with a porosity of 10%, area of 404685 m^2 (100 acres), and a thickness of 30.48 m (100 ft), the reservoir mass will be 30 x 10^9 kg. At 50^{o}C, the adsorbed methane is estimated to be 1500 x 10^6 kg. At the same pressure, if the reservoir temperature is raised to 100^{o}C, the amount of adsorbed methane will reduce to ~ 690 x 10^6 kg and the rest of adsorbed methane will be desorbed or produced which is ~ 810 x 10^6 kg. Further increase in the temperature from 100 to 150^{o}C will reduce the amount of adsorbed methane to ~372 x 10^6 kg. These calculations are estimated using carbonate rock adsorption capacity of 50, 23, and 12.4 mg/g at 50, 100, and 150^{o}C, respectively as shown in Figure 10. The reservoir temperature could be increased by injecting hot gases such a nitrogen or CO_2.

Figure 2.7 shows that adding 10% CO_2 to methane enhanced the adsorption from 23 for the pure methane to 30 mg/g for the 10% CO_2gas mixture at 100^{o}C. During production or desorption process the rock will only hold 23 mg/g methane and the rest will be desorbed. The difference between pure methane and the 10% CO_2 methane is attributed to CO_2 adsorption and sequestration, and replacement of methane. This enhanced methane production because of the CO_2 injection is a direct consequence of rock affinity towards CO_2 rather than methane. Adding 10% CO_2 to methane will force the rock to desorb 7 mg/g methane at 50 bars and this is equivalent to 210 x 10^6 kg of methane for the above-described reservoir.

3.5 Conclusion

The adsorption of CO_2 on Pink Desert limestone carbonate is far superior to that of CH_4 at the same pressure and temperature. CO_2 content in natural gas has a major influence on the adsorption/desorption of methane from carbonate rocks and gas adsorption amount increases with increasing CO_2/CH_4 ratio due to the high affinity of carbonate to CO_2, which gives a great prospect to use CO_2 in EGR applications in carbonates. Similarly, the thermodynamic analysis confirmed the high natural selectivity of carbonate toward CO_2 with lower heat of adsorption for CO_2 and the adsorption is spontaneous at low temperatures. As the temperature increases from 50^{o}C to 100^{o}C and 150^{o}C the positive values of ΔG_{ads} for the three gas systems (CO_2, CH_4 and 10% CO_2) increases demonstrating the un-favored spontaneity at high temperatures. Hence, the adsorption energy becomes less than the thermal energy. However, CH_4 adsorption requires more energy and it is not preferable at high temperatures. Methane adsorption on the surface of the carbonate rock reduced from 50 mg/g at 50^{o}C to 12.4 mg/g at 150^{o}C. Addition of 10% CO_2 to methane has enhanced the adsorption from 23 for the pure methane to 30 mg/g for the 10% CO_2 gas mixture at 100^{o}C. Furthermore, the pure CO_2 adsorption study supported that Pink Desert limestone is very good candidate for CO_2 sequestration. The temperature study suggests that low reservoir temperatures can store large amounts of CO_2 with less energy and they are greatly viable option for CO_2 storage. Gas recovery from carbonate reservoirs is predicted to be enhanced by hot gas injections such as injecting CO_2 into the reservoir because carbonates have higher affinity to adsorb CO_2 than methane. Further, this study will enhance the simulation and flow models that describe the flow of natural gas in carbonate reservoirs.

CHAPTER 3

ADSORPTION/DESORPTION OF CO_2/CH_4 BY SANDSTONE ROCKS

4.1 Summary

The results of the experimental studies showed that the CO_2 content in the natural gas has a big effect on the desorption of the natural gas from the tight sandstone rocks. The CO_2 content also affected the desorption isotherm model for the natural gas. Increasing CO_2 fraction in the mixture from 0% to 10% CO_2 the total gas uptake is increased to approximately 28%, 22% and 33% at 50^o C, 100^o C and 150^o C respectively which reflects the high Kentucky sandstone affinity toward CO_2. The tight sandstone mineralogy also affected the desorption behavior of the natural gas. The presence of water bearing clay minerals such as Illite exhibited a vast sensitivity to temperature causing damage to crystal structure and expulsion of bounded water which resulted in huge increase in the adsorption uptake. The output from this chapter is a robust model that explain the contribution of the desorption of the natural gas to gas production. Also, it will enhance the simulation and flow models that describe the flow of natural gas in porous media in tight sandstone reservoirs.

4.2 Introduction

Natural gas present a key power choice due to its fuel efficiency and cleanness when compared with other petroleum and coal products. Natural gas consumption projected by EIA will reach 3.4 trillion cubic meters in 2040. Unconventional tight gas resources will account for more than 20% of Natural gas production in the next two decades [56].

The high complexity of tight sandstone reservoirs in terms of mineralogical composition, ultra-low permeability (generally ≤ 0.1mD) and deprived petrophysical properties poses a great challenge in natural gas production analysis [111]. Furthermore, the diagenesis processes frequently alter the original pore structure which can diminish the pore throat typical diameter increasing the tortuosity and number of isolated pores [112]. Common formation evaluation practices often come short in providing satisfactory outcomes. Without advance drilling methods and gas recovery techniques the production from tight gas sands is marginal [113]. The most feasible economical way to produce natural gas from tight sands is fracturing methods especially multi-stage hydraulic fracturing [114].

The simulation of the gas flow in tight sandstone reservoir is a very complicated process [115]. Several mechanisms contributed to the natural gas production from tight sandstone reservoirs. One of the main mechanisms is gas desorption from the rock surface to the pore body. The existing models did not consider the effect of CO_2 content in the natural gas on the gas desorption from the rock. Also, the current models [115]–[119] used desorption models from the literature and they neglect the sorption and the effect of rock type and reservoir conditions on the gas desorption.

In this chapter, we investigated the effect of CO_2 content (0 to 10 Vol%) on the natural gas desorption from the tight sandstone rocks and accurate desorption isotherms were developed based on the rock type and gas composition. Adsorption/desorption experiments at high pressure and high temperature were conducted to develop a robust model for the natural gas desorption from the rock. Also, the effect of tight sandstone rock mineralogy was investigated on the adsorption/desorption of the natural gas by thermal decomposition analysis.

4.3 Experimental setup and procedure

Measuring the gas adsorption/desorption on the surface of rocks is often conducted using volumetric based or gravimeteric approaches [83]. In general, gravimeteric methods involve using a sensitive microbalance to quantify the variation in the sample weight related to the adsorption under controlled pressure and temperature[84]. These gravimeteric methods are extremely accurate and can be conducted using small size samples [85]. Whereas volumetric methods are conducted by allowing the pressure to expand from a reference cell to a measuring cell and record the change in pressure which will be related to gas adsorption. Although they are faster and permit the use of large sample volumes, but they lack the accuracy of gravimeteric methods [55]. shows a diagram of the setup used to conduct the adsorption experiment using (Rubotherm^{TM}) magnetic suspension balance which proofed to efficient elsewhere [85], [120]–[123]. In contrast with customary balances, the magnetic suspension balance is not directly associated with testing sample which is suspended by a suspension magnet. the suspension magnet system comprises of a permanent magnet, measuring load and a sensor core. then Control

frameworks maintain the electric magnet in free suspension and transmit the measured weight to the outer balance [84].

The measurements started with calibrating the measured weight of the intact cubic sample while heating the sample to 50^{o}C under vacuum for 1 hour which was sufficient to remove any adsorbed air and until a constant mass is attained. Then a Helium buoyancy experiment was conducted using (Rubotherm^{TM}) magnetic suspension balance at constant temperature of 50^{o}C and through eight pressurizing stages to a maximum pressure of 50 bars. At these low pressure and temperature, we can assume only buoyancy occurs and the helium adsorption is negligible, which has been reported by many researchers [55], [84], [86]. The blank and the buoyancy measurements has been adopted for every testing temperature to correct the sample apparent weight because of gas density and the weight of the sample holder. One segment of the helium buoyancy measurement at 100^{o}C (see Appendix B). Then the pressure and temperature absolute isotherm of adsorption is obtained after correcting the weight to accommodate the apparent weight loss caused by the buoyancy experiment and eliminate the sample holder effect [87]. Furthermore, the CH_4 adsorption isotherm is measured by recording the measured weight of the sample under constant temperature of 50^{o}C through eight pressure set points up to 50 bars. After that we investigated the effect of temperature covering 100^{o}C and 150^{o}C respectively. The same experimental procedures were carried out for pure CO_2 and 10% CO_2 - 90% CH_4 mixture at the three measurements temperatures.

4.4 Results and discussion

4.4.1 Characterization of Kentucky sandstone

The mineralogy of the Kentucky rock sample from XRD is shown in Table 3.1 and Figure 3.1 with a two thirds quartz, 14% Illite, 17% Plagioclase, 3% Potassium feldspar and traces of Kaolinite. Figure 3.2 shows the SEM analysis of the surface of the rock and the red circles points some of the locations of clay on the surface while the completely black sites are pores. The core permeability is 0.1 md and the porosity is 0.08.

Table 3.1 Mineralogy of Kentucky sandstone[124]

Mineral	wt. %
Quartz	66
Dolomite	0
Calcite	0
Kaolinite	Trace
Illite	14
Chlorite	0
Potassium feldspar	3
Plagioclase	17

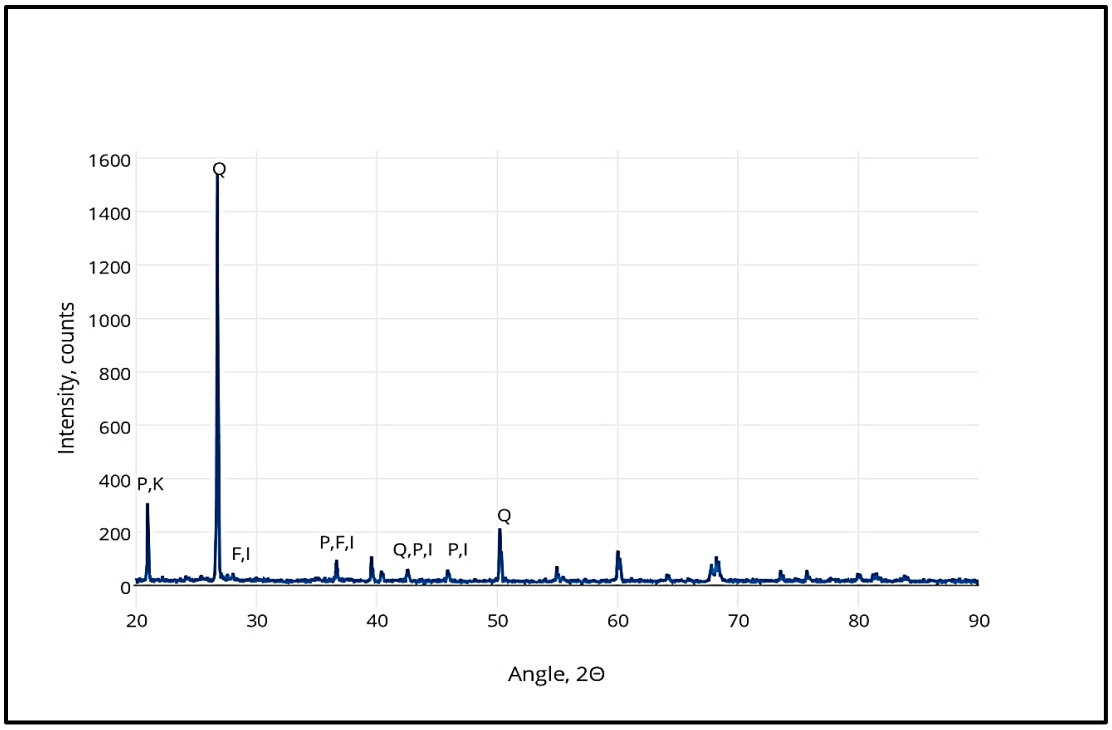

Figure 3.1 Kentucky sandstone XRD patterns, Quartz (Q), Kaolinite (K), Illite (I), Potassium feldspar (F) and Plagioclase (P).

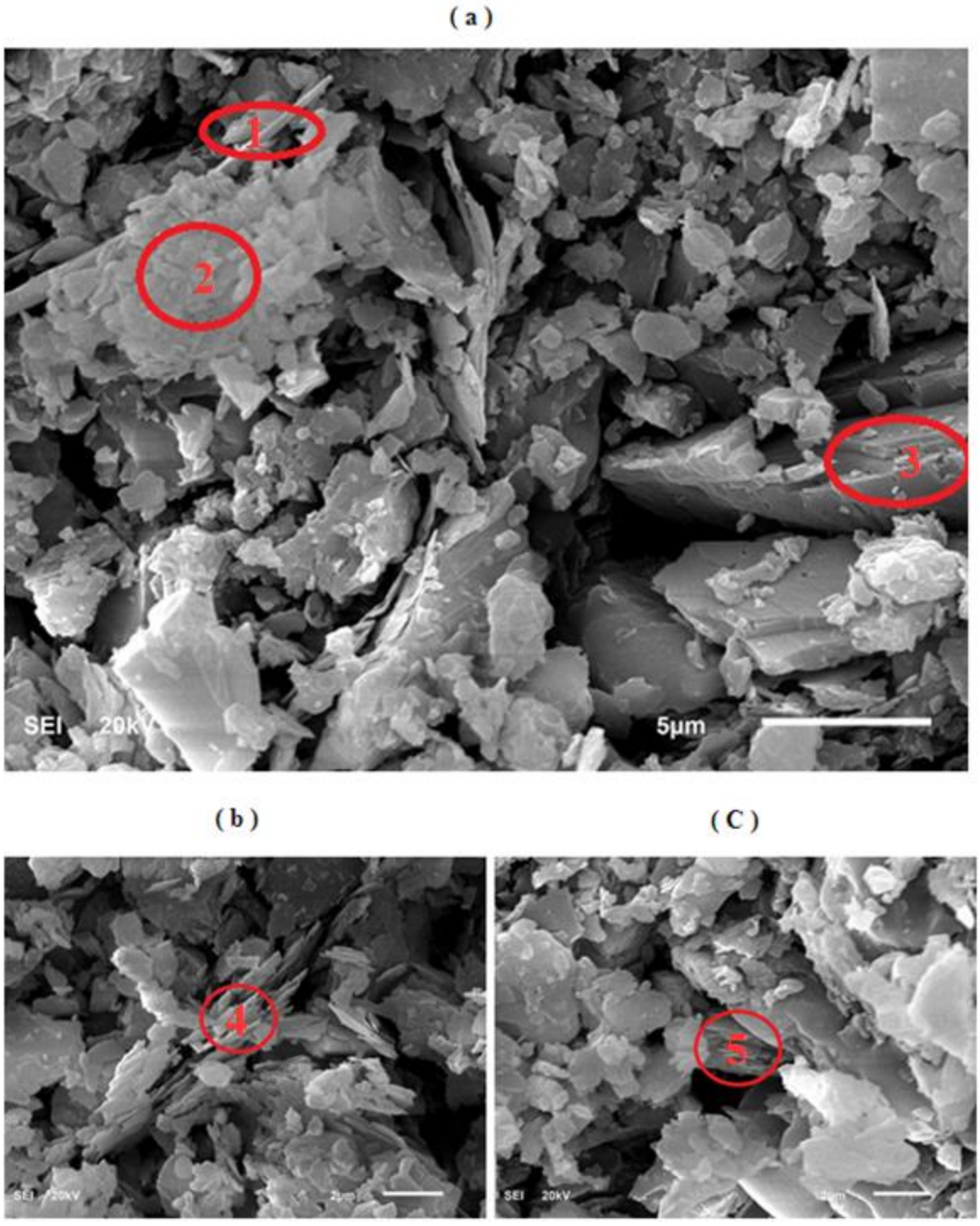

Figure 3.2 Kentucky sandstone SEM at different locations. The red circles highlight some of the locations of clay minerals. 1-Plagioclase, 2- Plagioclase, 3-K-feldspar, 4-Illite and 5-Illite.

4.4.2 Adsorption of CH_4 and CO_2

Determining the actual adsorption capacity of methane and carbon dioxide for different rocks is extremely important for comprehending the CO_2 storage and methane desorption processes [88]. The sorption phenomenon exists when the gas is attached to the surface of the substance and held into its pores physically or chemically. The physical sorption is due to van der Walls forces and electrostatic forces, and the chemical sorption is caused by strong chemical bonds [13]. This adsorption process is directly proportional to the pressure of the free gas; increasing the pressure increases the adsorption process. On the other hand, decreasing the pressure in the desorption process decreases the adsorbed gas [14]. Furthermore, the maximum volume of adsorbed gas is usually determined by the sorption isotherm which represents the equilibrium volume of the gas adsorbed on substance surface at isothermal conditions [15].

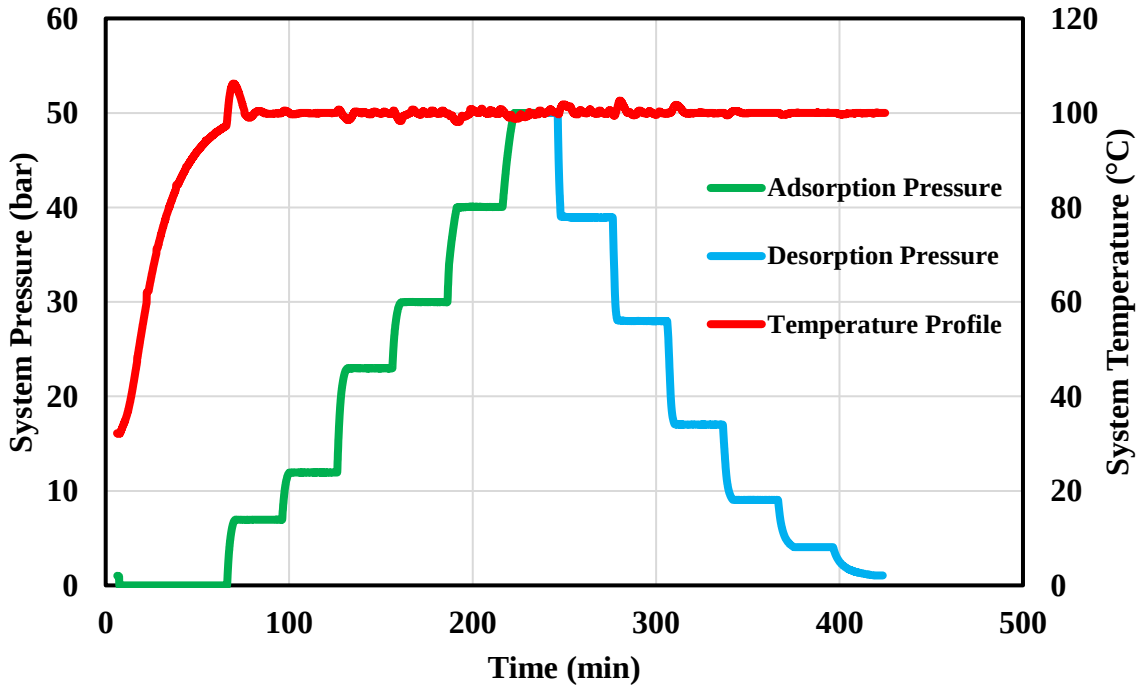

Figure 3.3 Pressure and temperature profiles through the adsorption/desorption measurement for CH_4 at 100°C and various pressure set points

Adsorption isotherms are generally utilized to describe adsorption characteristics of gases on the rock surface and as input parameters to model the gas flow and transport in porous media. Lacking the appropriate expression of the adsorption data can lead to severe errors in the transport modeling process [25]. Simple models such as Langmuir and Freundlich isotherms are widely used to fit and define the adsorption data, but they frequently lack the accuracy and more sophisticated complex models are applied [26]. Because the isotherm models are based on the idea of adsorption behavior at constant temperature (reservoir temperature) with different pressures (average reservoir pressure) which is the case in gas reservoirs since they often stay in the same temperature during the depletion phase for most of the reservoir life.

Langmuir is a monolayer model of equilibrium on the surface of the rock given by [10]:

$$q = \frac{Q_l k_l p}{1 + k_l p} \tag{14}$$

Where Q_l (mg/g) is the maximum mass of gas adsorbed per unit mass to cover the complete monolayer and k_l is the Langmuir constant of equilibrium (1/mg). The Freundlich isotherm is given by [29]:

$$q = k_f p^n \tag{15}$$

Where k_f and n are constants. The BET isotherm describes the multilayer adsorption on the surface of the rock [11]:

$$q = \frac{Q_m k_b p}{(p_s - p)[1 + (k_b - 1)\frac{p}{p_s}} \tag{16}$$

The Langmuir model includes three different types of isotherms; the Langmuir, the Freundlich, and the mixture of both Langmuir and Freundlich isotherms [16]. Langmuir

isotherm is being widely used in the literature to define the adsorption process [19] and the competitive adsorption process [20].

The maximum amount of pure methane adsorbed by the sandstone at 50^{o}C and a pressure of 50 bars shown in Figure 3.4 is 27.75 mg/g which is significantly less than the maximum adsorbed carbon dioxide amount (143.1 mg/g) in Figure 3.6 which gives an indication of the high desirability of the rock for capturing carbon dioxide molecules [90]. Correspondingly, increasing CO_2 percentage in pure methane to 10% in the mixture the uptake increased to more than 40 mg/g and that confirms the high selectivity of Kentucky sandstone toward CO_2 in the mixture which will lead to higher methane recapture and less CO_2 recovery. When the temperature increased to 100^{o}C the adsorption isotherms for methane, carbon dioxide and 10% CO_2 mixture exhibited a normal Physisorption behavior i.e. adsorption uptake amount decrease proportionally with increasing the temperature. However, increasing the temperature to 150^{o}C resulted in reverse behavior for all the three gases and the uptake for CH_4 increased to 121.55 mg/g, for CO_2 499.12 mg/g and for 10% carbon dioxide was 161.37 mg/g. This behavior type of desirable increasing in storage with elevating temperature has been reported for some rock types at high pressures when the temperature effect reversed which allows more gas to be accommodated depending on the porosity of formation [125].

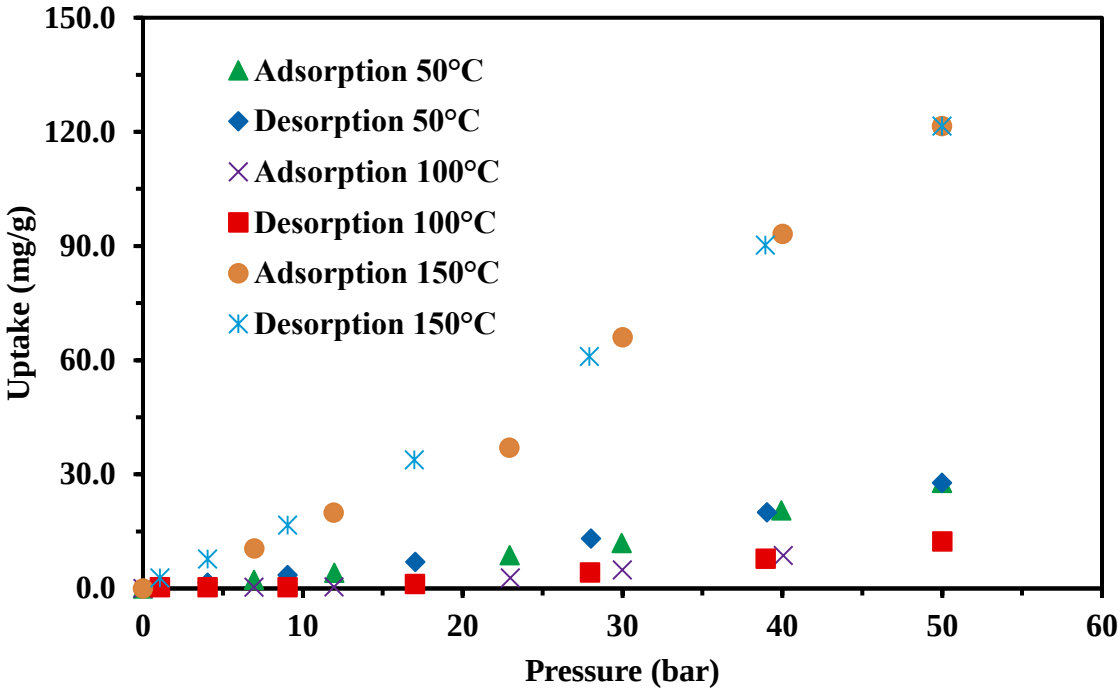

Figure 3.4 Effect of temperature on adsorption of CH_4 by Kentucky Sandstone

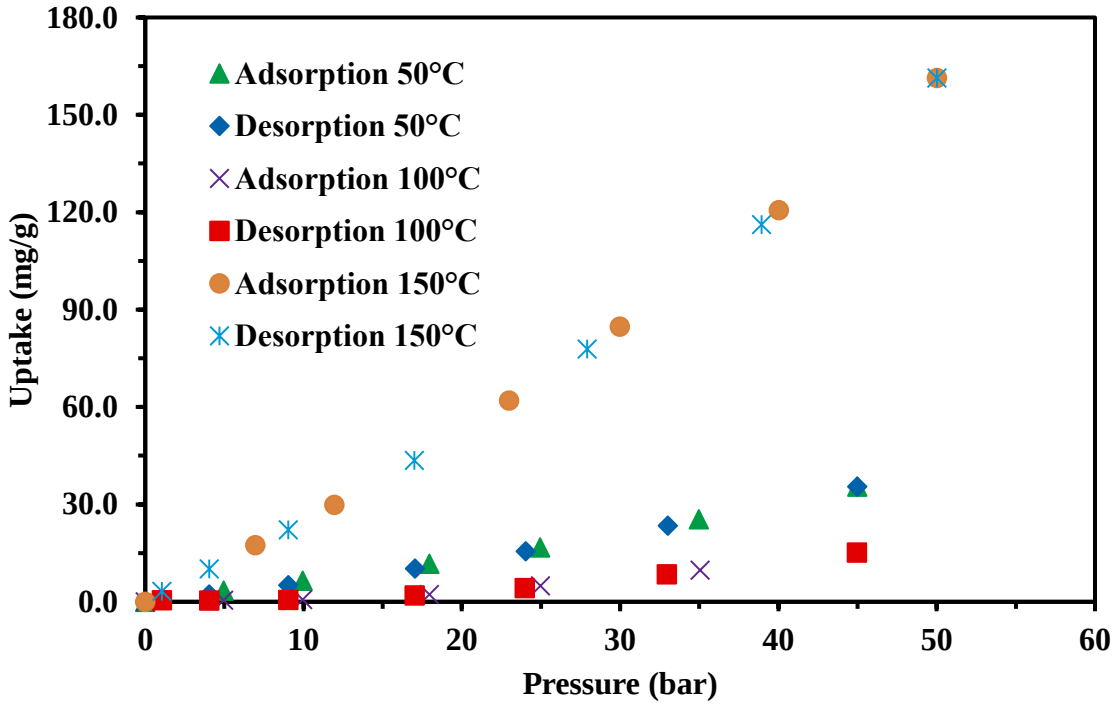

Figure 3.5 Effect of temperature on adsorption of 10% CO_2 by Kentucky Sandstone

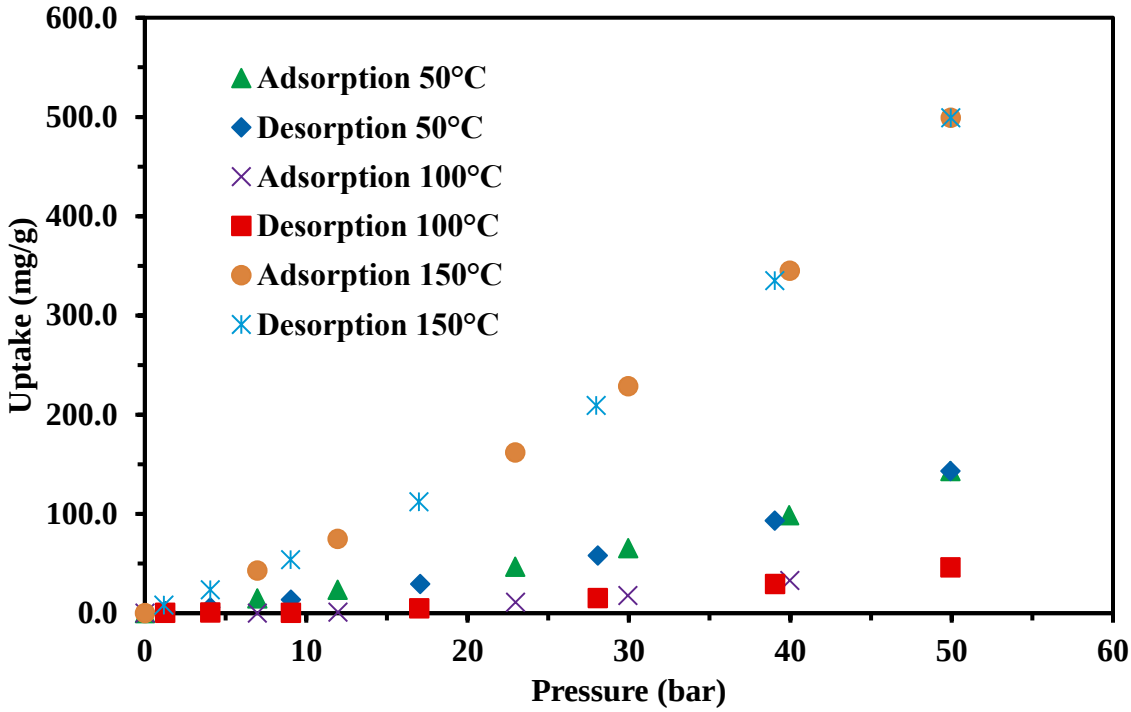

Figure 3.6 Effect of temperature on adsorption of CO_2 by Kentucky Sandstone.

Figure 3.7-Figure 3.9 illustration the fitting results to Langmuir, Freundlich and BET isotherms at 50°C, 100°C and 150°C, respectively. The results confirm that Langmuir isotherm is not representing the experimental data except at low pressures, while Freundlich isotherm is the best fit and BET isotherm is more accurate than Langmuir. However, when fitting adsorption data the high R^2 value for an adsorption isotherm does not certainly imply that the fitted model is the best in representing the experimental data [126]. The fitting parameters are exhibited in Table 3.2 also see Appendix B.

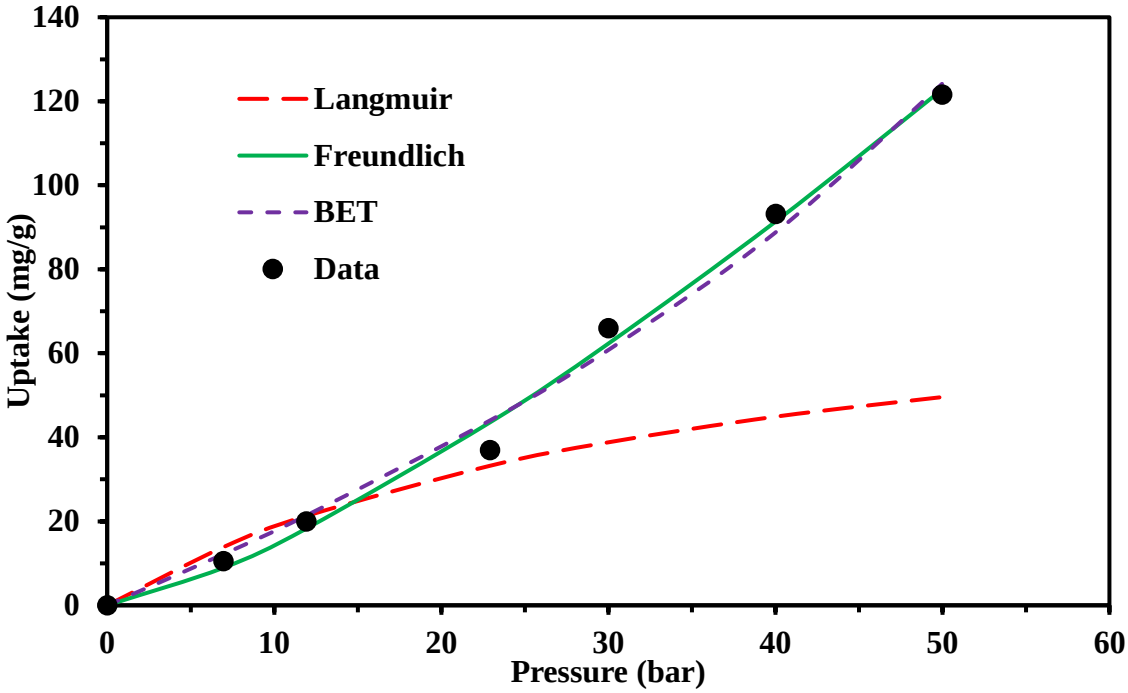

Figure 3.7 Fitting of CH_4 adsorption at 150 °C with Langmuir, Freundlich and BET.

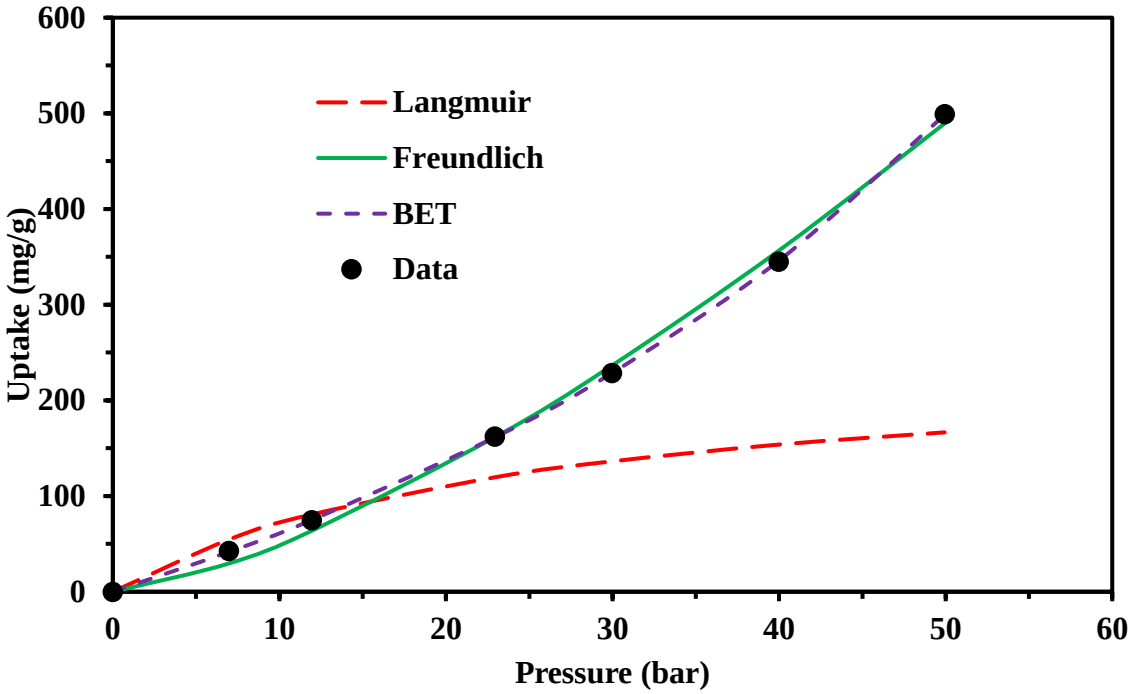

Figure 3.8 Fitting of CO_2 adsorption at 150 °C with Langmuir, Freundlich and BET.

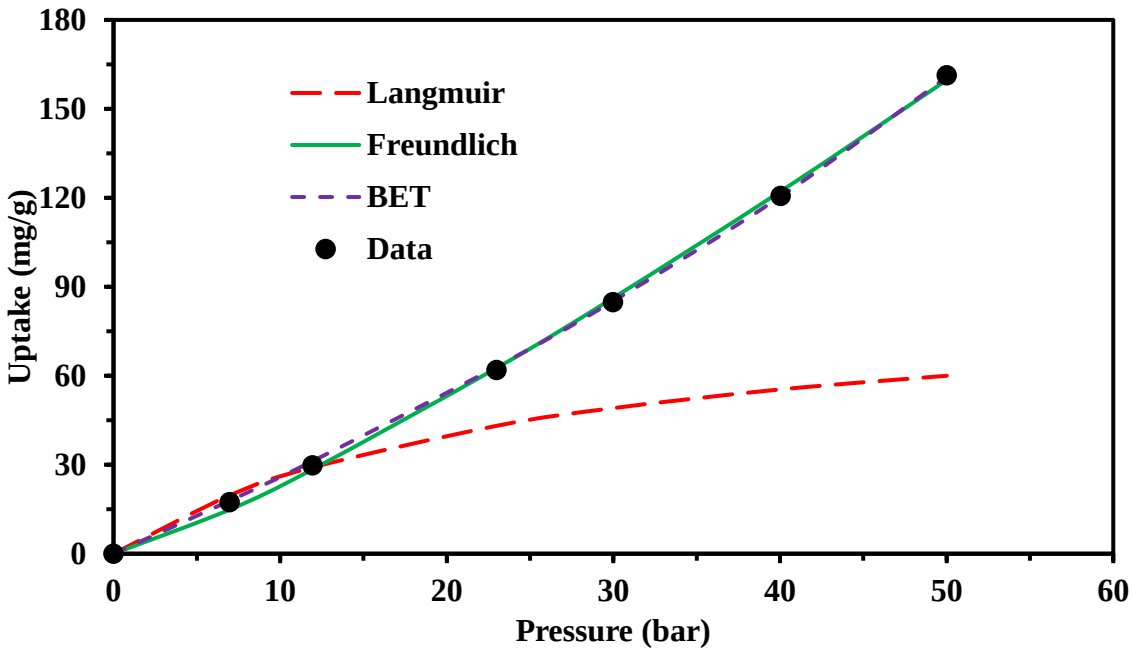

Figure 3.9 Fitting of 10% CO_2 adsorption at 150 ^oC with Langmuir, Freundlich and BET.

The study of temperature effect on the adsorption capacity yielded an uptake declining after raising the adsorption measurement temperature from 50^oC to 100^oC under all pressure set points. At a 50 bar pressure the reduction in adsorption for, and was 27.75 mg/g to 12.35 mg/g for pure methane, 143.10 mg/g to 46.13 mg/g for pure carbon dioxide and 35.51 mg/g to 15.18 for 10%CO_2/CH_4 mixture. However, after elevating the temperature to 150^oC under a pressure of 50 bar the uptake jumped to extremely high value for all the tested three gas systems; 121.56 mg/g for pure CH_4, 161.367 mg/g for pure CO_2 and 499.118 mg/g for 10% CO_2 which are extremely superior than uptake at 50^oC. This odd alteration in adsorption behavior can be attributed to expulsion of considerable amount of loosely bounded interlayer water mainly in Illite and thermal induced structural slight decomposition changes to the crystals of the clay minerals which guides the sample to an endothermic section for temperatures greater than 120^oC [127]–[129]. To verify this elucidation, XRD study was conducted for the samples at 50^oC, 100^oC and 150^oC.

Figure 3.11 displays the XRD patterns displaying bluntness at 100ºC when compared with the patterns at 50ºC and normal adsorption reduction when elevating the temperature. Furthermore, increasing the temperature to 150ºC resulted in sharper Illite and feldspar peaks signifying increase in crystallinity that happened during thermal treatment caused the particles of minerals to slightly enlarge in size, although the XRD also confirms that new peaks appeared but no new materials has emerged at the 150ºC [129], [130].

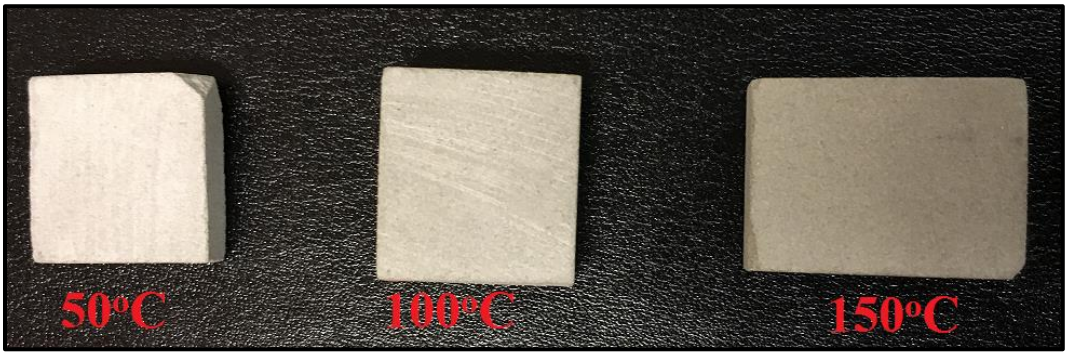

Figure 3.10 Samples treated to 50ºC,100ºC and 150ºC.

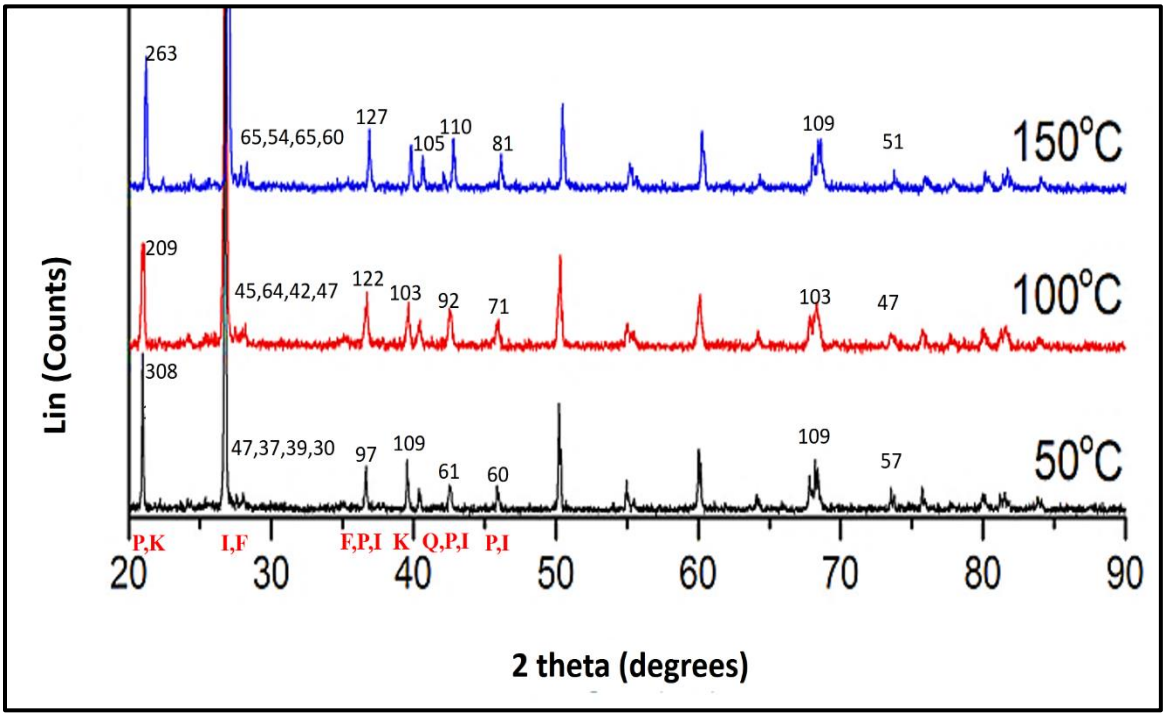

Figure 3.11 Thermal impacts on Kentucky sandstone XRD patterns, Quartz (Q), Kaolinite (K), Illite (I), Potassium feldspar (F) and Plagioclase (P).

Table 3.2 Isotherms model parameters fitting at 50°C, 100°C and 150°C for Langmuir, Freundlich and BET isotherms.

Gas		Langmuir				Freundlich				BET				
	Temperature (°C)	Q_l	k_l	R^2	SSE	k_f	n	R^2	SSE	Q_m	k_b	P_s	R^2	SSE
100% CH_4	50	13	0.035	0.980	8.743	0.089	1.466	0.996	2.648	76.666	0.539	138.164	0.998	1.944
	100	7	0.020	0.905	5.666	0.008	1.874	0.999	0.186	40	0.240	108.000	0.996	0.987
	150	85	0.028	0.930	27.277	0.678	1.329	0.997	66.780	120	1.554	109.940	0.995	107.528
10% CO_2/CH_4	50	22	0.040	0.931	6.517	0.385	1.185	0.998	2.087	63	1.335	141.505	0.999	2.087
	100	12	0.014	0.913	148.154	0.010	1.931	0.999	0.307	34	0.330	93.320	0.996	1.280
	150	90	0.040	0.925	5.318	1.432	1.205	0.999	15.561	250	1.500	150.000	0.999	3.797
100% CO_2	50	86	0.039	0.899	65.549	0.618	1.386	0.994	89.110	87.792	1.939	88.700	0.999	3.691
	100	23	0.030	0.856	76.473	0.031	1.873	0.997	9.299	48.246	0.728	93.317	0.992	30.990
	150	250	0.040	0.896	171.814	1.862	1.425	0.998	579.530	672.974	0.969	116.163	0.999	2.823

4.4.3 Thermodynamics of adsorption on Sandstone

The thermodynamic parameters shown in equations (17) to (19) are used to quantify the free energy of adsorption, heat of adsorption and standard heat of adsorption [102]:

$$\Delta G^0_{ads} = -RT \ln K_c \tag{17}$$

$$\ln K_c = \frac{\Delta S^0_{ads}}{R} - \frac{\Delta H^0_{ads}}{RT} \tag{18}$$

$$K_c = \frac{q_e}{C^b_e} \tag{19}$$

Where R stands for the universal gas constant (8.314J/mol K). ΔG^0_{ads} is the Gibbs standard free energy, ΔS^0_{ads} is the standard entropy, ΔH^0_{ads} is the heat of adsorption and Kc is Freundlich constant. All thermodynamic parameters can be computed from Freundlich model by plotting $\ln K_c$ vs. 1/T in Kelvin and ΔH^0_{ads} can be calculated from the slope while ΔS^0_{ads} is obtained from the intercept. and q_e and C^b_e are the equilibrium values of gas adsorption (see Table 3.3 and Appendix B).

Table 3.3 Pure CH_4, pure CO_2 and 10% CO_2 heat of adsorption Arrhenius plot fitting parameters between 50°C and 100°C.

	100% CH_4	10% CO_2/CH_4	100% CO_2
Slope	5756.3	8955.3	7213.2
Intercept	-20.226	-26.668	-22.803
R^2	0.9999	0.9999	0.9999

The values of ΔG_{ads}, ΔH_{ads} and ΔS_{ads} are computed in Table 3.4.The negative values of ΔH_{ads} confirms the exothermic nature of CH_4 and CO_2 adsorption [103][104]. At 50 °C the value of ΔG_{ads} for pure carbon dioxide is five times less than of pure methane and two times less than of 10% CO_2 methane mixture underlining the CO_2 unprompted adsorption nature onto the rock [105]. As the temperature raised up to 100°C the positive values of ΔG_{ads} for the three gas systems (CO_2, CH_4 and 10% CO_2) increases demonstrating the un-

favored spontaneity at high temperatures because the adsorption energy becomes less than the thermal energy. Correspondingly, these results suggest that at most reservoir temperatures the Kentucky sandstone adsorption of carbon dioxide is much more preferred to methane, which can be attributed to the high selectivity of clay minerals toward capturing carbon dioxide [106], [107].

Table 3.4 Pure CO2, pure methane and 10% CO2 thermodynamic parameters with the adsorption temperature.

	100% CO_2		100% CH_4		10% CO_2/CH_4	
Temperature (^oC)	K_c	ΔG_{ads} (KJ/mol)	K_c	ΔG_{ads} (KJ/mol)	K_c	ΔG_{ads} (KJ/mol)
50	0.618	1.293	0.0896	6.483	0.385	2.566
100	0.0310	10.773	0.008	14.891	0.009	14.484
ΔH_{ads} (KJ/mol)	-59.974		-47.861		-74.4585	
ΔS_{ads} (J/mol. K)	-189.595		-168.168		-238.359	

The ΔH_{ads} negative range is because of the physical adsorption exothermic nature of CO_2 and CH_4 since the adsorption is taking place due to van der Waals force between the rock surface and the two gases [108], [109]. Besides, the reversibility of the Physisorption process is very useful in EGR where we need to extract all the adsorbed methane by injecting carbon dioxide.

4.5 Conclusion

The results of the experimental studies showed that CO_2 content in the natural gas has a great effect on natural gas adsorption/desorption isotherms on tight Kentucky sandstone rock for all studied temperatures. As the CO_2 content increases more CO_2 will be adsorbed when competing with methane the desorption isotherm model for the natural gas. Also, the high affinity of the Kentucky sandstone toward CO_2 triggers the possibility to use CO_2 in EGR applications preferably in low to mid-range temperature reservoirs.

The tight sandstone mineralogy has also affected the desorption behavior of the natural gas. The thermal decomposing study shown that the presence of water bearing clay minerals such as Illite exhibited a vast sensitivity to temperature causing damage to crystal structure and expulsion of bounded water which resulted in huge increase in the adsorption uptake. Langmuir isotherm does not represent the adsorption on Kentucky sandstone while BET and Freundlich fits the experimental data.

CHAPTER 4

ADSORPTION/DESORPTION OF CO_2/CH_4 BY SHALE ROCKS

5.1 Summary

Adsorption of CH_4 and CO_2 on two shales (SH1 and SH2) from Saudi Arabia Qusaiba field was studied. The temperature changes have projected a tremendous effect on the desorption process of the natural gas. The results of the experimental studies showed that the CO_2 content in the natural gas has a big effect on the desorption of the natural gas from the two shale rocks. Increasing CO_2 fraction in the mixture from 0% to 10% CO_2 the total maximum gas uptake on SH1 is increased to approximately 24%, 26% and 31% at 50^{o}C, 100^{o}C and 150^{o}C respectively which reflects the high shale attraction toward CO_2. Furthermore, increasing the temperature from 50^{o}C to 100^{o}C tremendously increased the uptake on SH1 by 820%, 650% and 840% for CH_4, CO_2 and 10% CO_2 respectively at 44 bar. Nevertheless, SH2 exhibited very different behavior with temperature and gas composition; there was no CH4 adsorption at 50^{o}C and it increase slightly after increasing temperature to 16 mg/g at 100^{o}C and further increased to 145 mg/g at 150^{o}C. at 50^{o}C and 100^{o}C the CO_2 adsorption on SH2 was the approximately same value of 85 mg/g and increased to 555 mg/g at 150^{o}C and 44 bar. The TOC and shale mineralogy affected the adsorption behavior of CO_2 and CH_4 on SH1 and SH2. The presence of water bearing clay minerals which are sensitivity

to temperature causing damage to crystal structure which resulted in huge increase in the adsorption uptake.

5.2 Introduction

Due to the complexity of shale gas reservoirs gas is stored as both free gas in the pores and fractures, and adsorbed gas adhered to the mineral and organic matter (Kerogen) which greatly complicates the simulation of gas production. In these ultra-low permeability shale gas reservoirs, the gas is produced mainly by two mechanisms. Firstly, from the fractures where the production rate declined quickly as gas produced depending on the reservoir properties. Secondly, gas desorption which is characterized by less decline rate. However, the existing models used desorption isotherms from the literature and they neglected the effect of rock type and reservoir conditions on the gas desorption.

Natural gas present a key power choice due to its fuel efficiency and cleanness when compared with other petroleum and coal products. Natural gas consumption projected by EIA will reach 3.4 trillion cubic meters in 2040. Unconventional tight gas resources will account for more than 20% of Natural gas production in the next two decades [56].

The high complexity of shale gas reservoirs in terms of mineralogical composition, ultra-low permeability and deprived petrophysical properties poses a great challenge in natural gas production analysis [111]. Furthermore, the diagenesis processes frequently alter the original pore structure which can diminish the pore throat typical diameter increasing the tortuosity and number of isolated pores [112]. Common formation evaluation practices often come short in providing satisfactory outcomes. Without advance drilling methods and gas recovery techniques the production from shale gas is marginal [113]. The most

feasible economical way to produce natural gas from shale is fracturing methods especially multi-stage hydraulic fracturing [114].

The simulation of the gas flow in shale gas reservoir is a very complicated process [115], [131]–[134]. Several mechanisms contributed to the natural gas production from shale gas reservoirs. One of the main mechanisms is gas desorption from the rock surface to the pore body. The existing models did not consider the effect of CO_2 content in the natural gas on the gas desorption from the rock. Also, the current models [115]–[119] used desorption models from the literature and they neglect the sorption and the effect of rock type and reservoir conditions on the gas desorption.

5.3 Experimental setup and procedure

Measuring the gas adsorption/desorption on the surface of rocks is often conducted using volumetric based or gravimeteric approaches [83]. In general, gravimeteric methods involve using a sensitive microbalance to quantify the variation in the sample weight related to the adsorption under controlled pressure and temperature[84]. These gravimeteric methods are extremely accurate and can be conducted using small size samples [85]. Whereas volumetric methods are conducted by allowing the pressure to expand from a reference cell to a measuring cell and record the change in pressure which will be related to gas adsorption. Although they are faster and permit the use of large sample volumes, but they lack the accuracy of gravimeteric methods [55]. Figure 1.6 shows a diagram of the setup used to conduct the adsorption experiment using (Rubotherm^{TM}) magnetic suspension balance which proofed to efficient elsewhere [85], [120]–[123]. In contrast with customary balances, the magnetic suspension balance is not directly associated with testing sample which is suspended by a suspension magnet. the suspension

magnet system comprises of a permanent magnet, measuring load and a sensor core. then Control frameworks maintain the electric magnet in free suspension and transmit the measured weight to the outer balance [84].

The measurements started with calibrating the measured weight of the intact cubic sample while heating the sample to 50^{o}C under vacuum for 1 hour which was sufficient to remove any adsorbed air and until a constant mass is attained. Then a Helium buoyancy experiment was conducted using (Rubotherm^{TM}) magnetic suspension balance at constant temperature of 50^{o}C and through eight pressurizing stages to a maximum pressure of 50 bars. At these low pressure and temperature, we can assume only buoyancy occurs and the helium adsorption is negligible [55], [84], [86]. A blank and a buoyancy measurements has been adopted for every testing temperature to correct the sample apparent weight because of gas density and the weight of the sample holder. One segment of the helium buoyancy measurement at 100^{o}C is shown in Appendix C. Then the pressure and temperature absolute isotherm of adsorption is obtained after correcting the weight to accommodate the apparent weight loss caused by the buoyancy experiment and eliminate the sample holder effect [87]. Furthermore, the CH_4 adsorption isotherm is measured by recording the measured weight of the sample under constant temperature of 50^{o}C through eight pressure set points up to 50 bars Figure 4.3. After that we investigated the effect of temperature covering 100^{o}C and 150^{o}C respectively. The same experimental procedures were carried out for pure CO_2 and 10% CO_2 - 90% CH_4 mixture at the three measurements temperatures. The pyrolysis of the shale samples has been conducted at King Fahd University Research institute to obtain the Geomechanically data and TOC [135].

5.4 Results and discussion

5.4.1 Characterization of Shale

Two shale samples from Saudi Arabia SH1 and SH2 are used in the adsorption study. The shale sample mineralogy from XRD and thermal pyrolysis is shown in Table 4.1. the main differences between the two shales is TOC and total clays for their high surface area compared to other constituents.

Table 4.1 Mineralogy & Geochemical Data of Shale.

	Sample Type		Surface	
	Sample ID		SH1	SH2
Organic Geochemical Data	S1	mg/g	0.08	0.91
	S2	mg/g	4.23	9.78
	Tmax	°C	419	417
	S3	mg/g	1.91	4.09
	TOC	%	3.16	6.10
	HI		134	160
	OI		60.00	67.00
Inorganic Geochemical Data	Total Clays	%	39.00	54.00
	Calcite	%	1	2
	Dolomite	%	1.00	1.00
	Quartz	%	31.00	24.00
	K-spar	%	18	8
	Pyrite	%	10.00	0.91

Figure 4.1 shows SEM image of rock surface. The red letters point some of the locations of clay on the surface while the completely black sites are pores. It also shows a randomly-oriented mica sheets (MC), filling the space between quartz detrital grain and created micro-porosity with few microns wide (P). Few scattered organic particles are also encountered (O).

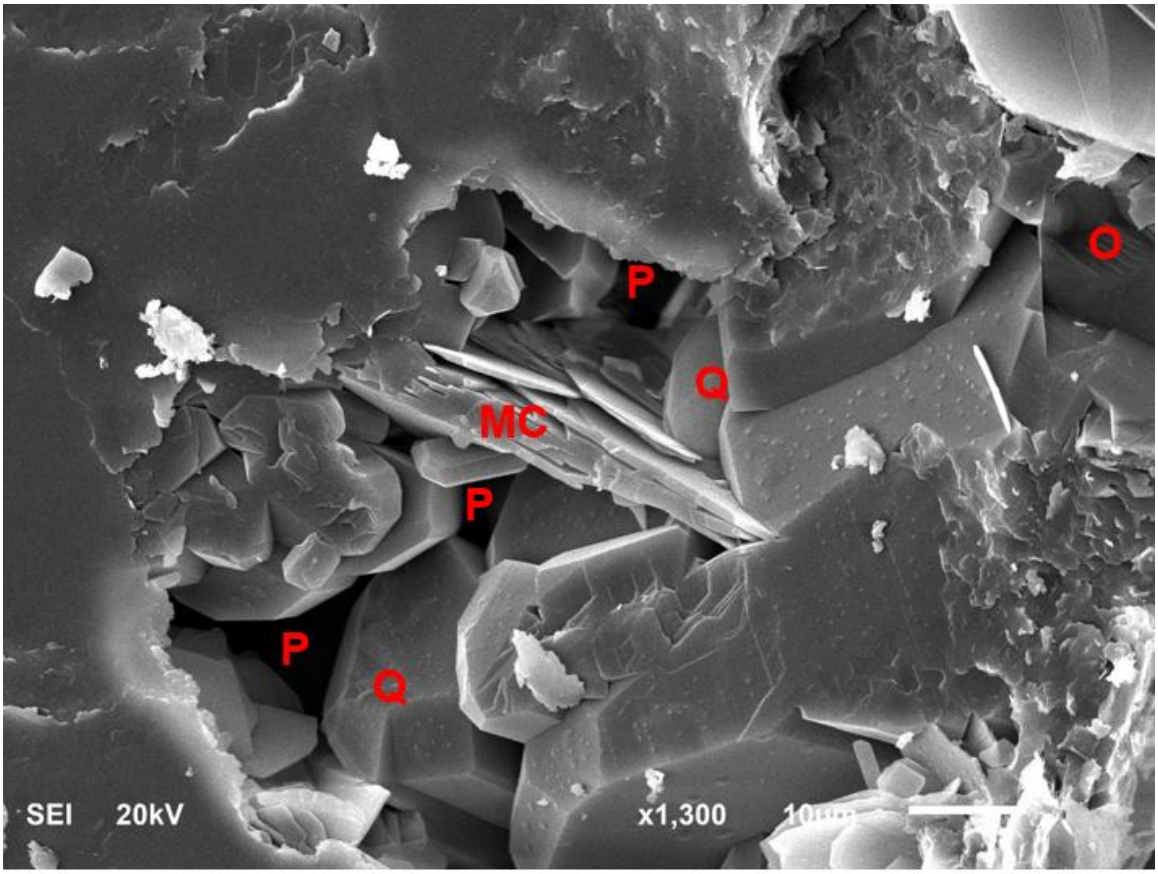

Figure 4.1 SEM photo of SH1 Shale.

Figure 4.2 SEM photo shows some of the constituent minerals of SH2 shale; Clay flakes with preferred horizontal orientation (C); Mica platelets (M) in addition to euhedral pyrite crystal (Py) which is masked with organic matter (O).

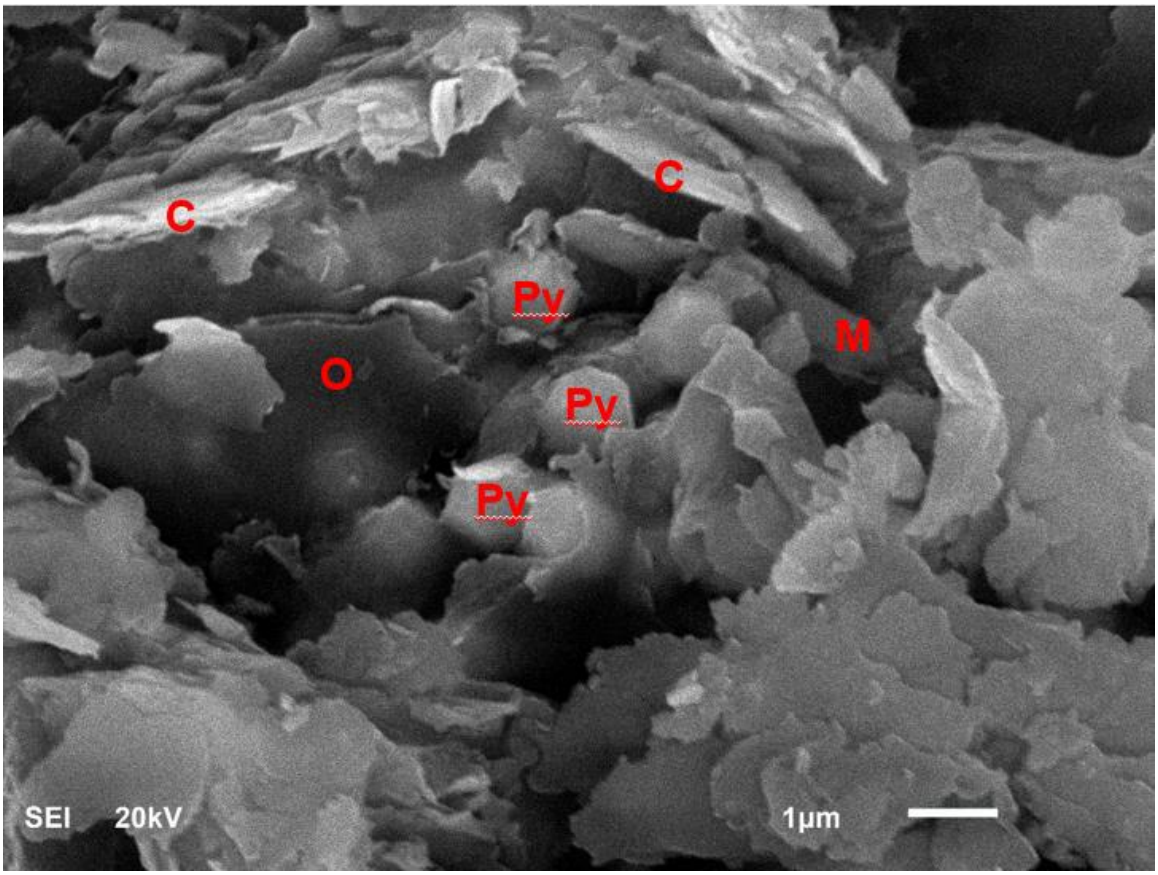

Figure 4.2 SEM photo of SH2 Shale.

5.4.2 Adsorption of CH_4 and CO_2

Determining the actual adsorption capacity of methane and carbon dioxide for different rocks is extremely important for comprehending the CO_2 storage and methane desorption processes [88]. The sorption phenomenon exists when the gas is attached to the surface of the substance and held into its pores physically or chemically. The physical sorption is due to Vander Walls forces and electrostatic forces, and the chemical sorption is caused by strong chemical bonds [13]. This adsorption process is directly proportional to the pressure of the free gas; increasing the pressure increases the adsorption process. On the other hand, decreasing the pressure in the desorption process decreases the adsorbed gas [14]. Furthermore, the maximum volume of adsorbed gas is usually determined by the sorption

isotherm which represents the equilibrium volume of the gas adsorbed on substance surface at isothermal conditions [15].

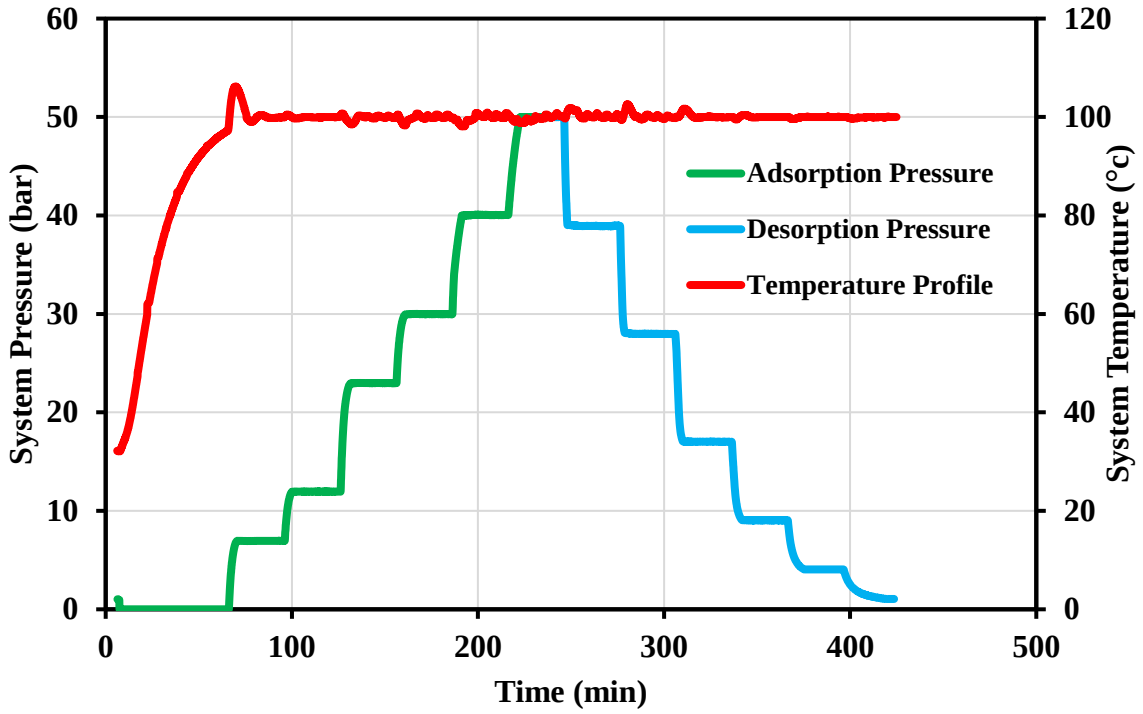

Figure 4.3 Pressure and temperature profiles through the adsorption/desorption on SH1 measurement for CH_4 at 100°C and various pressure set points.

Adsorption isotherms are generally utilized to describe adsorption characteristics of gases on the rock surface and as input parameters to model the gas flow and transport in porous media. Lacking the appropriate expression of the adsorption data can lead to severe errors in the transport modeling process [25]. Simple models such as Langmuir and Freundlich isotherms are widely used to fit and define the adsorption data, but they frequently lack the accuracy and more sophisticated complex models are applied [26]. Because the isotherm models are based on the idea of adsorption behavior at constant temperature (reservoir temperature) with different pressures (average reservoir pressure) which is the case in gas reservoirs since they often stay in the same temperature during the depletion phase for most of the reservoir life.

Langmuir is a monolayer model of equilibrium on the surface of the rock given by [10]:

$$q = \frac{Q_l k_l p}{1 + k_l p} \tag{20}$$

Where Q_l (mg/g) is the maximum mass of gas adsorbed per unit mass to cover the complete monolayer and k_l is the Langmuir constant of equilibrium (1/mg). The Freundlich isotherm is given by [29]:

$$q = k_f p^n \tag{21}$$

Where k_f and n are constants. The BET isotherm describes the multilayer adsorption on the surface of the rock [11]:

$$q = \frac{Q_m k_b p}{(p_s - p)[1 + (k_b - 1)\frac{p}{p_s}} \tag{22}$$

The Langmuir model includes three different types of isotherms; the Langmuir, the Freundlich, and the mixture of both Langmuir and Freundlich isotherms [16]. Langmuir isotherm is being widely used in the literature to define the adsorption process [19] and the competitive adsorption process [20].

The maximum amount of pure methane adsorbed by the shale SH1 at 50°C and a pressure of 45 bar shown in Figure 4.4 is 19.19 mg/g which is significantly less than the maximum adsorbed carbon dioxide amount 89.23 mg/g in Figure 4.6 which gives an indication of the high desirability of the rock for capturing carbon dioxide molecules [90]. Correspondingly, increasing CO_2 percentage in pure methane to 10% in the mixture the uptake increased to more than 23.97 mg/g (Figure 4.5) and that confirms the high selectivity of shale toward CO_2 in the mixture which will lead to higher methane recapture and less CO_2 recovery. When the temperature increased to 100°C the adsorption isotherms for methane, carbon dioxide and 10%CO_2 mixture exhibited an abnormal Physisorption behavior i.e. adsorption

uptake amount increased proportionally with increasing the temperature. However, increasing the temperature to 150^{o}C resulted in reverse behavior for all the three gases and the uptake for CH_4 decreased to 80.01 mg/g, for CO_2 196.82 mg/g and for 10% carbon dioxide was 70.02 mg/g. This behavior type of desirable increasing in storage with elevating temperature has been reported for some rock types at high pressures when the temperature effect reversed which allows more gas to be accommodated depending on the porosity of formation [125].

The study of temperature effect on the adsorption capacity of SH1 yielded an adsorption increasing after raising the measurement temperature from 50^{o}C to 100^{o}C under all pressure set points. At a 44 bar pressure the growth in adsorption was 19.19 mg/g to 158.86 mg/g for pure methane, 89.23 mg/g to 584.36 mg/g for pure carbon dioxide and 23.96 mg/g to 201.10 for 10% carbon dioxide - 90% methane mixture. However, after elevating the temperature to 150^{o}C under a pressure of 44 bar the uptake fell to lower value for all the tested three gas systems; 80.01 mg/g for pure CH_4, 315.67 mg/g for pure CO_2 and 105.04 mg/g for 10% CO_2 which are extremely superior than uptake at 50^{o}C. This alteration in adsorption behavior is associated to the considerable amount of TOC between the crystals and loosely bounded interlayer water and thermal induced structural slight decomposition changes to the crystals of the clay minerals and kerogen which guides the sample to an endothermic section on high temperatures [127]–[129]. Nevertheless, SH2 exhibited very different behavior with temperature and gas composition; there was no CH_4 adsorption at 50^{o}C due to poor access to surface of intact rock sample due to the high TOC. The adsorption increased after increasing temperature to 16 mg/g at 100^{o}C and further increased to 145 mg/g at 150^{o}C. at 50^{o}C and 100^{o}C the CO_2 adsorption on SH2 was the approximately

same value of 85 mg/g and increased to 555 mg/g at 150°C and 44 bar. Furthermore, increasing CO_2 percentage enhanced the adsorption for SH1 and SH2 at all temperatures. High TOC shale SH2 high increase in adsorption at 150°C can be attributed to degradation of organic matter at high temperatures opens access to previously blocked nanopores uncovering more surface area, and confirms the high adsorption potential of matured and over matured kerogens [136]–[138].

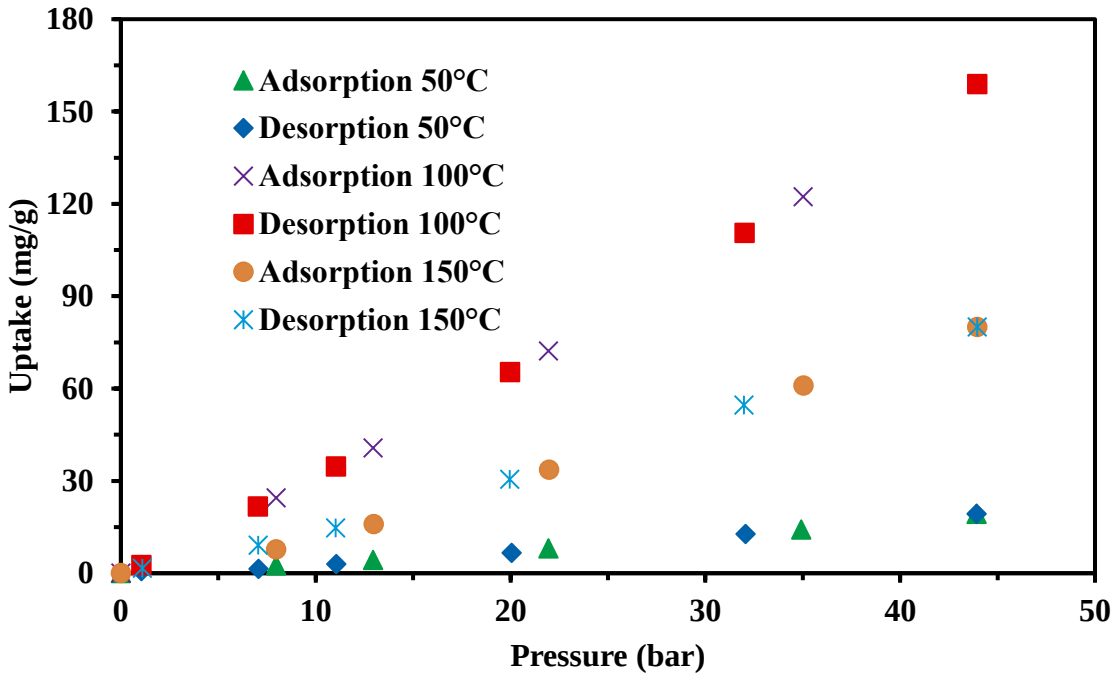

Figure 4.4 Effect of temperature on adsorption of CH_4 by SH1

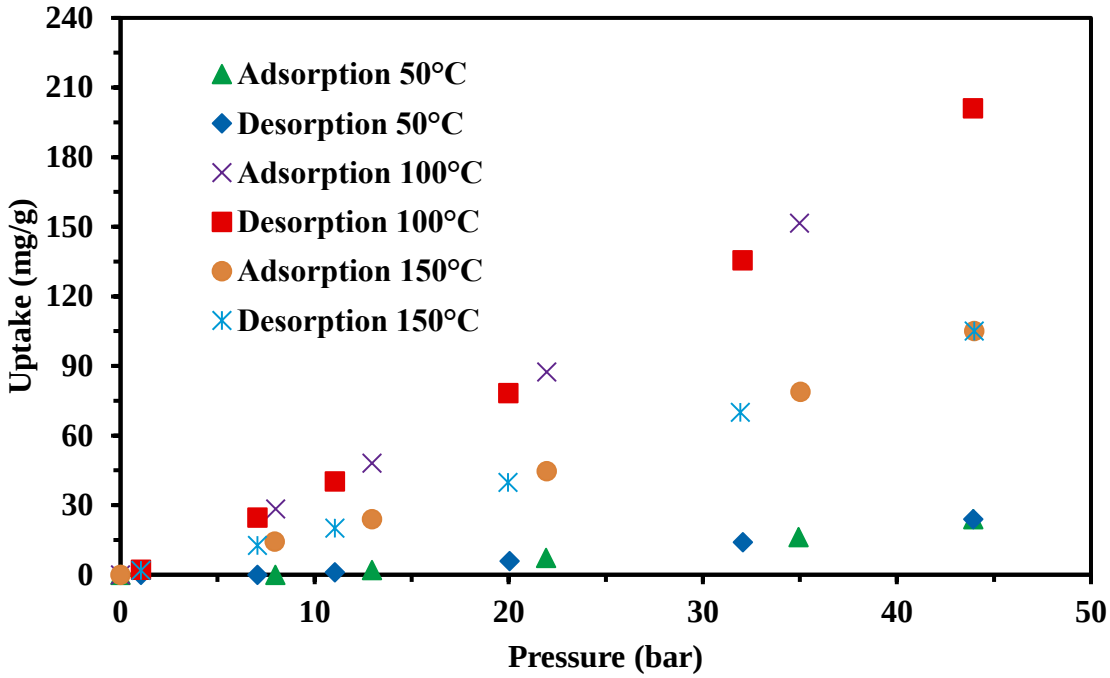

Figure 4.5 Effect of temperature on adsorption of 10% CO_2 by SH1

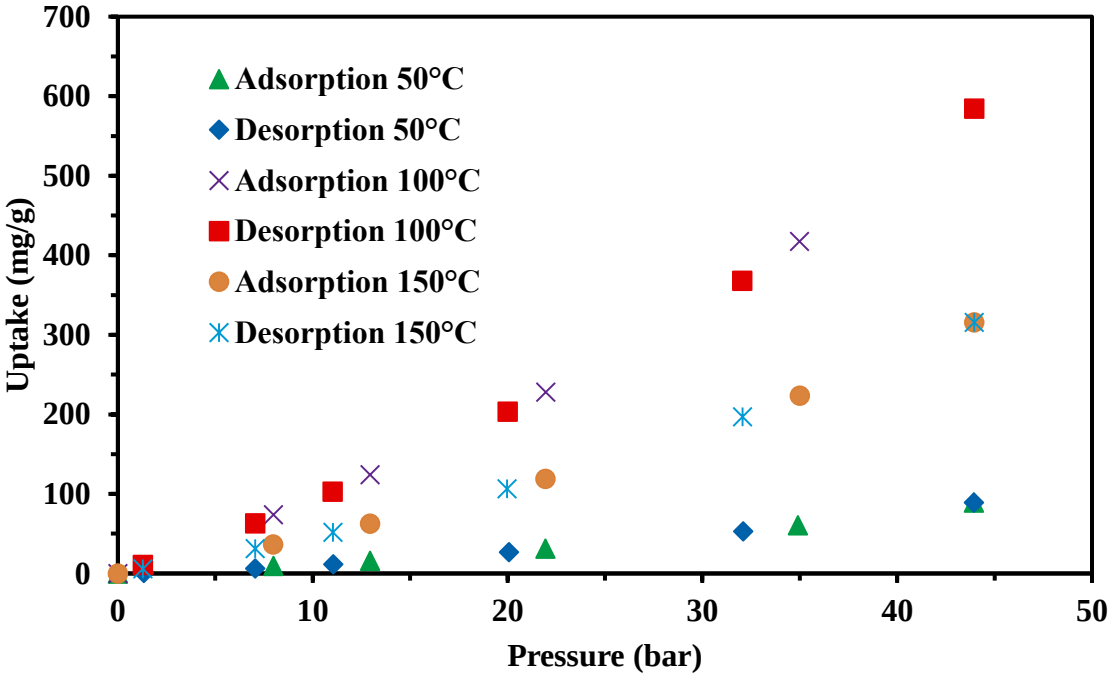

Figure 4.6 Effect of temperature on adsorption of CO_2 by SH1

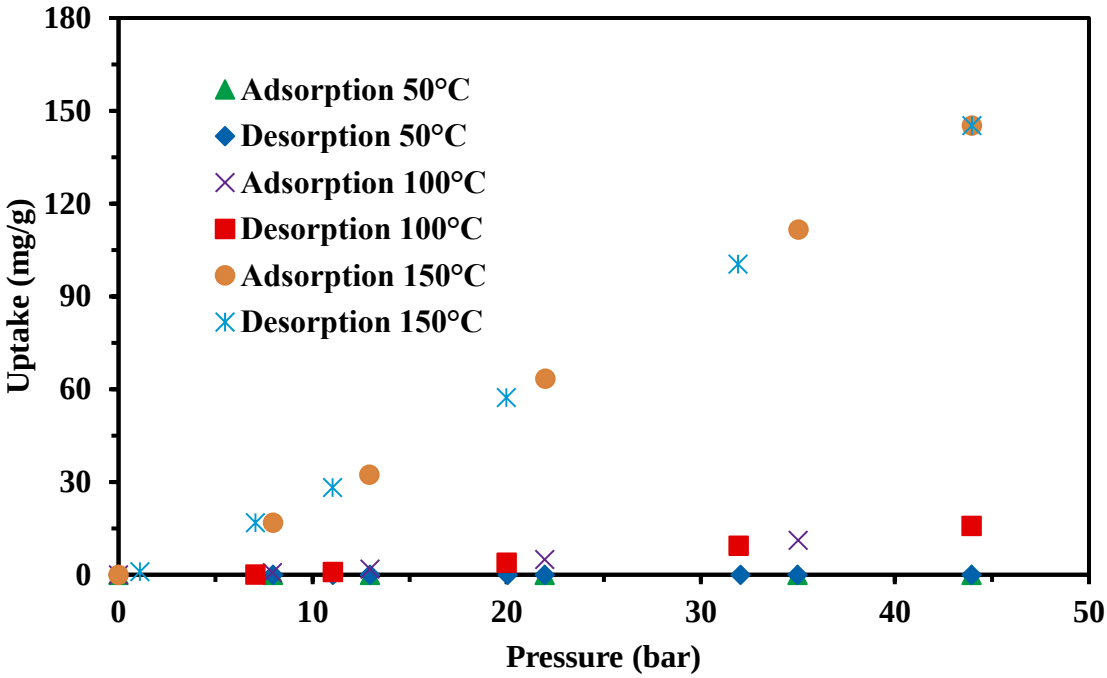

Figure 4.7 Effect of temperature on adsorption of CH_4 by SH2

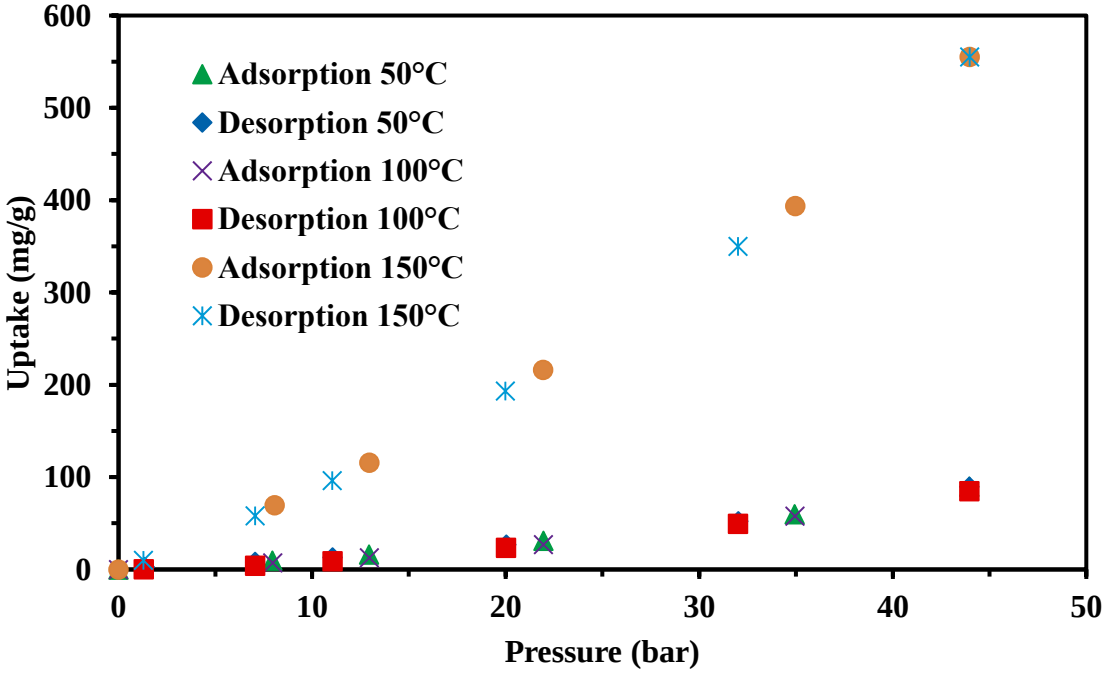

Figure 4.8 Effect of temperature on adsorption of 10% CO_2 by SH2

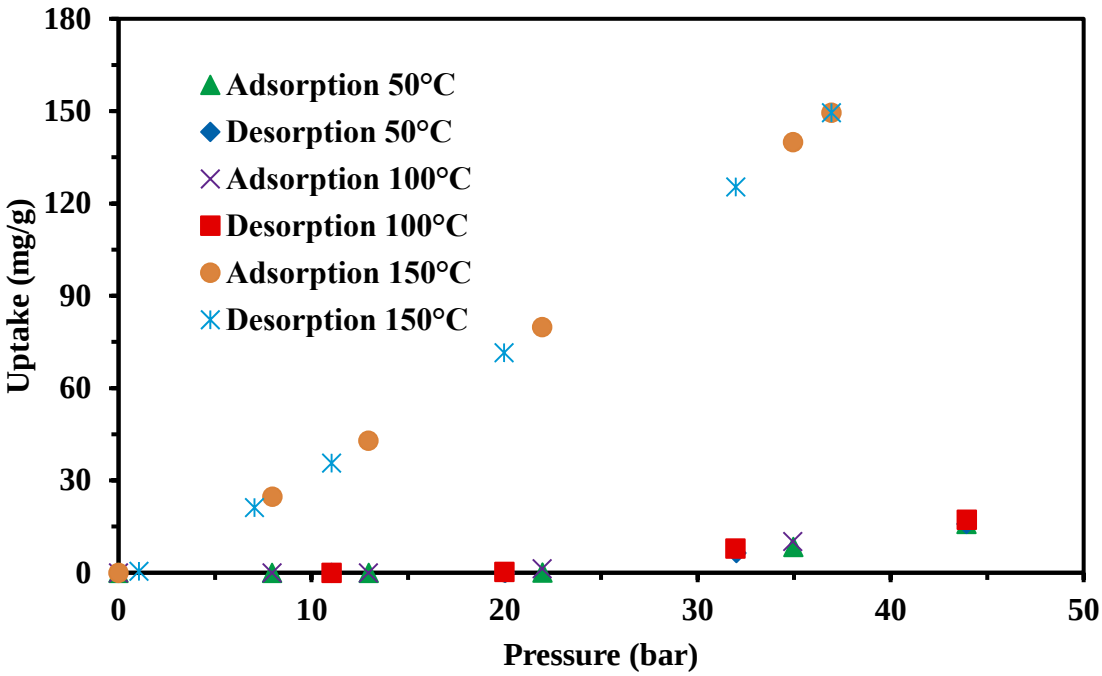

Figure 4.9 Effect of temperature on adsorption of CO_2 by SH2

Figure 4.10-Figure 4.15 illustrate the adsorption of CO_2, CH_4 and 10%CO_2/CH_4 on SH1 and SH2 fitting results to Langmuir, Freundlich and BET isotherms at 150^{o}C. The results confirm that Langmuir isotherm is not representing the experimental data except at low pressures, while Freundlich isotherm is the best fit and BET isotherm is more accurate than Langmuir. However, when fitting adsorption data the high R^2 value for an adsorption isotherm does not certainly imply that the fitted model is the best in representing the

experimental data [126]. Fitting results for 50°C, 100°C and 150°C are summarized in Table 4.2 and

Table **4.3** also see Appendix C.

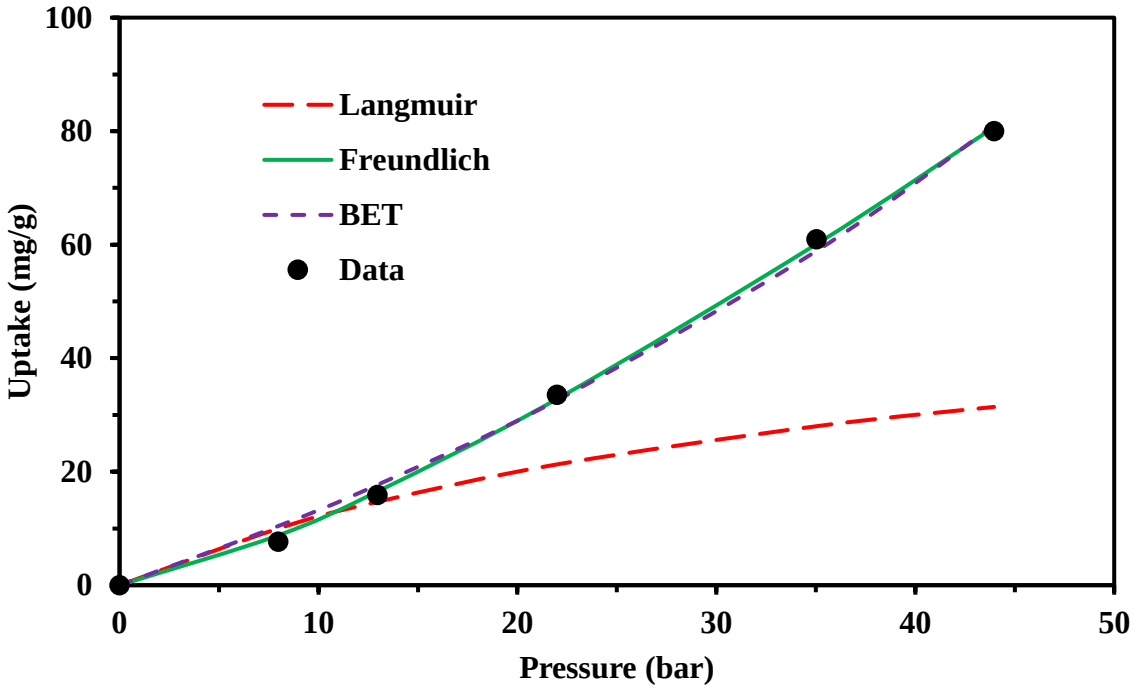

Figure 4.10 Fitting of CH_4 adsorption on SH1 at 150°C with Langmuir, Freundlich and BET.

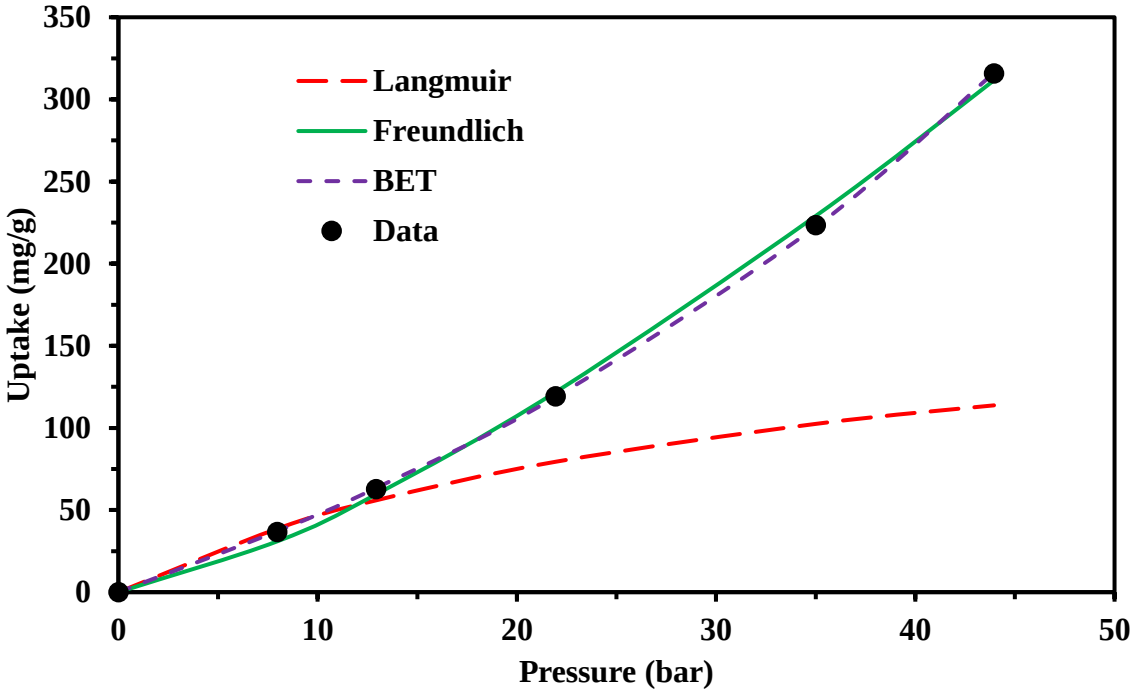

Figure 4.11 Fitting of CO_2 adsorption on SH1 at 150°C with Langmuir, Freundlich and BET.

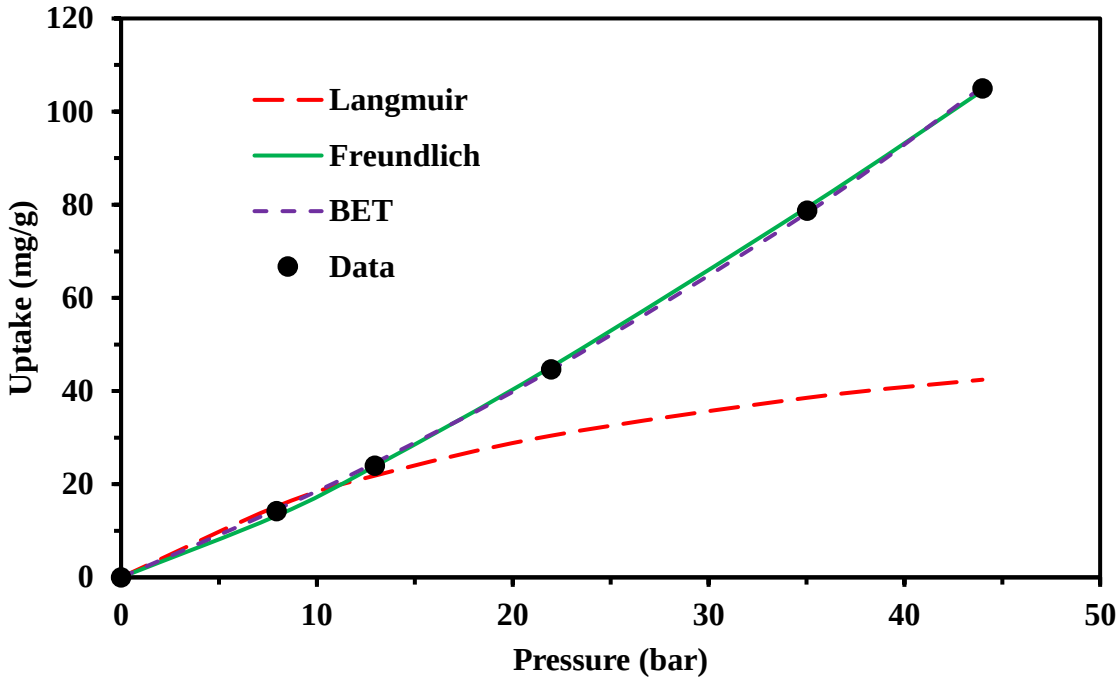

Figure 4.12 Fitting of 10% CO_2 adsorption on SH1 at 150°C with Langmuir, Freundlich and BET.

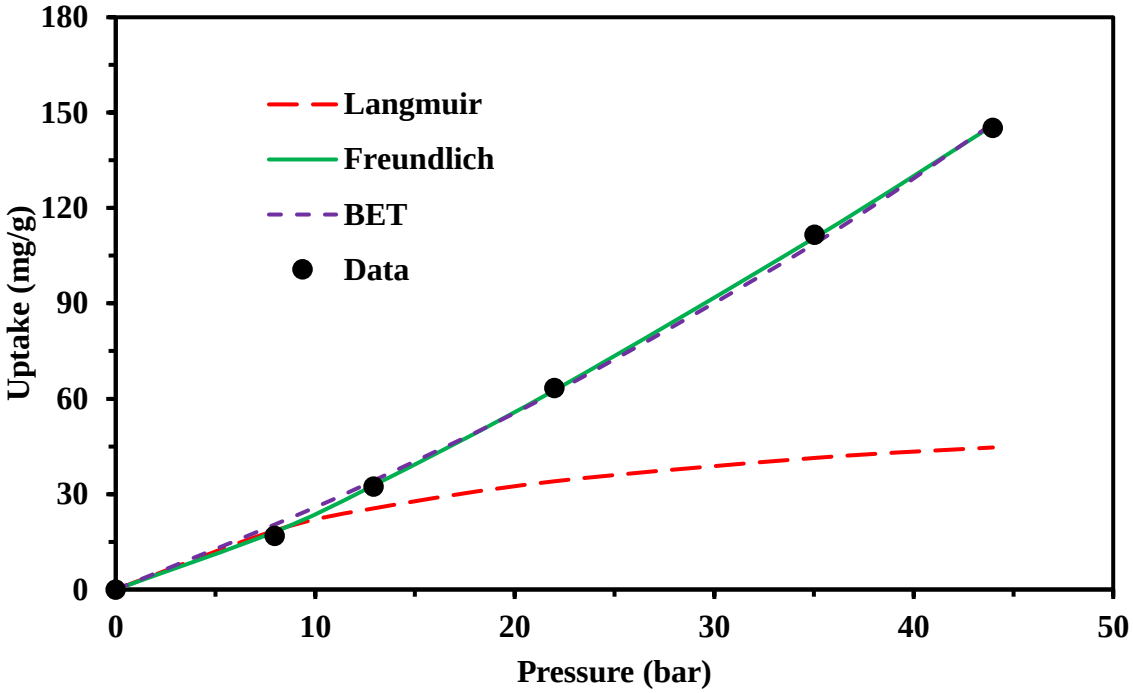

Figure 4.13 Fitting of CH_4 adsorption on SH2 at 150°C with Langmuir, Freundlich and BET.

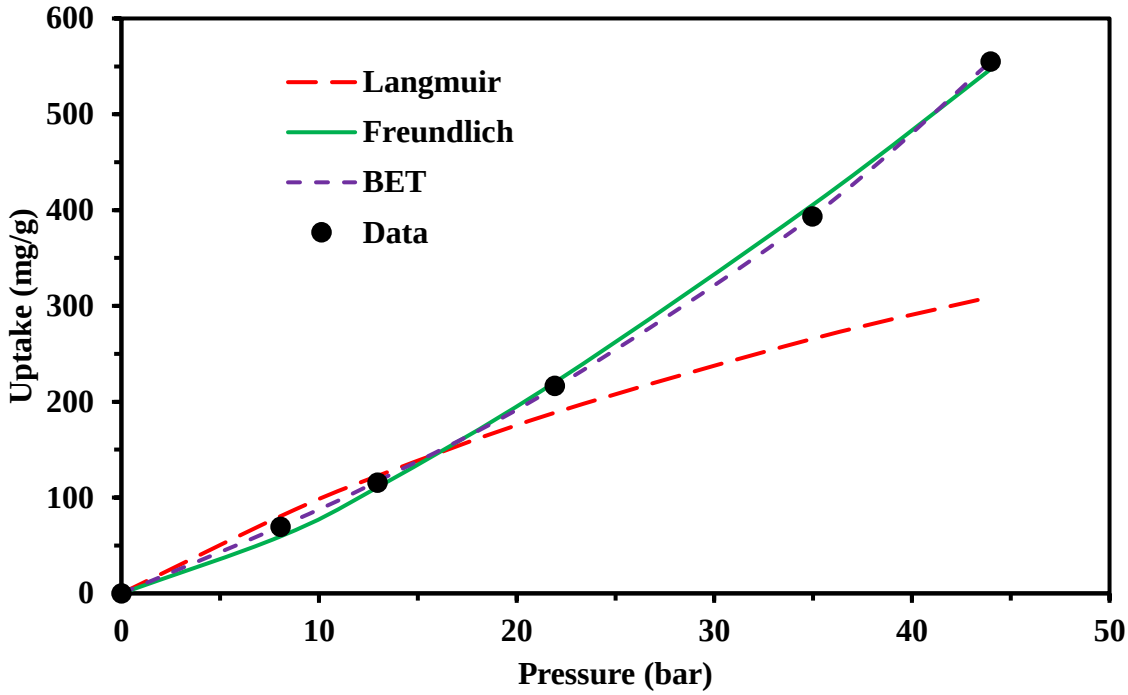

Figure 4.14 Fitting of CO_2 adsorption on SH2 at 150°C with Langmuir, Freundlich and BET.

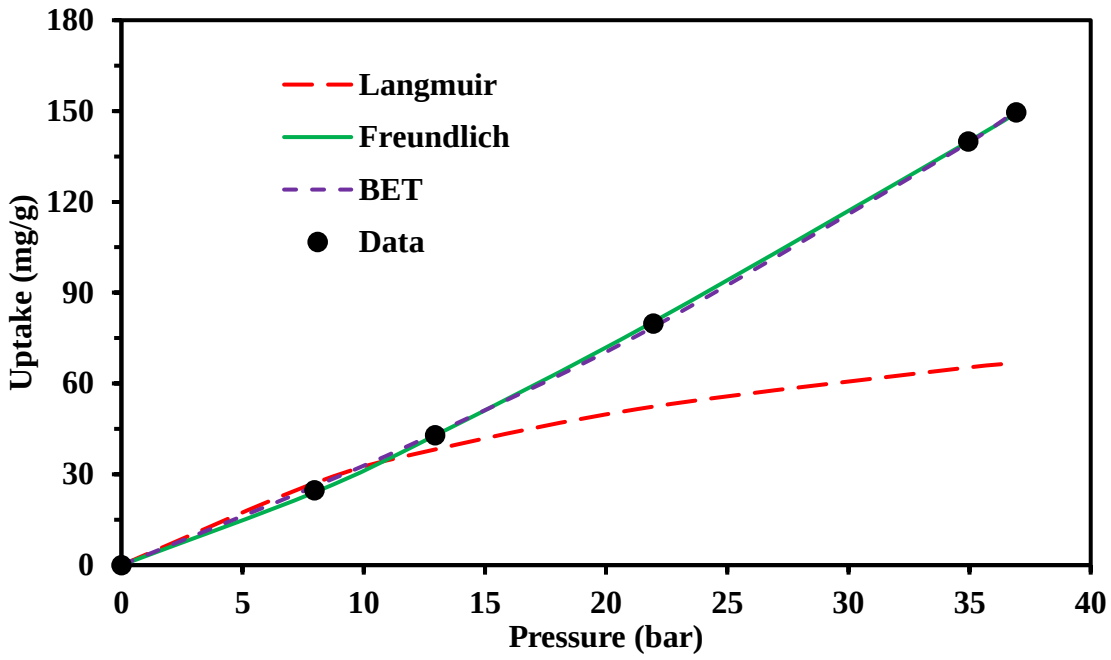

Figure 4.15 Fitting of 10% CO_2 adsorption on SH2 at 150°C with Langmuir, Freundlich and BET.

5.4.3 Thermodynamics of adsorption on shale

The thermodynamic parameters shown in equations (23) to (25) are used to quantify the free energy of adsorption, heat of adsorption and standard heat of adsorption [102]:

$$\Delta G^0_{ads} = -RT \ln K_c \tag{23}$$

$$\ln K_c = \frac{\Delta S^0_{ads}}{R} - \frac{\Delta H^0_{ads}}{RT} \tag{24}$$

$$K_c = \frac{q_e}{C_e^b} \tag{25}$$

Where R stands for the universal gas constant (8.314J/mol K). ΔG^0_{ads} is the Gibbs standard free energy, ΔS^0_{ads} is the standard entropy, ΔH^0_{ads} is the heat of adsorption and K_c is Freundlich constant. All thermodynamic parameters can be computed from Freundlich model by plotting $\ln K_c$ vs. 1/T in Kelvin and ΔH^0_{ads} can be calculated from the slope while ΔS^0_{ads} is obtained from the intercept. and q_e and C_e^b are the equilibrium values of gas adsorption (see Table 4.4, Table 4.5 and Appendix C).

Table 4.2 Isotherms model parameters fitting for SH1 at 50°C, 100°C and 150°C for Langmuir, Freundlich and BET isotherms.

Gas		Langmuir				Freundlich				BET				
	Temperature (°C)	Q_l	k_l	R^2	SSE	k_f	n	R^2	SSE	Q_m	k_b	P_s	R^2	SSE
100% CH_4	50	10	0.05	0.9	7.86	0.179	1.234	0.999	0.102	87.436	0.649	186.318	0.999	0.019
	100	87	0.06	0.91	535.715	2.307	1.118	0.999	2.08	357.81	1.496	175.327	0.999	1.246
	150	60	0.025	0.95	157.341	0.592	1.299	0.99	3.352	340.186	0.775	151.86	0.998	17.334
10% CO_2/CH_4	50	11	0.02	0.908	152.442	0.0273	1.793	0.999	0.598	64.156	0.336	99.15	0.996	3.291
	100	120	0.046	0.923	2135	2.315	1.179	0.999	7.166	534.42	1.111	169.751	0.999	1.879
	150	70	0.035	0.939	5.613	1.083	1.208	0.999	1.947	237.669	1.128	151.846	0.999	1.411
100% CO_2	50	60	0.025	0.931	103.542	0.358	1.454	0.998	13.114	111.942	0.947	97.4	0.999	0.222
	100	350	0.04	0.918	4290	4.256	1.297	0.999	383.224	922.274	1.096	117.318	0.999	0.734
	150	200	0.03	0.931	48.538	1.866	1.353	0.999	96.819	562.568	0.895	116.8324	0.999	2.303

Table 4.3 Isotherms model parameters fitting for SH2 at 50°C, 100°C and 150°C for Langmuir, Freundlich and BET isotherms.

Gas		Langmuir				Freundlich				BET				
	Temperature (°C)	Q_l	k_l	R^2	SSE	k_f	n	R^2	SSE	Q_m	k_b	P_s	R^2	SSE
100% CH_4	50	0	0	-	-	0	0	-	-	0	0	0	-	-
	100	15	0.01	0.953	4.928	0.026	1.7	0.999	0.196	14.46	0.933	82.3	0.996	1.935
	150	65	0.05	0.913	912.67	1.441	1.221	0.999	3.978	468.194	0.909	174.569	0.999	28.154
10% CO_2/CH_4	50	1	0.02	0.802	299.597	0.0004	3.41	0.993	3.199	62	0.08	73	0.986	11.44
	100	25	0.004	0.9	235.239	0.007	2.033	0.989	10.063	119.596	0.044	74	0.988	7.791
	150	112	0.04	0.944	27.159	2.03	1.191	0.999	0.754	282.429	1.333	121.046	0.999	4.02
100% CO_2	50	60	0.025	0.929	99.733	0.358	1.454	0.998	19.44	11.942	0.947	97.4	0.999	0.426
	100	48	0.03	0.907	68.06	0.208	1.587	0.999	4.684	460.914	0.397	161.518	0.997	52.375
	150	302	0.045	0.907	137.632	3.89	1.307	0.999	340.915	707.774	1.239	107.251	0.999	3.914

Table 4.4 Pure CH_4, pure CO_2 and 10% CO_2 heat of adsorption on SH1 Arrhenius plot fitting parameters between 100°C and 150°C.

	100% CH_4	10% CO_2/CH_4	100% CO_2
Slope	-4297.816	-2399.559	-2603.328
Intercept	-10.682	-5.591	-5.528
R2	0.999	0.999	0.999

Table 4.5 Pure CH_4, pure CO_2 and 10% CO_2 heat of adsorption on SH2 Arrhenius plot fitting parameters between 100°C and 150°C.

	100% CH_4	10% CO_2/CH_4	100% CO_2
Slope	12729	17792	9255.7
Intercept	30.446	42.754	23.232
R2	0.999	0.999	0.999

The values of ΔG_{ads}, ΔH_{ads} and ΔS_{ads} for SH1 are computed in Table 4.6. The negative values of ΔH_{ads} confirms the exothermic nature of CH_4 and CO_2 adsorption [103][104]. At 100°C the value of ΔG_{ads} for pure carbon dioxide is 200% less than of pure methane and less than of 10% CO_2 methane mixture underlining the CO_2 unprompted adsorption nature onto the rock [105]. As the temperature raised up to 150°C the positive values of ΔG_{ads} for the three gas systems (CO_2, CH_4 and 10% CO_2) increases demonstrating the un-favored spontaneity at high temperatures because the adsorption energy becomes less than the thermal energy. Correspondingly, these results suggest that at most reservoir temperatures the shale adsorption of carbon dioxide is much more preferred to methane, which can be attributed to the high selectivity of clay minerals toward capturing carbon dioxide [106], [107]. The ΔH_{ads} negative range is because of the physical adsorption exothermic nature of CO_2 and CH_4 since the adsorption is taking place due to van der Waals force between the rock surface and the two gases [108], [109]. Besides, the reversibility of Physisorption

Table 4.6 Pure CO_2, pure methane and 10% CO_2 thermodynamic parameters with the adsorption temperature for SH1.

	Pure CO_2		Pure CH_4		10% CO_2	
Temperature (^oC)	K_c	ΔG_{ads} (KJ/mol)	K_c	ΔG_{ads} (KJ/mol)	K_c	ΔG_{ads} (KJ/mol)
100	4.256	-4.494	2.307	0.836	2.315	0.839
150	1.866	-2.196	0.592	-0.525	1.083	0.080
ΔH_{ads} (KJ/mol)	-21.645		-35.734		-19.951	
ΔS_{ads} (J/mol. K)	-45.964		-88.815		-46.487	

process is very useful in EGR where we need to extract all the adsorbed methane by injecting carbon dioxide. Table 4.7 summarizes the values of ΔG_{ads}, ΔH_{ads} and ΔS_{ads} for SH2. As the temperature increased, the ΔG_{ads} decreased indicating favorable adsorption at high temperature and the favorability increases with increasing CO_2 percent in the gas. The high positive values of ΔH_{ads} highlights and endothermic nature of Chemisorption and the positive ΔG_{ads} indicates the high randomness of the system.

Table 4.7 Pure CO_2, pure methane and 10% CO_2 thermodynamic parameters with the adsorption temperature for SH2.

	Pure CO_2		Pure CH_4		10% CO_2	
Temperature (^oC)	K_c	ΔG_{ads} (KJ/mol)	K_c	ΔG_{ads} (KJ/mol)	K_c	ΔG_{ads} (KJ/mol)
100	0.208	4.878	0.026	11.371	0.007	15.283
150	3.890	-4.78	1.441	-1.287	2.030	-2.491
ΔH_{ads} (KJ/mol)	76.956		105.834		147.931	
ΔS_{ads} (J/mol. K)	193.162		253.142		355.476	

5.5 Conclusion

The results of the experimental studies showed that CO_2 content in the natural gas has a great effect on natural gas adsorption/desorption isotherms on SH1 and SH2 shales rock for all studied temperatures. As the CO_2 content increases more CO_2 will be adsorbed when competing with methane the desorption isotherm model for the natural gas. Also, the high affinity of the shale toward CO_2 triggers the possibility to use CO_2 in EGR applications preferably in low to mid-range temperature reservoirs. The shale TOC and mineralogy has also affected the desorption behavior of the natural gas and as TOC increases the adsorption at low temperature decreases due to the restriction of organic matter to nanopores. The thermal decomposing study on shale showed that the presence organic matter and clay minerals such exhibited a vast sensitivity to temperature causing alterations in adsorption behavior due to crystal structure changes which resulted in huge increase in the adsorption uptake at 150^{o}C in SH2 shale and 100^{o}C in SH1. Shale rocks from the same field adsorption properties are different and comprehensive testing is required to quantify the adsorption behavior due to the heterogeneity of shale. Langmuir isotherm does not describe the adsorption behavior of the studied shales.

CHAPTER 5

CONCLUSION

The adsorption/desorption behavior of CO_2 and CH_4 and their mixture was investigated on different reservoir rock types including; carbonate, tight sandstone and shale at different temperatures. The experiments were conducted using intact cube rock samples of Pink Desert limestone, Kentucky tight sandstone and two Qusaiba shales SH1 and SH2 at 50^{o}C, 100^{o}C and 150^{o}C.The CO_2 adsorption on the studied rocks was approximately 4-5 times higher than of CH_4 and as CO_2 percentage increased in the mixture the adsorption of the gas increased at all tested temperatures. The adsorption behavior on limestone was exothermic physisorption i.e. adsorption decreases as the temperature increases. However, the adsorption on tight sandstone was exothermic from 50-100^{o}C and increased tremendously at 150^{o}C due to changes of crystallinity and expulsion of bounded water from clay minerals. The adsorption on shale was different on the two studied samples; on SH1 shale which has low TOC the adsorption from 50-100^{o}C was endothermic due to the high temperature degradation of organic matter covering the nanopores and from 100-150^{o}C was exothermic physisorption. The adsorption on SH2 shale which has high TOC was endothermic i.e. adsorption increases as temperature increases. Adsorption isotherms analysis concluded that Langmuir isotherm does not represent the adsorption behavior of the studied rocks at different temperatures and using Freundlich or BET is more representative.

REFERENCES

[1] T. Ertekin, G. A. King, and F. C. Schwerer, “Dynamic Gas Slippage: A Unique Dual-Mechanism Approach to the Flow of Gas in Tight Formations,” *SPE Form. Eval.*, vol. 1, no. 1, pp. 43–52, Apr. 1986.

[2] L. J. Klinkenberg, “The Permeability Of Porous Media To Liquids And Gases,” *Drilling and Production Practice*. American Petroleum Institute, 01-Jan-1941.

[3] C. R. Clarkson, M. Nobakht, D. Kaviani, and T. Ertekin, “Production Analysis of Tight Gas and Shale Gas Reservoirs Using the Dynamic-Slippage Concept,” in *North American Unconventional Gas Conference and Exhibition*, 2011.

[4] F. O. Jones and W. W. Owens, “A Laboratory Study of Low-Permeability Gas Sands,” *J. Pet. Technol.*, vol. 32, no. 9, pp. 1631–1640, Apr. 1980.

[5] E. Ozkan, R. S. Raghavan, and O. G. Apaydin, “Modeling of Fluid Transfer From Shale Matrix to Fracture Network,” in *SPE Annual Technical Conference and Exhibition*, 2010.

[6] F. Javadpour, “Nanopores and apparent permeability of gas flow in mudrocks (shales and siltstone),” *J. Can. Pet. Technol.*, vol. 48, no. 8, pp. 16–21, 2009.

[7] G. R. L. Chalmers and R. M. Bustin, “The organic matter distribution and methane capacity of the Lower Cretaceous strata of Northeastern British Columbia, Canada,” *Int. J. Coal Geol.*, vol. 70, no. 1–3, pp. 223–239, Apr. 2007.

[8] D. J. K. Ross and R. M. Bustin, “Investigating the use of sedimentary geochemical proxies for paleoenvironment interpretation of thermally mature organic-rich strata: Examples from the Devonian–Mississippian shales, Western Canadian Sedimentary Basin,” *Chem. Geol.*, vol. 260, no. 1–2, pp. 1–19, Mar. 2009.

[9] C. R. Clarkson and M. Bustin, “Coalbed Methane: Current Field-Based Evaluation Methods,” *SPE Reserv. Eval. Eng.*, vol. 14, no. 1, pp. 60–75, Apr. 2011.

[10] I. Langmuir, “THE ADSORPTION OF GASES ON PLANE SURFACES OF GLASS, MICA AND PLATINUM.,” *J. Am. Chem. Soc.*, vol. 40, no. 9, pp. 1361–1403, Sep. 1918.

[11] S. Brunauer, P. H. Emmett, and E. Teller, “Adsorption of Gases in Multimolecular Layers,” *J. Am. Chem. Soc.*, vol. 60, no. 2, pp. 309–319, Feb. 1938.

[12] V. Swami and A. Settari, “A Pore Scale Gas Flow Model for Shale Gas Reservoir,” *Proc. SPE Am. Unconv. Resour. Conf.*, no. June, pp. 5–7, 2012.

[13] F. G. Helfferich, “Principles of adsorption & adsorption processes, by D. M. Ruthven, John Wiley & Sons, 1984, xxiv + 433 pp,” *AIChE J.*, vol. 31, no. 3, pp. 523–524, Mar. 1985.

[14] G. J. Bell and K. C. Rakop, “Hysteresis Of Methane/Coal Sorption Isotherms,” in *SPE Annual Technical Conference and Exhibition*, 1986.

[15] D. Yee, J. P. Seidle, and W. B. Hanson, “Gas Sorption on Coal and Measurement of Gas Content: Chapter 9,” vol. 180, pp. 203–218, 1993.

[16] R. T. Yang, “Gas separation by adsorption processes,” Jan. 1986.

[17] J. T. Saunders, B. M. C. Tsai, and R. T. Yang, “Adsorption of gases on coals and heattreated coals at elevated temperature and pressure,” *Fuel*, vol. 64, no. 5, pp. 621–626, May 1985.

[18] M. D. Stevenson, W. V. Pinczewski, M. L. Somers, and S. E. Bagio, “Adsorption/Desorption of Multicomponent Gas Mixtures at In-Seam Conditions,” in *SPE Asia-Pacific Conference*, 1991.

[19] Halliburton, “Coalbed Methane: Principles and Practices,” 2007.

[20] R. I. Masel, *Principles of Adsorption and Reaction on Solid Surfaces*. John Wiley & Sons, 1996.

[21] A. Agbaji, B. Lee, H. Kumar, R. Belvalker, S. Eslambolchi, S. Guiadem, and S. Park, “Sustainable Development and Design of Marcellus Shale Play in Susquehanna, PA,” 2009.

[22] A. M. Belyadi, K. Aminian, and S. Ameri, “Production Performance of the Multiply-Fractured Horizontal Wells,” in *SPE Western Regional Meeting*, 2013.

[23] B. Nelson, F. Belyadi, A. Mashayekhi, K. Aminian, and S. Ameri, “Predicting Long-term Production Behavior of the Marcellus Shale,” in *SPE Western North American and Rocky Mountain Joint Meeting*, 2014.

[24] Y.-S. Wu, J. Li, D. Ding, C. Wang, and Y. Di, “A Generalized Framework Model for the Simulation of Gas Production in Unconventional Gas Reservoirs,” *SPE J.*, vol. 19, no. October, pp. 845–857, Oct. 2014.

[25] C. Hinz, “Description of sorption data with isotherm equations,” *Geoderma*, vol. 99, no. 3–4, pp. 225–243, Feb. 2001.

[26] D. G. Kinniburgh, “General purpose adsorption isotherms.,” *Environ. Sci. Technol.*, vol. 20, no. 9, pp. 895–904, Sep. 1986.

[27] C. H. Giles, D. Smith, and A. Huitson, “A general treatment and classification of the solute adsorption isotherm. I. Theoretical,” *J. Colloid Interface Sci.*, vol. 47, no. 3, pp. 755–765, Jun. 1974.

[28] K. J. Farley, D. A. Dzombak, and F. M. . Morel, “A surface precipitation model for the sorption of cations on metal oxides,” *J. Colloid Interface Sci.*, vol. 106, no. 1, pp. 226–242, Jul. 1985.

[29] H. Freundlich, *Kolloidchemie*. Leipzig, Germany, 1909.

[30] J. Tóth, “Thermodynamical Correctness of Gas/Solid Adsorption Isotherm Equations,” *J. Colloid Interface Sci.*, vol. 163, no. 2, pp. 299–302, Mar. 1994.

[31] G. L. Aranovich and M. D. Donohue, “An Equation of State for Multilayer Adsorption,” *J. Colloid Interface Sci.*, vol. 175, no. 2, pp. 492–496, Nov. 1995.

[32] V. P. M. J. Temkin, “Recent Modifications to Langmuir Isotherms,” *Acta Phys. Chem.*, vol. 12, pp. 217–222, 1940.

[33] R. H. Fowler and E. A. Guggenheim, *Statistical thermodynamics; A version of statistical mechanics for students of physics and chemistry*, 2nd ed. Cambridge, England: Cambridge University Press, 1960.

[34] D. Biswas, “Shale Gas Predictive Model (SGPM)--An Alternate Approach To Model Shale Gas Production,” in *SPE Eastern Regional Meeting*, 2011.

[35] G. R. King, “Material-Balance Techniques for Coal-Seam and Devonian Shale Gas Reservoirs With Limited Water Influx,” *SPE Reserv. Eng.*, vol. 8, no. 1, pp. 67–72, Apr. 1993.

[36] M. O. Eshkalak and U. Aybar, “The Effect of Desorption-induced Porosity-Permeability Changes and Geomechanics on Production from U.S. Shale Gas Formations,” *49th U.S. Rock Mechanics/Geomechanics Symposium*. American Rock Mechanics Association, 13-Nov-2015.

[37] Y. Wang, Y. Zhu, S. Liu, and R. Zhang, “Methane adsorption measurements and modeling for organic-rich marine shale samples,” *Fuel*, vol. 172, pp. 301–309, May 2016.

[38] A. Leahy-Dios, M. Das, A. Agarwal, and R. D. Kaminsky, “Modeling of Transport Phenomena and Multicomponent Sorption for Shale Gas and Coalbed Methane in an Unstructured Grid Simulator,” in *SPE Annual Technical Conference and Exhibition*, 2011.

[39] T. F. Rexer, E. J. Mathia, A. C. Aplin, and K. M. Thomas, “High-pressure methane adsorption and characterization of pores in posidonia shales and isolated kerogens,” *Energy and Fuels*, 2014.

[40] D. Silin and T. J. Kneafsey, “Shale Gas: Nanometer-Scale Observations and Well Modelling,” *J. Can. Pet. Technol.*, vol. 51, no. 6, pp. 464–475, Apr. 2012.

[41] H. G. Reading, *Sedimentary Environments: Processes, Facies and Stratigraphy*, 3rd Editio. Blackwell Publishing, 1996.

[42] S. Rani, B. K. Prusty, and S. K. Pal, “Methane adsorption and pore characterization of Indian shale samples,” *J. Unconv. Oil Gas Resour.*, vol. 11, pp. 1–10, Sep. 2015.

[43] W. Yu, K. Sepehrnoori, and T. W. Patzek, “Evaluation of Gas Adsorption in Marcellus Shale,” in *SPE Annual Technical Conference and Exhibition*, 2014.

[44] a. Sakhaee-Pour and S. L. Bryant, “Gas permeability of shale,” *SPE Reserv. Eval. Eng.*, vol. 15, no. 4, pp. 401–409, 2012.

[45] I. Y. Akkutlu and E. Fathi, “Multiscale Gas Transport in Shales With Local Kerogen Heterogeneities,” *SPE J.*, vol. 17, no. 4, pp. 1002–1011, 2012.

[46] H. Singh and F. Javadpour, “Nonempirical Apparent Permeability of Shale,” *Unconv. Resour. Technol. Conf.*, vol. 2, no. 1, pp. 1258–1273, 2013.

[47] F. Civan, “Effective Correlation of Apparent Gas Permeability in Tight Porous Media,” *Transp. Porous Media*, vol. 82, no. 2, pp. 375–384, Jul. 2009.

[48] H. Wang and M. Marongiu-Porcu, “Impact of Shale-Gas Apparent Permeability on Production: Combined Effects of Non-Darcy Flow/Gas-Slippage, Desorption, and Geomechanics,” *SPE Reserv. Eval. Eng.*, vol. 18, no. 4, pp. 495–507, Nov. 2015.

[49] W. J. Lee and R. Sidle, “Gas-Reserves Estimation in Resource Plays,” *SPE Econ. Manag.*, vol. 2, no. 2, pp. 86–91, Oct. 2010.

[50] B. P. Ramagost and F. F. Farshad, “P/Z Abnormally Pressured Gas Reservoirs,” in *SPE Annual Technical Conference and Exhibition*, 1981.

[51] G. R. King, “Material-Balance Techniques for Coal-Seam and Devonian Shale Gas Reservoirs With Limited Water Influx,” *SPE Reserv. Eng.*, vol. 8, no. 1, pp. 67–72, Feb. 1993.

[52] S. Moghadam, O. Jeje, and L. Mattar, “Advanced Gas Material Balance in Simplified Format,” *J. Can. Pet. Technol.*, vol. 50, no. 1, pp. 90–98, Apr. 2011.

[53] D. J. K. Ross and R. Marc Bustin, “Impact of mass balance calculations on adsorption capacities in microporous shale gas reservoirs,” *Fuel*, vol. 86, no. 17–18, pp. 2696–2706, Dec. 2007.

[54] S. A. Mengal and R. A. Wattenbarger, “Accounting For Adsorbed Gas in Shale Gas Reservoirs,” in *SPE Middle East Oil and Gas Show and Conference*, 2011.

[55] R. Heller and M. Zoback, “Adsorption of methane and carbon dioxide on gas shale and pure mineral samples,” *J. Unconv. Oil Gas Resour.*, vol. 8, pp. 14–24, Dec. 2014.

[56] EIA, “International Energy Outlook 2016 (IEO2016),” Washington, DC, 2016.

[57] Schlumberger Limited, “Schlumberger Annual Report 2009,” Houston, Texas, 2009.

[58] A. Bashari, “Khuff formation Permian-Triassic carbonate in the Qatar-South Fars arch hydrocarbon province of the Persian Gulf,” *First Break*, vol. 23, no. 11, 2005.

[59] R. Sloan, “Quantification of Uncertainty in Recovery Efficiency Predictions: Lessons Learned from 250 Mature Carbonate Fields,” in *SPE Annual Technical Conference and Exhibition*, 2003.

[60] Edward Bryant, *Climate Process and Change | Climatology and Climate Change | Cambridge University Press*. 1997.

[61] S. Bachu, "Sequestration of CO2 in geological media: criteria and approach for site selection in response to climate change," *Energy Convers. Manag.*, vol. 41, no. 9, pp. 953–970, 2000.

[62] C. M. Oldenburg and S. M. Benson, "CO2 Injection for Enhanced Gas Production and Carbon Sequestration," in *SPE International Petroleum Conference and Exhibition in Mexico*, 2002.

[63] J. P. Laille, J. E. Molinard, and A. Wents, "Inert Gas Injection as Part of the Cushion of the Underground Storage of Saint-Clair-Sur-Epte, France," in *SPE Gas Technology Symposium*, 1988.

[64] J. F. Carriere, G. Fasanino, and M. R. Tek, "Mixing in Underground Storage Reservoirs," in *SPE Annual Technical Conference and Exhibition*, 1985.

[65] K. Blok, R. H. Williams, R. E. Katofsky, and C. A. Hendriks, "Hydrogen production from natural gas, sequestration of recovered CO2 in depleted gas wells and enhanced natural gas recovery," *Energy*, vol. 22, no. 2, pp. 161–168, 1997.

[66] S. Bachu and W. D. Gunter, "Acid-gas injection in the Alberta basin, Canada: a CO_2 -storage experience," *Geol. Soc. London, Spec. Publ.*, vol. 233, no. 1, pp. 225–234, 2004.

[67] M. Algharaib and N. A. Al-Soof, "Economical Modeling of CO2 Capturing and Storage Projects," in *SPE Saudia Arabia Section Technical Symposium*, 2008.

[68] S. Cavenati, C. A. Grande, and A. E. Rodrigues, "Adsorption Equilibrium of Methane, Carbon Dioxide, and Nitrogen on Zeolite 13X at High Pressures," *J. Chem. Eng. Data*, vol. 49, no. 4, pp. 1095–1101, Jul. 2004.

[69] J. Zhu, K. Jessen, A. R. Kovscek, and F. M. Orr, "Analytical Theory of Coalbed Methane Recovery by Gas Injection," *SPE J.*, vol. 8, no. 4, pp. 371–379, Dec. 2003.

[70] S. Duan, M. Gu, X. Du, and X. Xian, "Adsorption Equilibrium of CO_2 and CH_4 and Their Mixture on Sichuan Basin Shale," *Energy & Fuels*, vol. 30, no. 3, pp. 2248–2256, Mar. 2016.

[71] K. C. Schepers, B. C. Nuttall, A. Y. Oudinot, and R. J. Gonzalez, "Reservoir Modeling and Simulation of the Devonian Gas Shale of Eastern Kentucky for Enhanced Gas Recovery and CO2 Storage," in *SPE International Conference on CO2 Capture, Storage, and Utilization*, 2009.

[72] S. H. Stevens, D. Spector, and P. Riemer, "Enhanced Coalbed Methane Recovery Using CO2 Injection: Worldwide Resource and CO2 Sequestration Potential," in *SPE International Oil and Gas Conference and Exhibition in China*, 1998.

[73] R. L. Petrusak, D. E. Riestenberg, P. L. Goad, K. C. Schepers, J. Pashin, R. A. Esposito, and R. C. Trautz, "World Class CO2 Sequestration Potential in Saline Formations, Oil and Gas Fields, Coal, and Shale: The US Southeast Regional Carbon Sequestration Partnership Has It All," in *SPE International Conference on CO2 Capture, Storage, and Utilization*, 2009.

[74] C. Liner, P. J. A. McCurdy, and K. C. Noyes, "Carbon Capture and Sequestration: Overview and Offshore Aspects," in *Offshore Technology Conference*, 2010.

[75] S. M. Kang, E. Fathi, R. J. Ambrose, I. Y. Akkutlu, and R. F. Sigal, "Carbon Dioxide Storage Capacity of Organic-Rich Shales," *SPE J.*, vol. 16, no. 4, pp. 842–855, Dec. 2011.

[76] H. Yu, W. Guo, J. Cheng, and Q. Hu, "Impact of experimental parameters for manometric equipment on CO2 isotherms measured: Comment on 'Inter-laboratory comparison II: CO2 isotherms measured on moisture-equilibrated Argonne premium coals at 55°C and up to 15 MPa' by Goodman et al. (2007)," *Int. J. Coal Geol.*, vol. 74, no. 3–4, pp. 250–258, May 2008.

[77] Y. Gensterblum, A. Busch, and B. M. Krooss, "Molecular concept and experimental evidence of competitive adsorption of H2O, CO2 and CH4 on organic material," *Fuel*, vol. 115, pp. 581–588, 2014.

[78] D. D. Mamora and J. G. Seo, "Enhanced Gas Recovery by Carbon Dioxide Sequestration in Depleted Gas Reservoirs," in *SPE Annual Technical Conference and Exhibition*, 2002.

[79] P. F. Fulton, C. A. Parente, B. A. Rogers, N. Shah, and A. A. Reznik, "A Laboratory Investigation Of Enhanced Recovery Of Methane From Coal By Carbon Dioxide Injection," in *SPE Unconventional Gas Recovery Symposium*, 1980.

[80] R. Heller and M. Zoback, "Adsorption of methane and carbon dioxide on gas shale and pure mineral samples," *J. Unconv. Oil Gas Resour.*, vol. 8, pp. 14–24, 2014.

[81] J. He, Y. Shi, S. Ahn, J. W. Kang, and C.-H. Lee, "Adsorption and Desorption of CO_2 on Korean Coal under Subcritical to Supercritical Conditions," *J. Phys. Chem. B*, vol. 114, no. 14, pp. 4854–4861, Apr. 2010.

[82] D.-F. Zhang, Y.-J. Cui, B. Liu, S.-G. Li, W.-L. Song, and W.-G. Lin, "Supercritical Pure Methane and CO 2 Adsorption on Various Rank Coals of China: Experiments and Modeling," *Energy & Fuels*, vol. 25, no. 4, pp. 1891–1899, Apr. 2011.

[83] N. Siemons and A. Busch, "Measurement and interpretation of supercritical CO2 sorption on various coals," *Int. J. Coal Geol.*, vol. 69, no. 4, pp. 229–242, Mar. 2007.

[84] A. Herbst and P. Harting, "Thermodynamic Description of Excess Isotherms in

High-Pressure Adsorption of Methane, Argon and Nitrogen," *Adsorption*, vol. 8, no. 2, pp. 111–123, 2002.

[85] J. U. Keller, F. Dreisbach, H. Rave, R. Staudt, and M. Tomalla, "Measurement of Gas Mixture Adsorption Equilibria of Natural Gas Compounds on Microporous Sorbents," *Adsorption*, vol. 5, no. 3, pp. 199–214, 1999.

[86] P. Chareonsuppanimit, S. A. Mohammad, R. L. Robinson, and K. A. M. Gasem, "High-pressure adsorption of gases on shales: Measurements and modeling," *Int. J. Coal Geol.*, vol. 95, pp. 34–46, Jun. 2012.

[87] I. A. A. C. Esteves, M. S. S. Lopes, P. M. C. Nunes, and J. P. B. Mota, "Adsorption of natural gas and biogas components on activated carbon," *Sep. Purif. Technol.*, vol. 62, no. 2, pp. 281–296, Sep. 2008.

[88] T. Tajnik, L. K. Bogataj, E. Jurač, C. R. Lasnik, J. Likar, and B. Debelak, "Investigation of adsorption properties of geological materials for CO 2 storage," *Int. J. Energy Res.*, vol. 37, no. 8, pp. 952–958, Jun. 2013.

[89] I. Quiñones and G. Guiochon, "Extension of a Jovanovic–Freundlich isotherm model to multicomponent adsorption on heterogeneous surfaces," *J. Chromatogr. A*, vol. 796, no. 1, pp. 15–40, 1998.

[90] H. Zhao, W. Yan, Z. Bian, J. Hu, and H. Liu, "Investigation of Mg modified mesoporous silicas and their CO2 adsorption capacities," *Solid State Sci.*, vol. 14, no. 2, pp. 250–257, Feb. 2012.

[91] S. L. Suib, A. Zukal, P. Nachtigall, and J. Čejka, *New and Future Developments in Catalysis*. Elsevier, 2013.

[92] A. Zukal, J. Pastva, and J. Čejka, "MgO-modified mesoporous silicas impregnated by potassium carbonate for carbon dioxide adsorption," *Microporous Mesoporous Mater.*, vol. 167, pp. 44–50, Feb. 2013.

[93] F. Su, C. Lu, and H. Chen, "Adsorption , Desorption , and Thermodynamic Studies of CO 2 with High-Amine-Loaded Multiwalled Carbon Nanotubes," *Langmuir*, vol. 27, pp. 8090–8098, 2011.

[94] E. Battistutta, P. van Hemert, M. Lutynski, H. Bruining, and K.-H. Wolf, "Swelling and sorption experiments on methane, nitrogen and carbon dioxide on dry Selar Cornish coal," *Int. J. Coal Geol.*, vol. 84, no. 1, pp. 39–48, 2010.

[95] H. Wu, C. G. Thibault, H. Wang, K. A. Cychosz, M. Thommes, and J. Li, "Effect of temperature on hydrogen and carbon dioxide adsorption hysteresis in an ultramicroporous MOF," *Microporous Mesoporous Mater.*, vol. 219, pp. 186–189, 2016.

[96] F. van Bergen, C. Spiers, G. Floor, and P. Bots, "Strain development in unconfined coals exposed to CO2, CH4 and Ar: Effect of moisture," *Int. J. Coal Geol.*, vol. 77, no. 1–2, pp. 43–53, Jan. 2009.

[97] M. Abunowara, M. A. Bustam, S. Sufian, and U. Eldemerdash, “Description of Carbon Dioxide Adsorption and Desorption onto Malaysian Coals under Subcritical Condition,” *Procedia Eng.*, vol. 148, pp. 600–608, 2016.

[98] S. Ottiger, R. Pini, G. Storti, and M. Mazzotti, “Measuring and modeling the competitive adsorption of CO2, CH4, and N2 on a dry coal.,” *Langmuir*, vol. 24, no. 17, pp. 9531–40, Sep. 2008.

[99] H. J. Kim, Y. Shi, J. He, H.-H. Lee, and C.-H. Lee, “Adsorption characteristics of CO2 and CH4 on dry and wet coal from subcritical to supercritical conditions,” *Chem. Eng. J.*, vol. 171, no. 1, pp. 45–53, Jun. 2011.

[100] P. C. Gravelle, “Methods for the determination of heats of adsorption,” *J. Therm. Anal.*, vol. 14, no. 1–2, pp. 53–77, Oct. 1978.

[101] S. Lowell, J. E. Shields, M. A. Thomas, and M. Thommes, *Characterization of Porous Solids and Powders: Surface Area, Pore Size and Density*, vol. 16. Dordrecht: Springer Netherlands, 2004.

[102] Q. Bkour, N. Faqir, R. Shawabkeh, A. Ul-Hamid, and H.-J. Bart, “Synthesis of a Ca/Na-aluminosilicate from kaolin and limestone and its use for adsorption of CO2,” *J. Environ. Chem. Eng.*, vol. 4, no. 1, pp. 973–983, Mar. 2016.

[103] L. Hauchhum and P. Mahanta, “Kinetic , Thermodynamic and Regeneration Studies for CO 2 Adsorption onto Activated Carbon,” *Int. J. Adv. Mech. Eng.*, vol. 4, no. 1, pp. 27–32, 2014.

[104] G. Yue, Z. Wang, X. Tang, H. Li, and C. Xie, “Physical Simulation of Temperature Influence on Methane Sorption and Kinetics in Coal (II): Temperature Evolvement during Methane Adsorption in Coal Measurement and Modeling,” *Energy & Fuels*, vol. 29, no. 10, pp. 6355–6362, Oct. 2015.

[105] M. A. Saad, M. J. Al-marri, A. L. Yaumi, I. A. Hussein, and R. Shawabkeh, “An Experimental and Kinetic Study of the Sorption of Carbon Dioxide onto Amine-Treated Oil Fly Ash,” *J. Chem.*, vol. 2016, p. 11, 2016.

[106] P. Van Cuong, T. Kuznetsova, B. Kvamme, and B. Jensen, “Adsorption energy and stability of H2O and CO2 on calcite effect by short-range force field parameters and temperature,” pp. 66–72, Mar. 2012.

[107] Y. Belmabkhout and A. Sayari, “Adsorption of CO2 from dry gases on MCM-41 silica at ambient temperature and high pressure. 2: Adsorption of CO2/N2, CO2/CH4 and CO2/H2 binary mixtures,” *Chem. Eng. Sci.*, vol. 64, no. 17, pp. 3729–3735, Sep. 2009.

[108] P. W. (Peter W. Atkins and J. De Paula, *Physical chemistry*. .

[109] A. Dąbrowski, “Adsorption — from theory to practice,” *Adv. Colloid Interface Sci.*, vol. 93, no. 1, pp. 135–224, 2001.

[110] C. . Oldenburg, S. . Stevens, and S. . Benson, “Economic feasibility of carbon sequestration with enhanced gas recovery (CSEGR),” *Energy*, vol. 29, no. 9–10, pp. 1413–1422, Jul. 2004.

[111] J. Ailin, H. Dongbo, J. Chengye, J. Guang, and W. Yunsheng, “Challenges of Horizontal Well and Successful Cases for Tight Gas Development in China,” in *International Petroleum Technology Conference*, 2013.

[112] J. A. Rushing, K. E. Newsham, and T. A. Blasingame, “Rock Typing: Keys to Understanding Productivity in Tight Gas Sands,” in *SPE Unconventional Reservoirs Conference*, 2008.

[113] W. J. Lee and C. W. Hopkins, “Characterization of Tight Reservoirs,” *J. Pet. Technol.*, vol. 46, no. 11, pp. 956–964, Nov. 1994.

[114] D. H. Le, H. N. Hoang, and J. Mahadevan, “Gas Recovery From Tight Sands: Impact of Capillarity,” *SPE J.*, vol. 17, no. 4, pp. 981–991, Dec. 2012.

[115] L. Zhang, D. Li, L. Wang, D. Lu, L. Zhang, D. Li, L. Wang, and D. Lu, “Simulation of Gas Transport in Tight/Shale Gas Reservoirs by a Multicomponent Model Based on PEBI Grid,” *J. Chem.*, vol. 2015, pp. 1–9, 2015.

[116] D. Li, C. Xu, J. Y. Wang, and D. Lu, “Effect of Knudsen diffusion and Langmuir adsorption on pressure transient response in tight- and shale-gas reservoirs,” *J. Pet. Sci. Eng.*, vol. 124, pp. 146–154, Dec. 2014.

[117] F. Javadpour, “Nanopores and Apparent Permeability of Gas Flow in Mudrocks (Shales and Siltstone),” *J. Can. Pet. Technol.*, vol. 48, no. 8, pp. 16–21, Aug. 2009.

[118] C. M. Freeman, G. J. Moridis, and T. A. Blasingame, “A Numerical Study of Microscale Flow Behavior in Tight Gas and Shale Gas Reservoir Systems,” *Transp. Porous Media*, vol. 90, no. 1, pp. 253–268, Oct. 2011.

[119] C. M. Freeman, G. J. Moridis, and T. A. Blasingame, “Modeling and Performance Interpretation of Flowing Gas Composition Changes in Shale Gas Wells with Complex Fractures,” in *International Petroleum Technology Conference*, 2013.

[120] R. Pini, S. Ottiger, G. Storti, and M. Mazzotti, “Prediction of competitive adsorption on coal by a lattice DFT model,” *Adsorption*, vol. 16, no. 1–2, pp. 37–46, Oct. 2009.

[121] K. Lorenz and M. Wessling, “How to determine the correct sample volume by gravimetric sorption measurements,” *Adsorption*, vol. 19, no. 6, pp. 1117–1125, Dec. 2013.

[122] J. U. Keller and E. Robens, “A note on sorption measuring instruments,” *J. Therm. Anal. Calorim.*, vol. 71, no. 1, pp. 37–45, 2003.

[123] T. Fujii, S. Nakagawa, Y. Sato, H. Inomata, and T. Hashida, “Sorption Characteristics of CO₂ on Rocks and

Minerals in Storing CO₂ Processes," *Nat. Resour.*, vol. 1, no. 1, pp. 1–10, 2010.

[124] M. A. Mahmoud, H. A. Nasr-El-Din, and C. A. De Wolf, "High-Temperature Laboratory Testing of Illitic Sandstone Outcrop Cores With HCl-Alternative Fluids," *SPE Prod. Oper.*, vol. 30, no. 1, pp. 43–51, Feb. 2015.

[125] D. Li, Q. Liu, P. Weniger, Y. Gensterblum, A. Busch, and B. M. Krooss, "High-pressure sorption isotherms and sorption kinetics of CH4 and CO2 on coals," *Fuel*, vol. 89, no. 3, pp. 569–580, 2010.

[126] Ü. Sòukand, R. Sõukand, A. Maširin, and T. Tenno, "The Langmuir two-surface equation as a model for cadmium adsorption on peat," *Environ. Sci. Pollut. Res.*, vol. 9, no. S1, pp. 43–48, Jan. 2002.

[127] H. E. Gaudette and H. E., "The Nature of Illite," *Clays Clay Miner.*, vol. 13, no. 1, pp. 33–48, 1964.

[128] G. Sedmale, a Cimmers, and U. Sedmalis, "Characteristics of illite clay and compositions for porous building ceramics production," *Chem. Technol.*, vol. 2, no. 2, pp. 2–5, 2009.

[129] N. D. Hutson*, S. A. S. and, and E. A. Payzant, "Structural Effects on the High Temperature Adsorption of CO2 on a Synthetic Hydrotalcite," 2004.

[130] M. Al-Harahsheh, R. Shawabkeh, M. Batiha, A. Al-Harahsheh, and K. Al-Zboon, "Sulfur Dioxide Removal using Natural Zeolitic Tuff," *Fuel Process. Technol.*, vol. 126, pp. 249–258, 2014.

[131] D. J. K. Ross and R. Marc Bustin, "The importance of shale composition and pore structure upon gas storage potential of shale gas reservoirs," *Mar. Pet. Geol.*, vol. 26, no. 6, pp. 916–927, 2009.

[132] X. Luo, S. Wang, Z. Wang, Z. Jing, M. Lv, Z. Zhai, and T. Han, "Adsorption of methane, carbon dioxide and their binary mixtures on Jurassic shale from the Qaidam Basin in China," *Int. J. Coal Geol.*, vol. 150–151, pp. 210–223, Oct. 2015.

[133] B. Zhou, R. Xu, and P. Jiang, "Novel molecular simulation process design of adsorption in realistic shale kerogen spherical pores," *Fuel*, vol. 180, pp. 718–726, Sep. 2016.

[134] H. Sun and A. Chawathe, "Understanding Shale Gas Flow Behavior Using Numerical Simulation," no. February, 2015.

[135] M. O. Abouelresh, "Quantitative and Qualitative Evaluation of Micro-Porosity in Qusaiba Hot Shale, Saudi Arabia," in *Unconventional Resources Technology Conference*, 2015.

[136] H. Hu, "Methane adsorption comparison of different thermal maturity kerogens in shale gas system," *Chinese J. Geochemistry*, vol. 33, no. 4, pp. 425–430, Dec.

2014.

[137] J. Zhong, G. Chen, C. Lv, W. Yang, Y. Xu, S. Yang, and L. Xue, “Experimental study of the impact on methane adsorption capacity of continental shales with thermal evolution,” *J. Nat. Gas Geosci.*, vol. 1, no. 2, pp. 165–172, 2016.

[138] Y. Yang, K. Wu, T. Zhang, and M. Xue, “Characterization of the pore system in an over-mature marine shale reservoir: A case study of a successful shale gas well in Southern Sichuan Basin, China,” *Petroleum*, vol. 1, no. 3, pp. 173–186, 2015.

Appendix A

Adsorption/Desorption by Carbonate

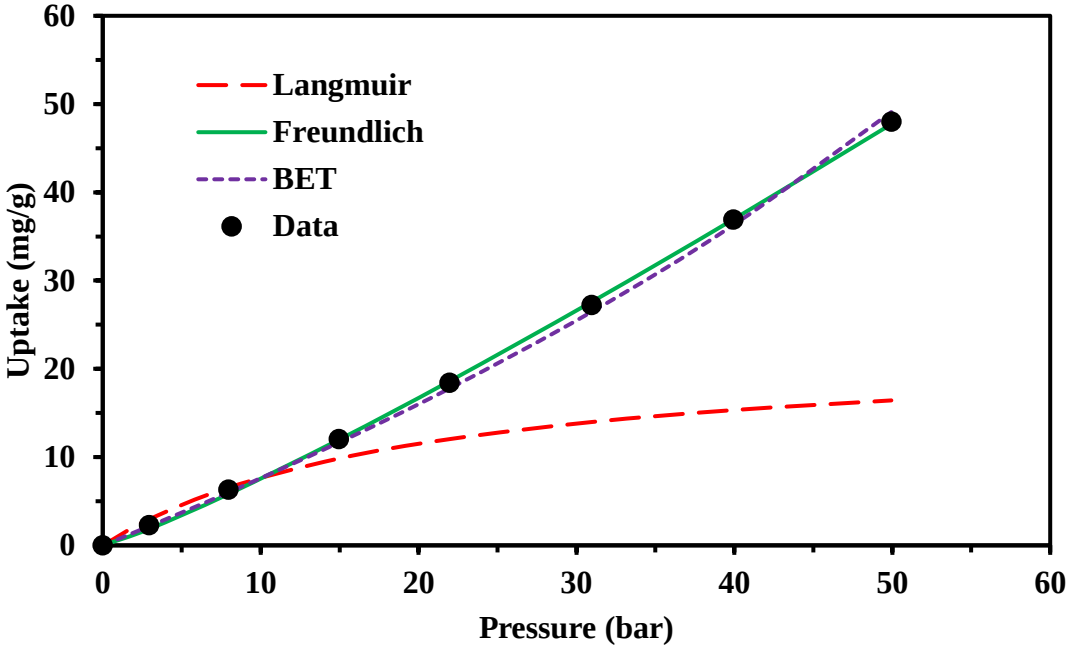

Figure A1 Fitting of CH_4 adsorption on Pink Desert Limestone at 50°C with Langmuir, Freundlich and BET.

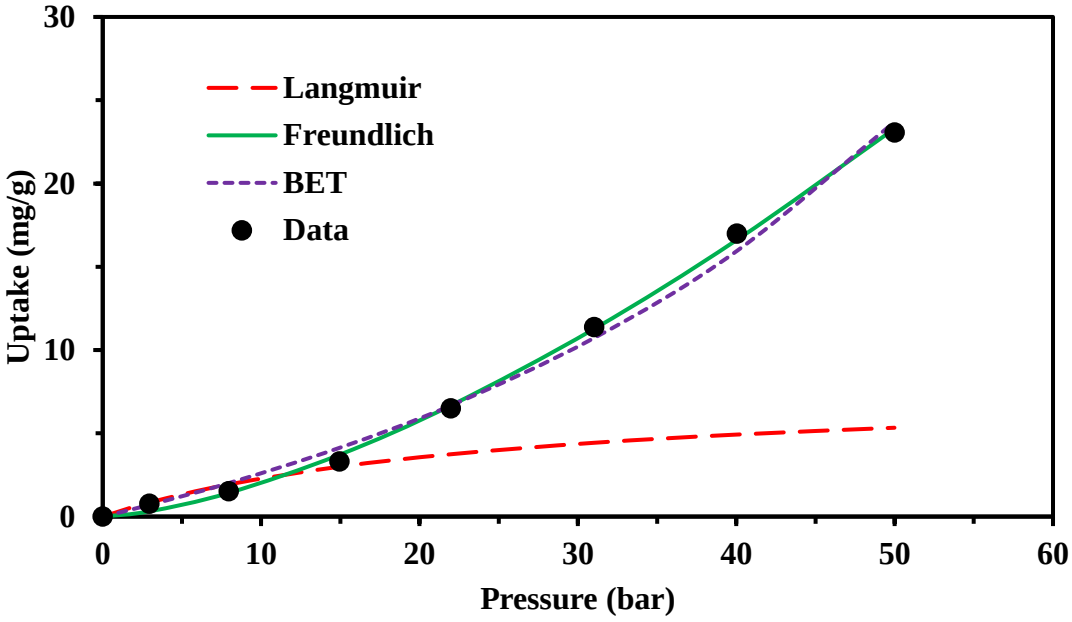

Figure A2 Fitting of CH_4 adsorption on Pink Desert Limestone at 100°C with Langmuir, Freundlich and BET.

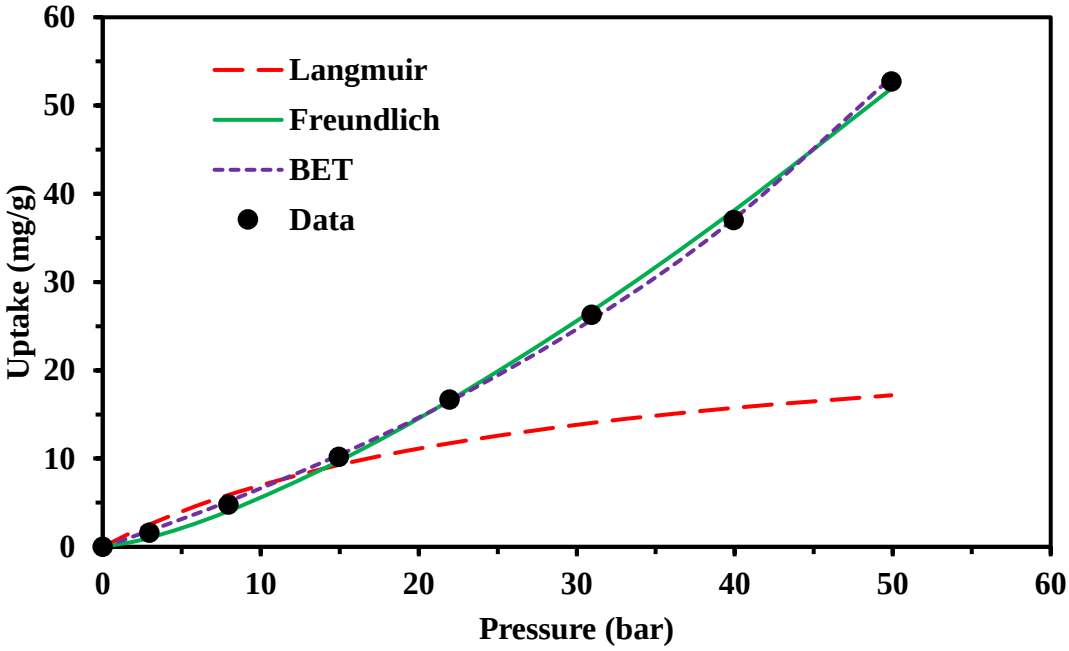

Figure A3 Fitting of 10%CO_2 adsorption on Pink Desert Limestone at 50°C with Langmuir, Freundlich and BET.

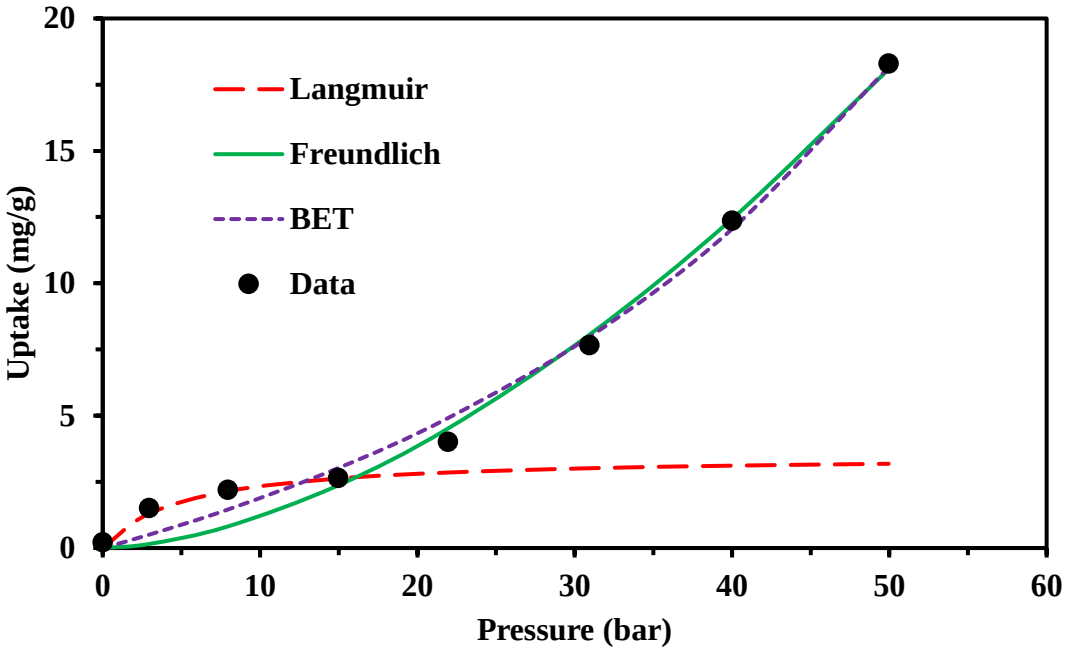

Figure A4 Fitting of 10%CO_2 adsorption on Pink Desert Limestone at 150°C with Langmuir, Freundlich and BET.

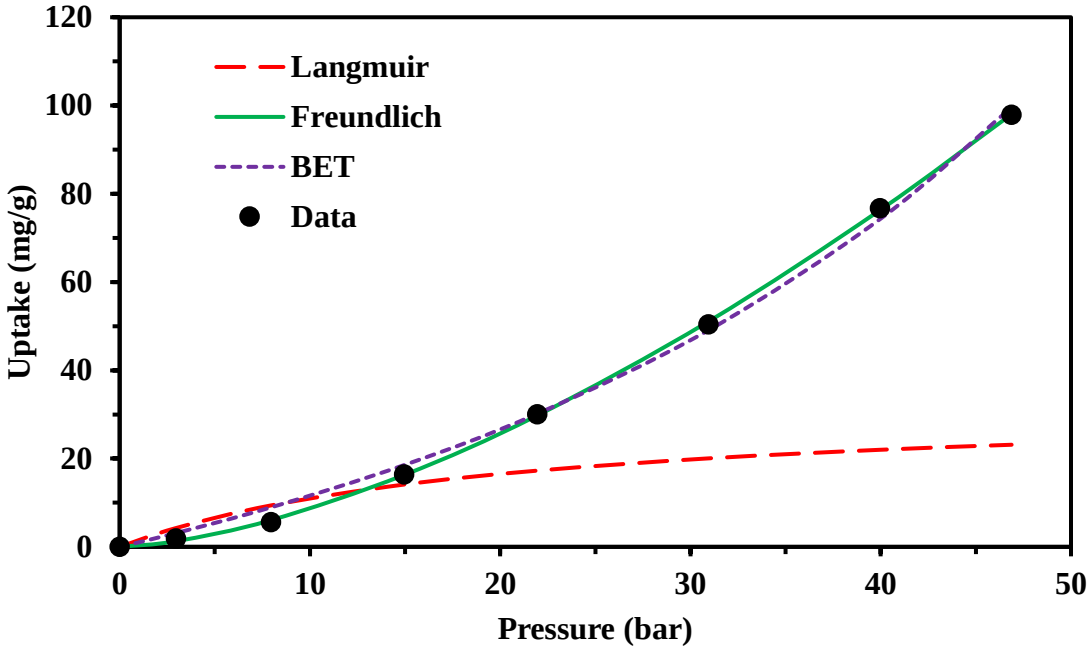

Figure A5 Fitting of CO_2 adsorption on Pink Desert Limestone at 100°C with Langmuir, Freundlich and BET.

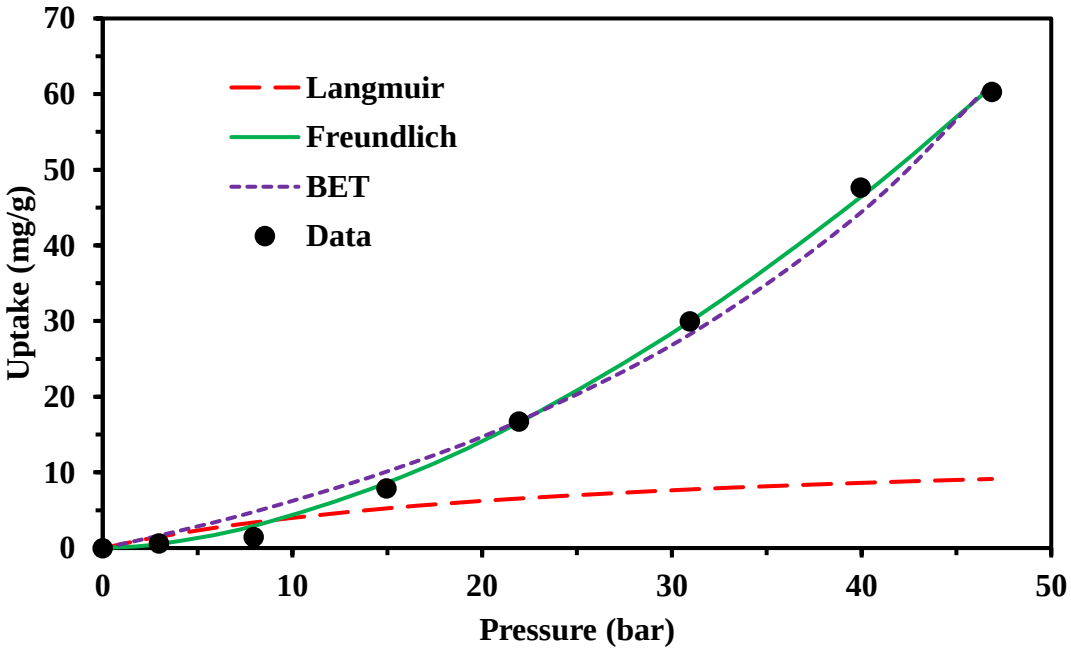

Figure A6 Fitting of CO_2 adsorption on Pink Desert Limestone at 150°C with Langmuir, Freundlich and BET.

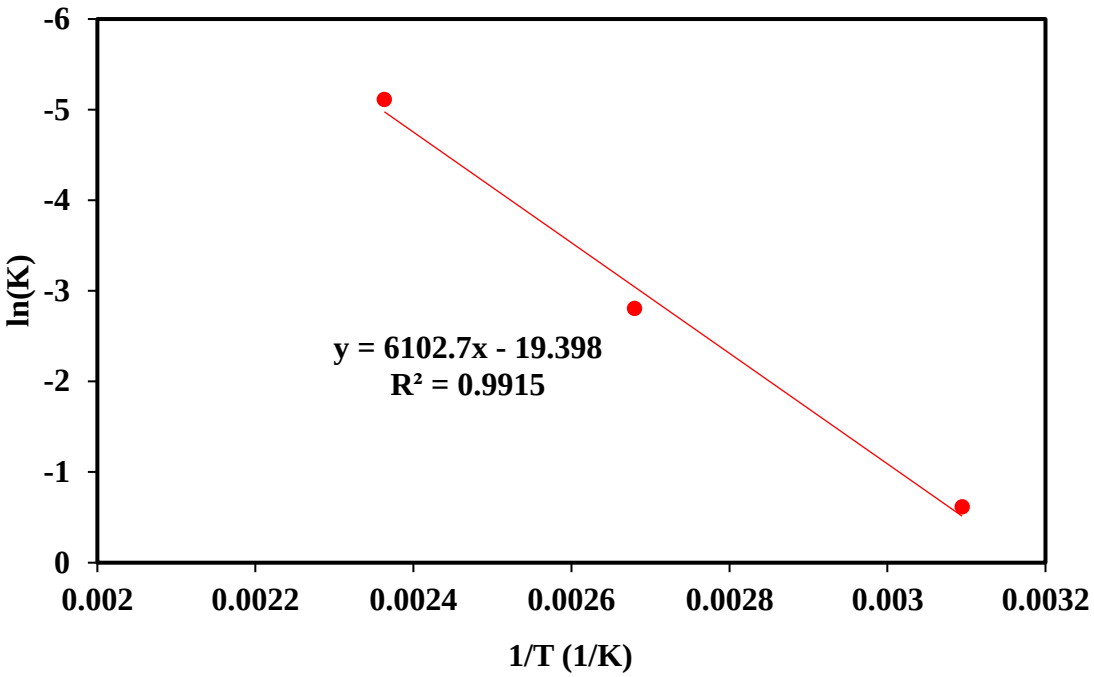

Figure A7 Pure methane heat of adsorption Arrhenius plot.

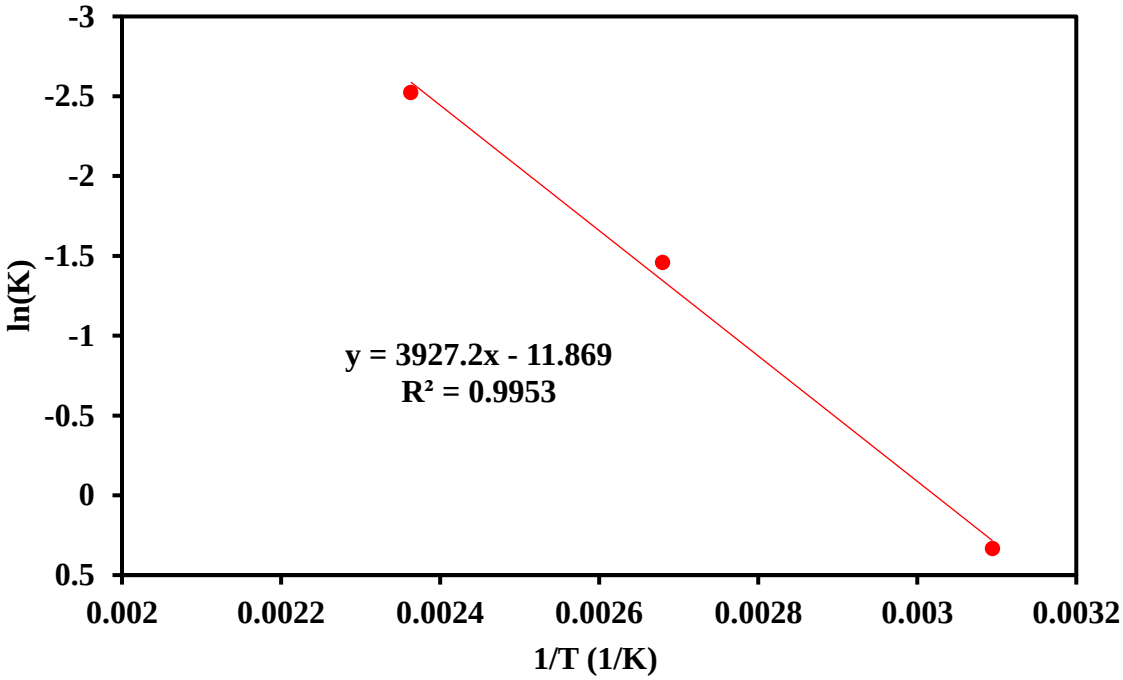

Figure A8 Pure carbon dioxide heat of adsorption Arrhenius plot.

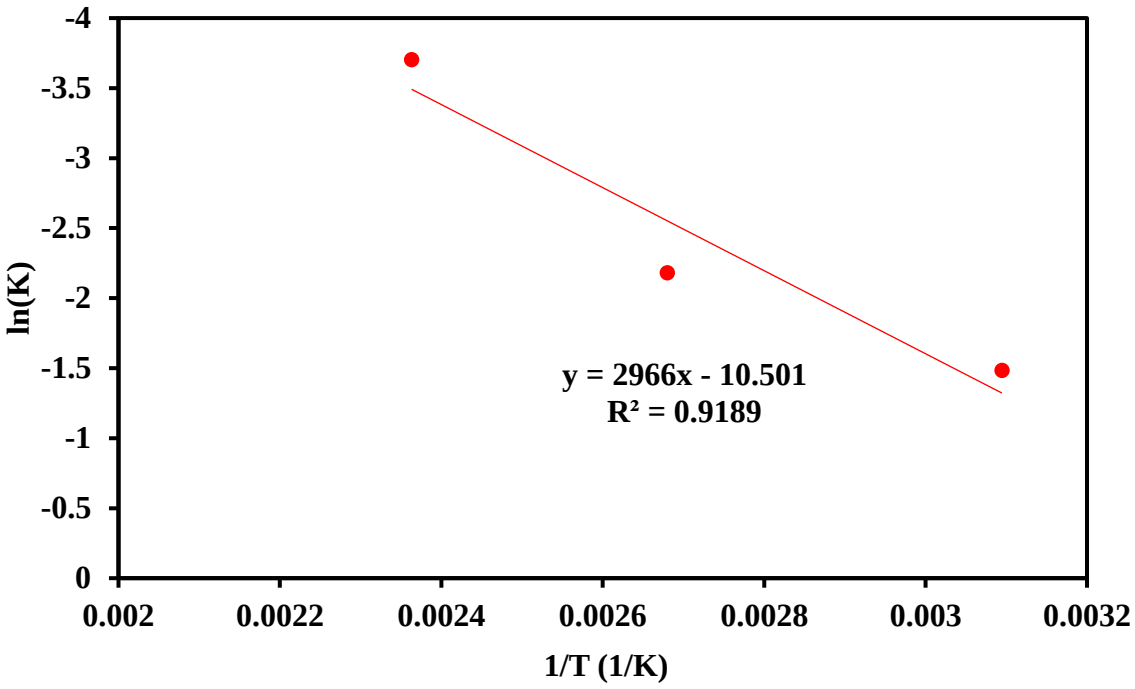

Figure A9 10% CO_2 & 90% CH_4 heat of adsorption Arrhenius plot.

Appendix B

Adsorption/Desorption by Tight Sandstone

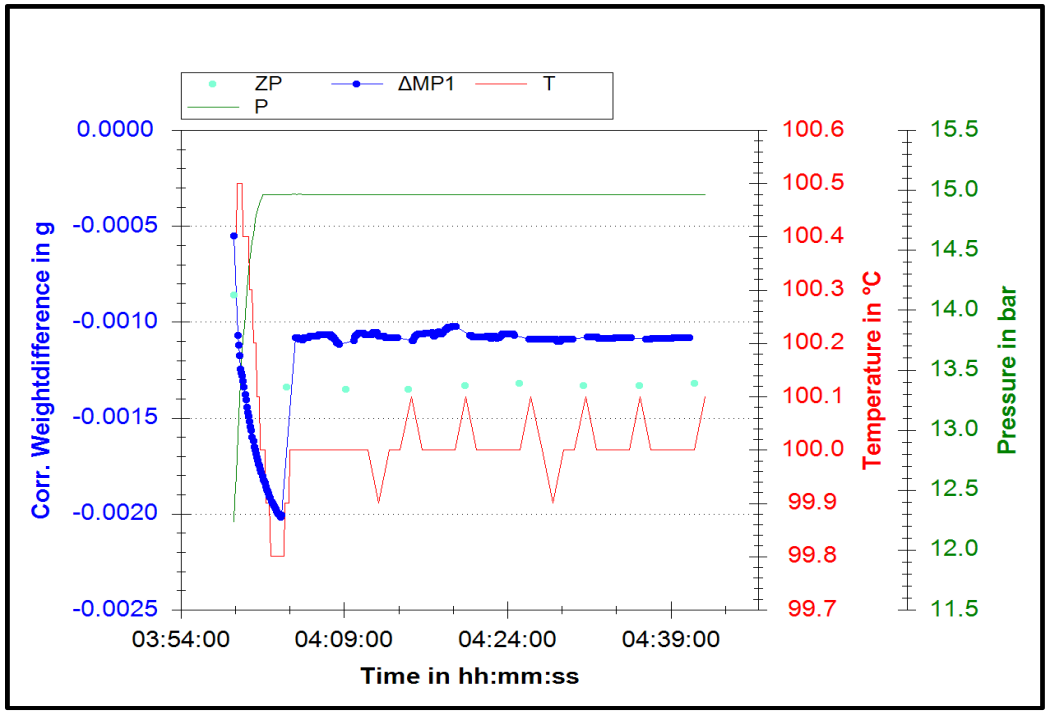

Figure B1 One pressure set point of the Helium Buoyancy measurement at 100°C.

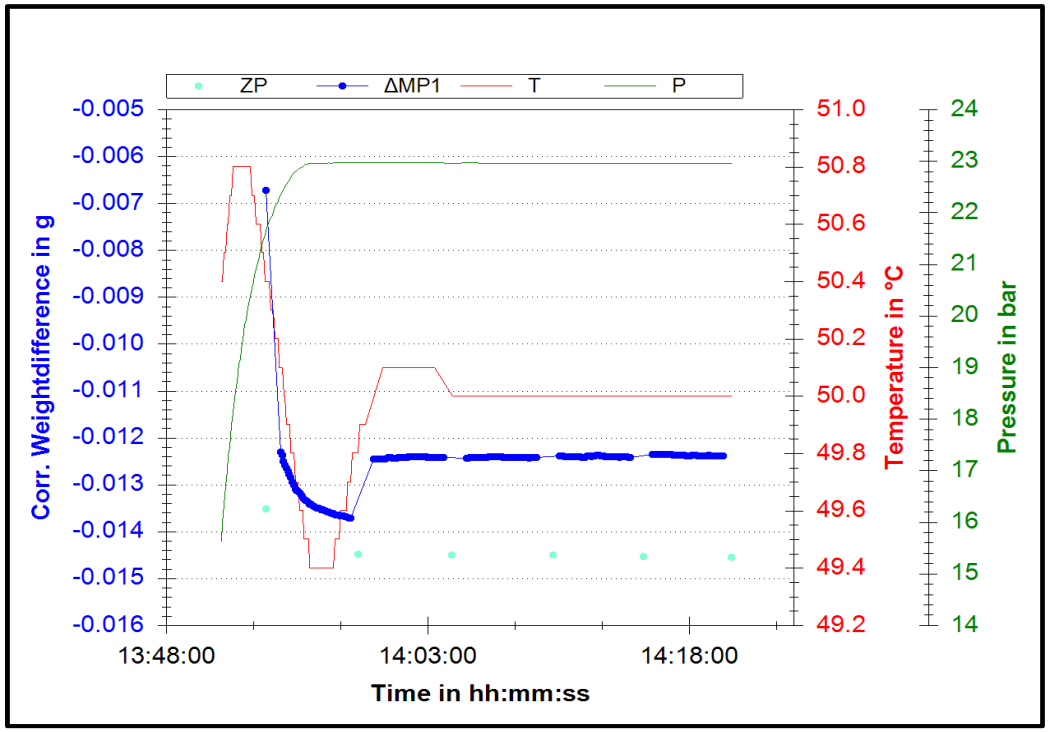

Figure B2 One pressure set point of CH_4 adsorption measurement at 50°C.

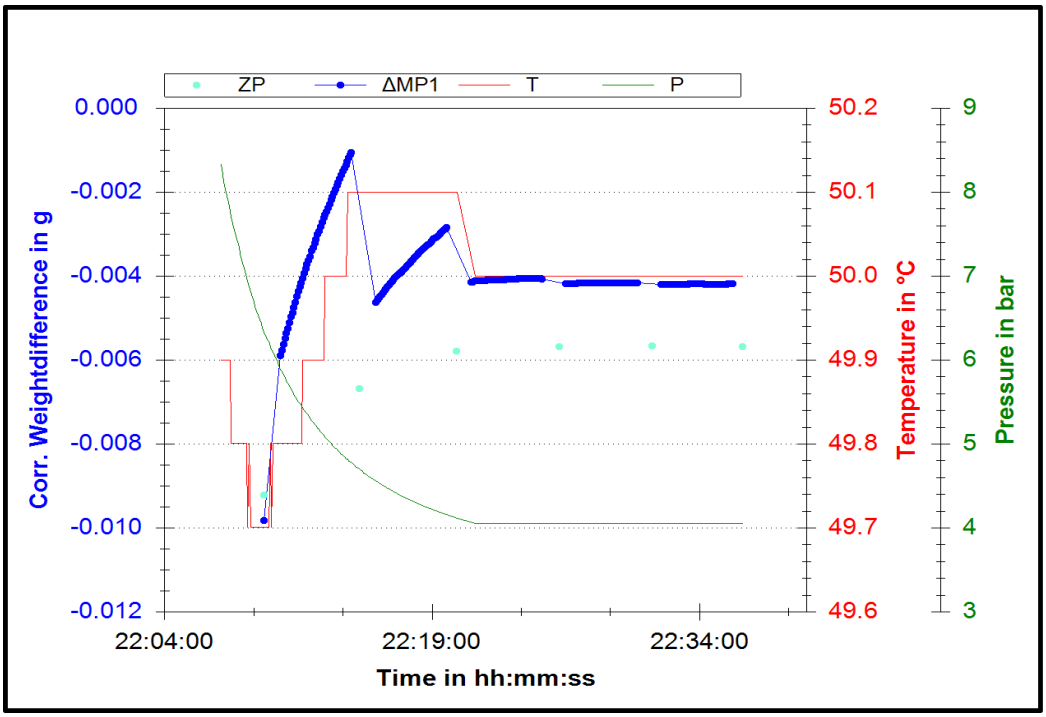

Figure B3 One pressure set point of CO_2 desorption measurement at 50°C.

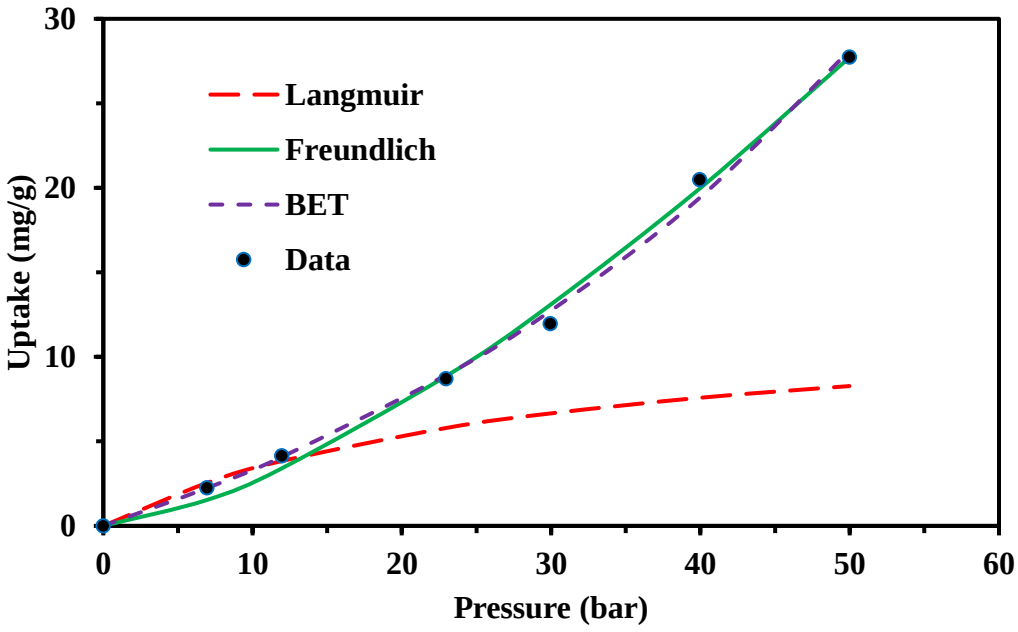

Figure B4 Fitting of CH_4 adsorption on Kentucky sandstone at 50°C with Langmuir, Freundlich and BET.

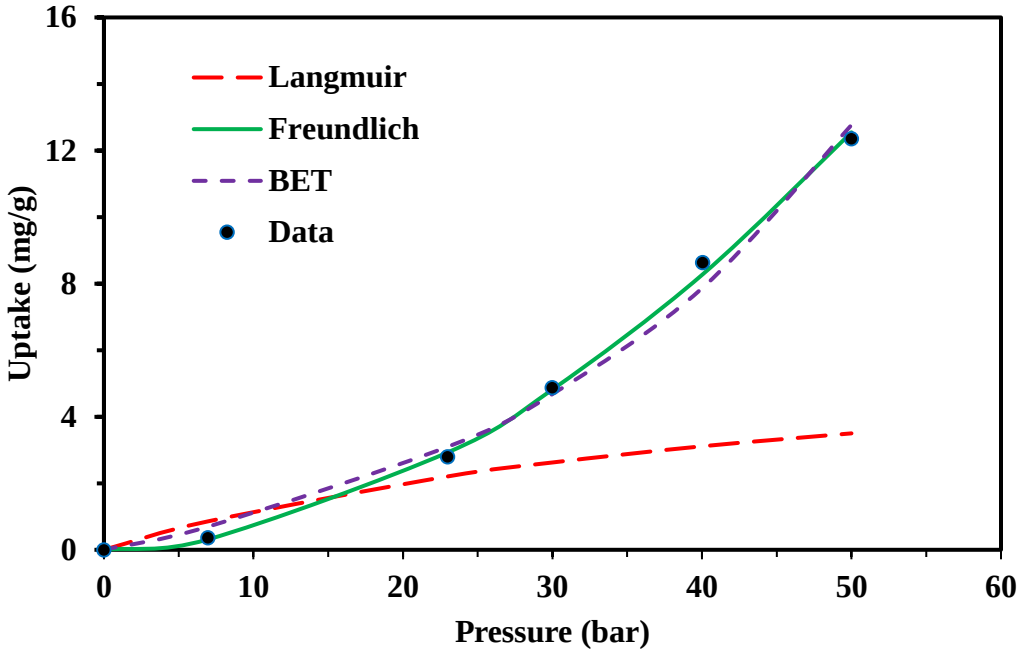

Figure B5 Fitting of CH_4 adsorption on Kentucky sandstone at 100°C with Langmuir, Freundlich and BET.

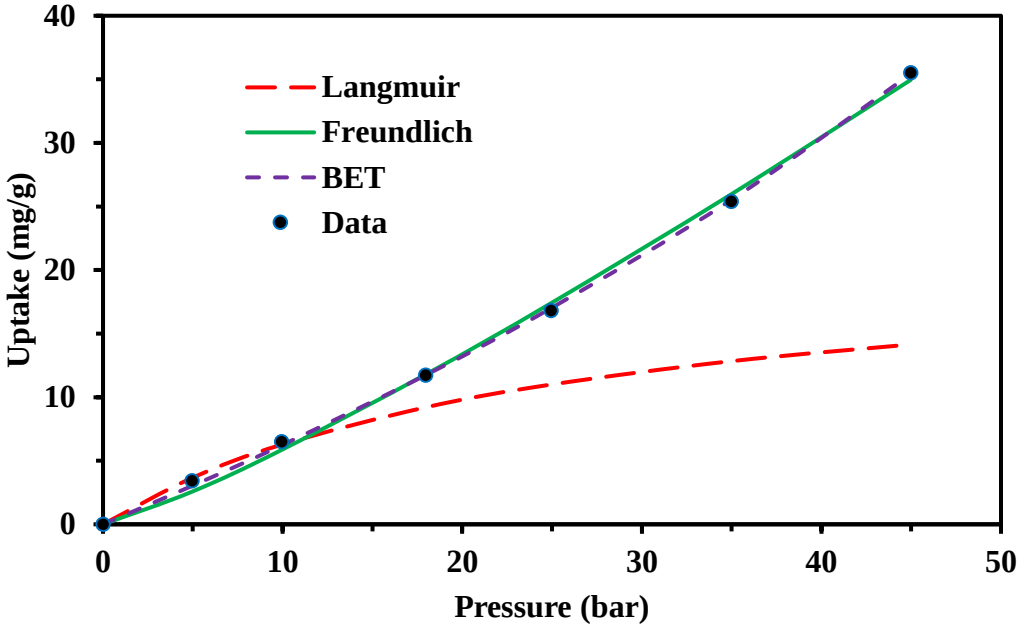

Figure B6 Fitting of 10%CO_2 adsorption on Kentucky sandstone at 50°C with Langmuir, Freundlich and BET.

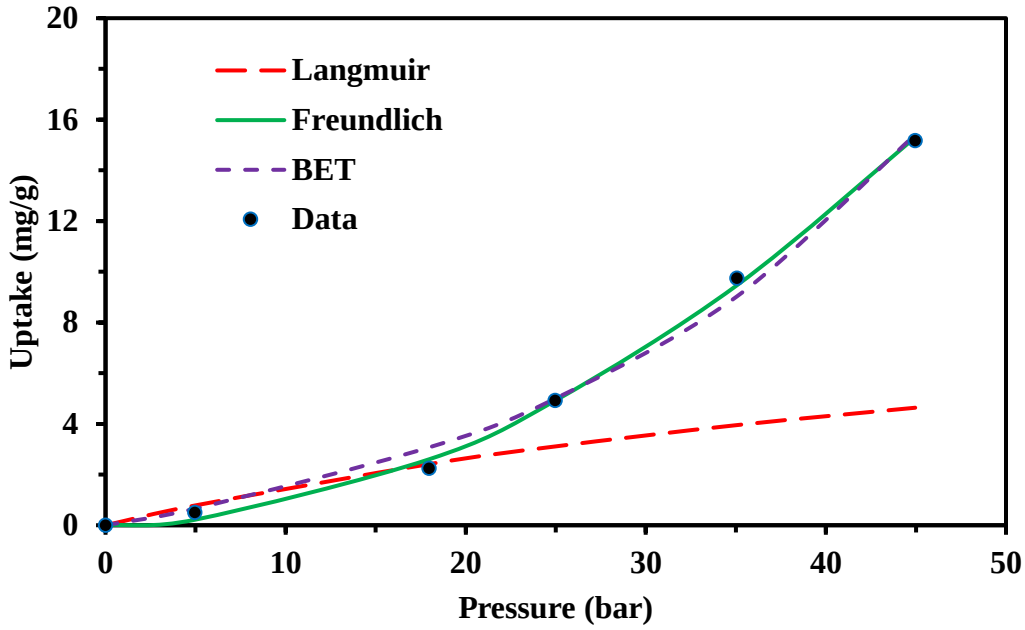

Figure B7 Fitting of 10%CO_2 adsorption on Kentucky sandstone at 100^oC with Langmuir, Freundlich and BET.

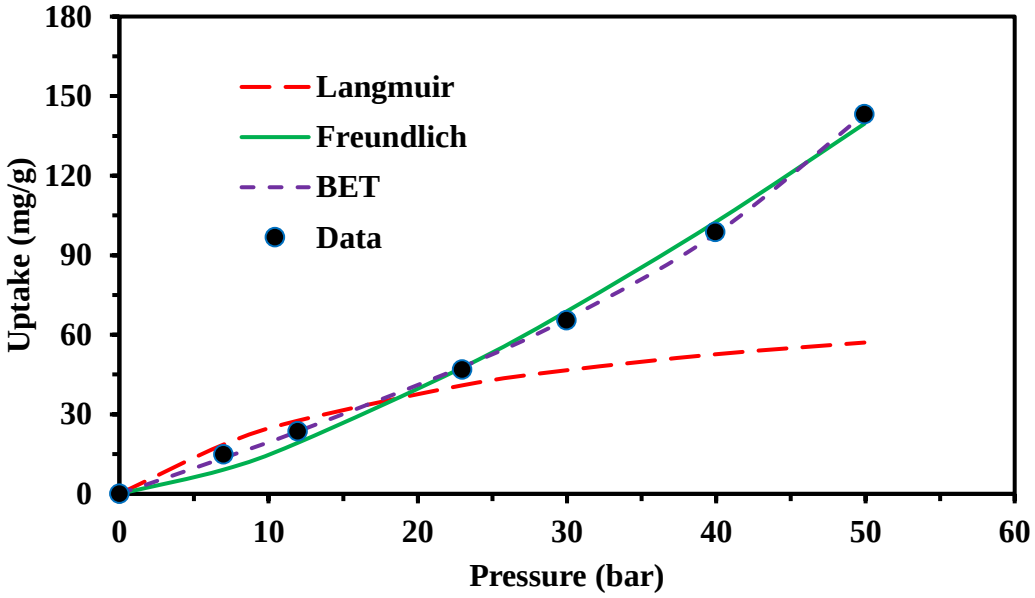

Figure B8 Fitting of CO_2 adsorption on Kentucky sandstone at 50^oC with Langmuir, Freundlich and BET.

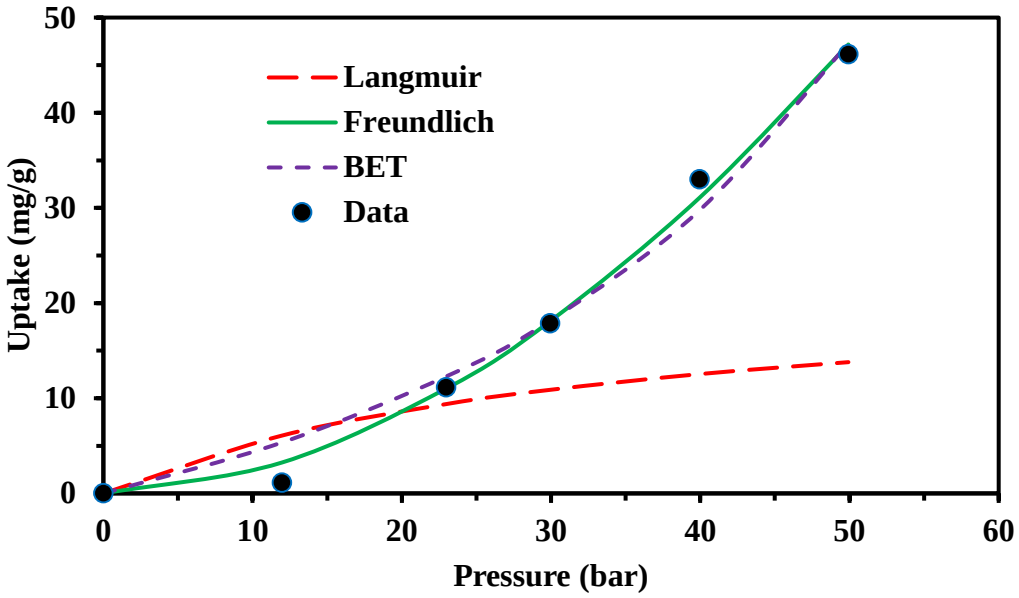

Figure B9 Fitting of CO_2 adsorption on Kentucky sandstone at 100°C with Langmuir, Freundlich and BET.

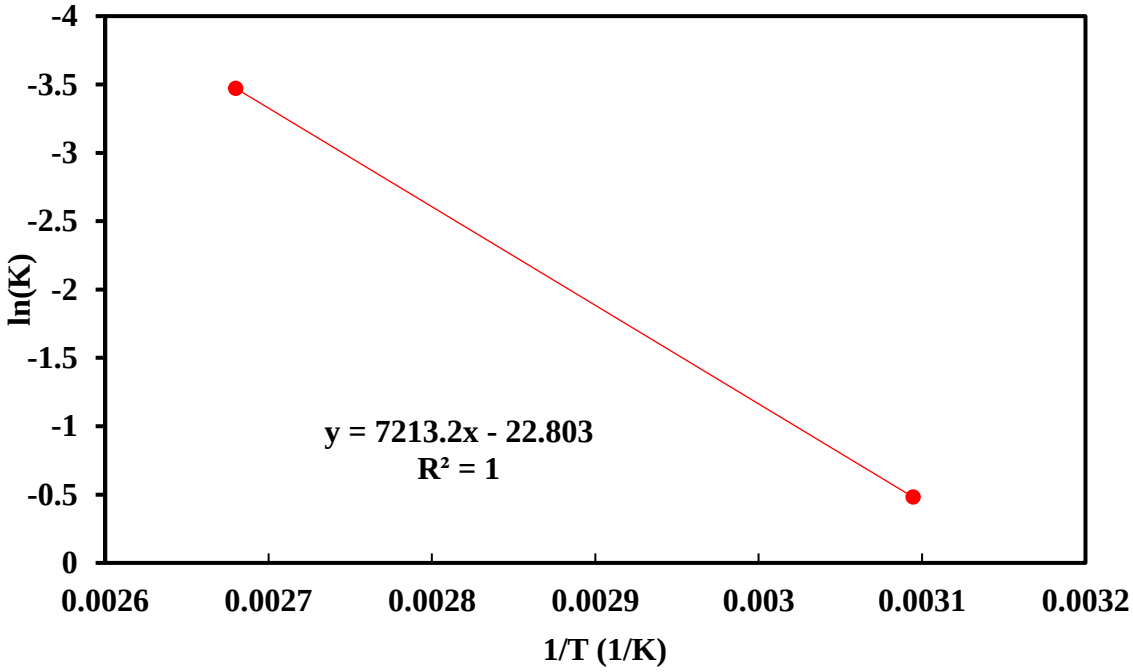

Figure B10 Pure CO_2 heat of adsorption Arrhenius plot.

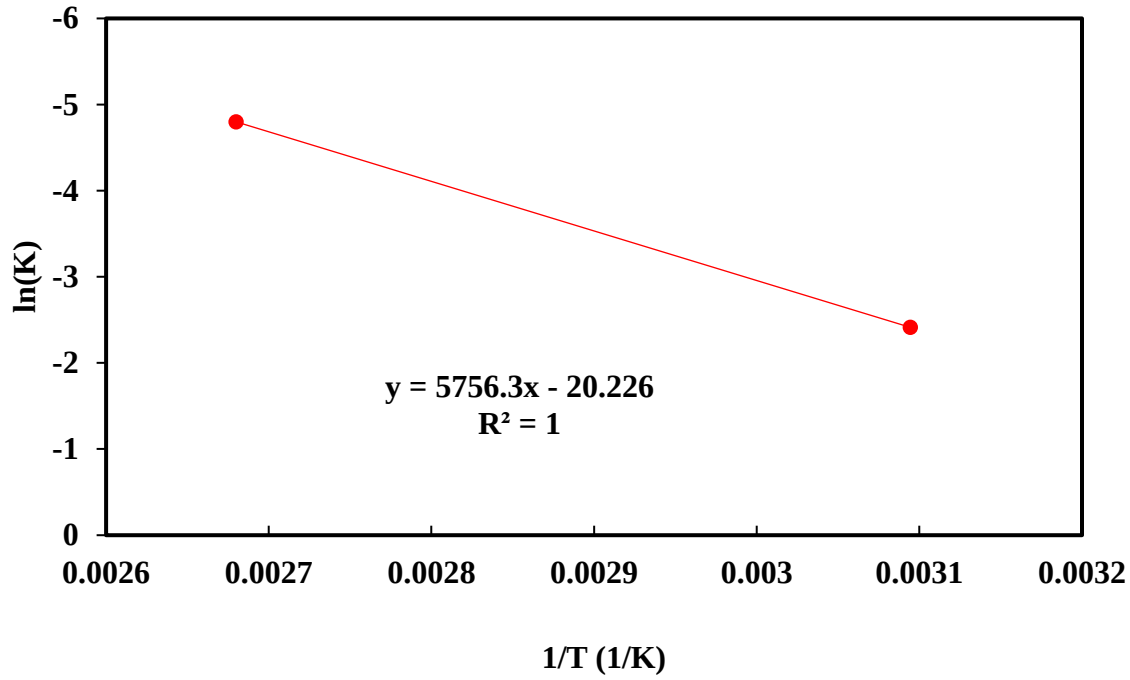

Figure B11 Pure CH_4 heat of adsorption Arrhenius plot.

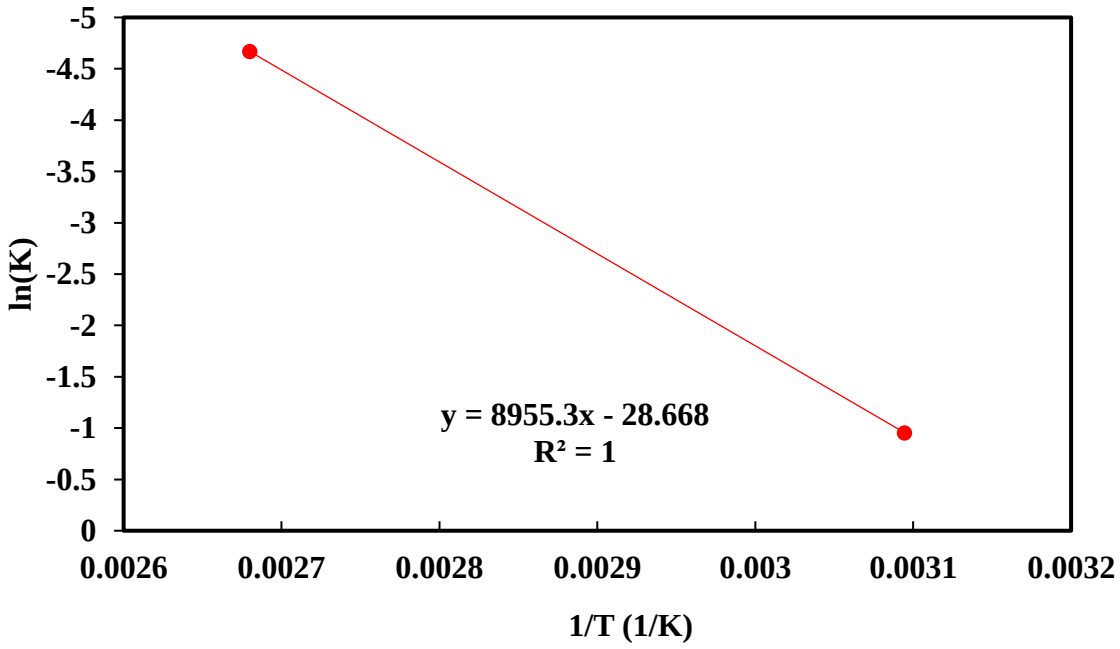

Figure B12 10% CO2-90% CH_4 heat of adsorption Arrhenius plot.

Appendix C

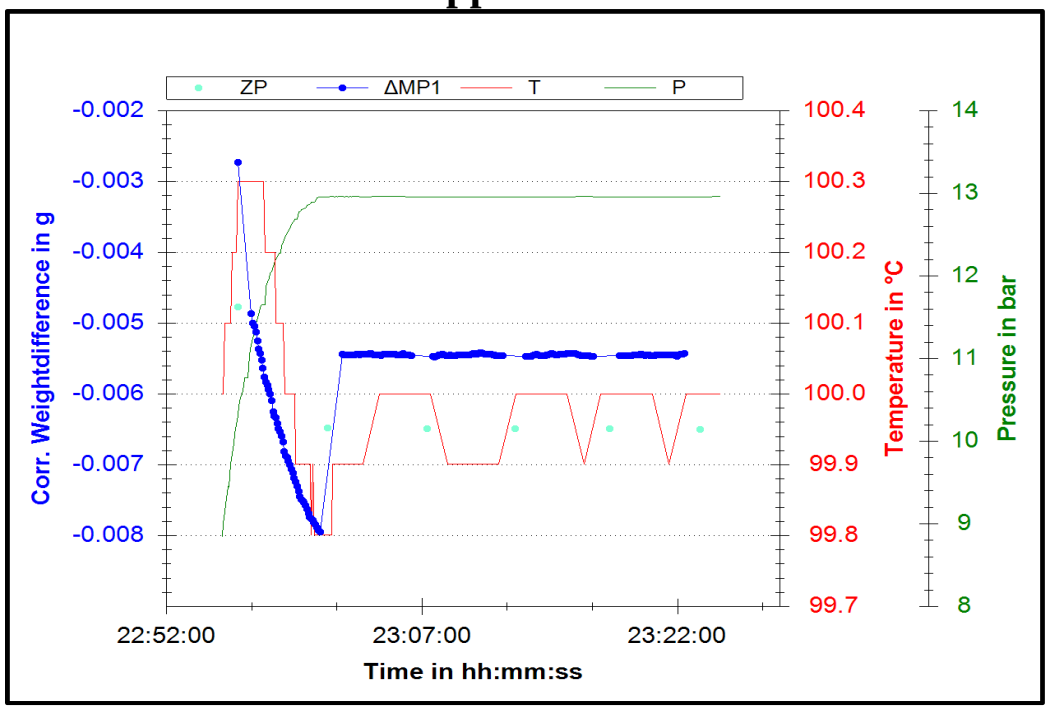

Figure C1 One pressure set point of the Helium Buoyancy measurement on SH1 at 100°C.

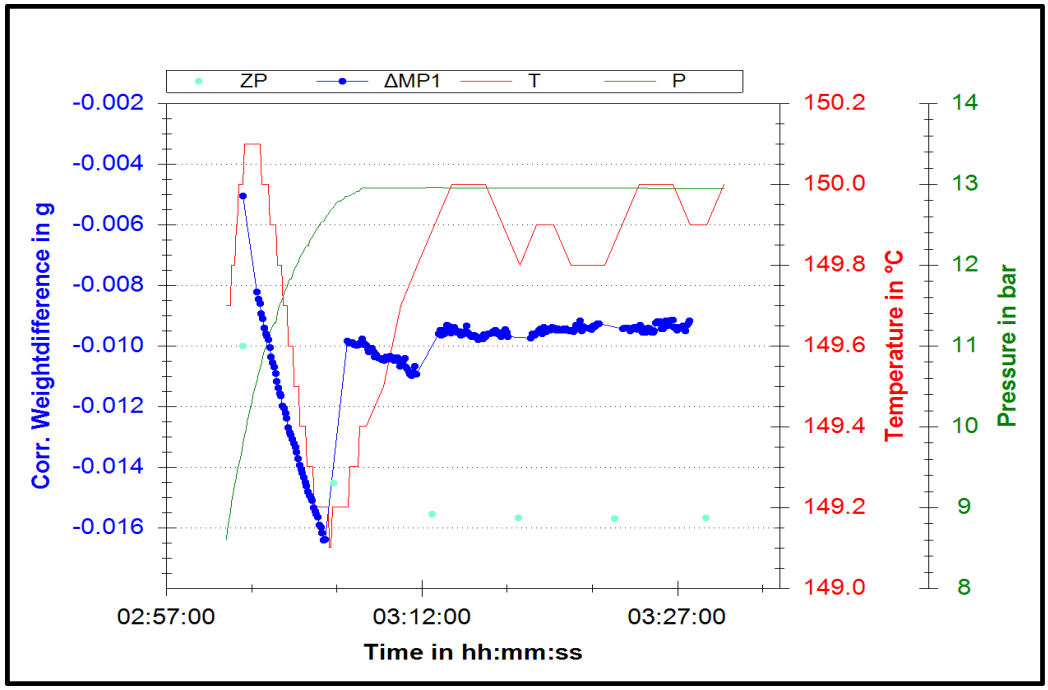

Figure C2 One pressure set point of CO_2 adsorption measurement on SH1 at 150°C.

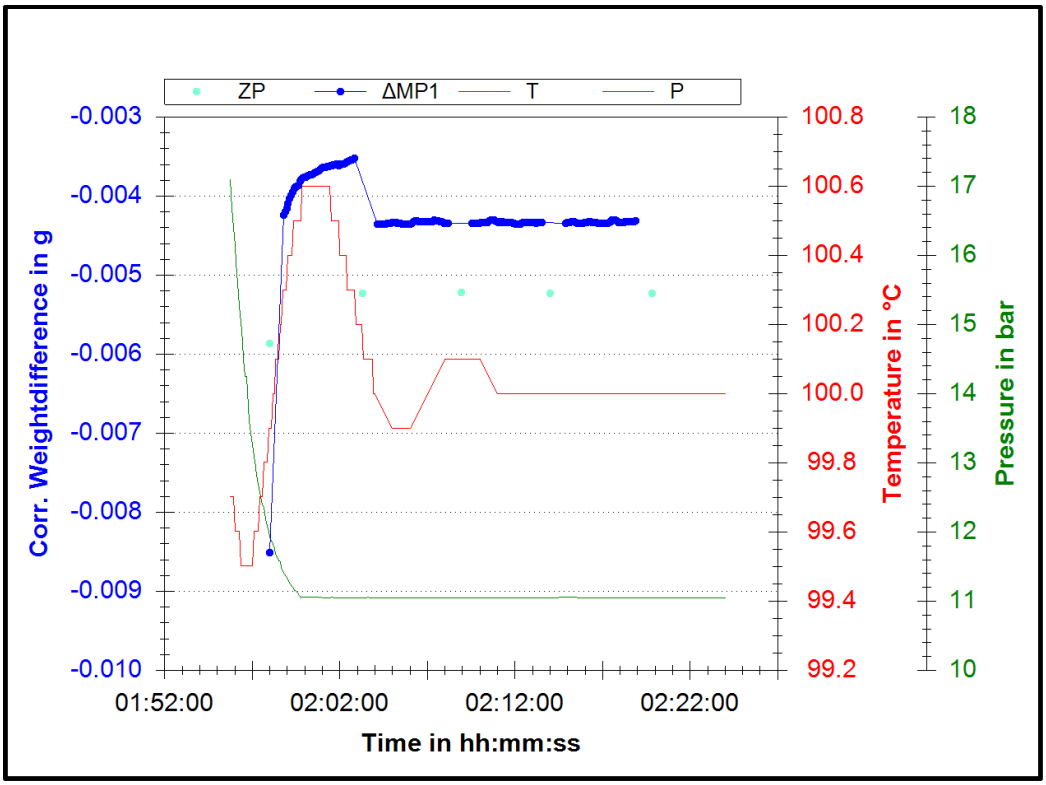

Figure C3 One pressure set point of CH_4 desorption measurement on SH1 at 100°C.

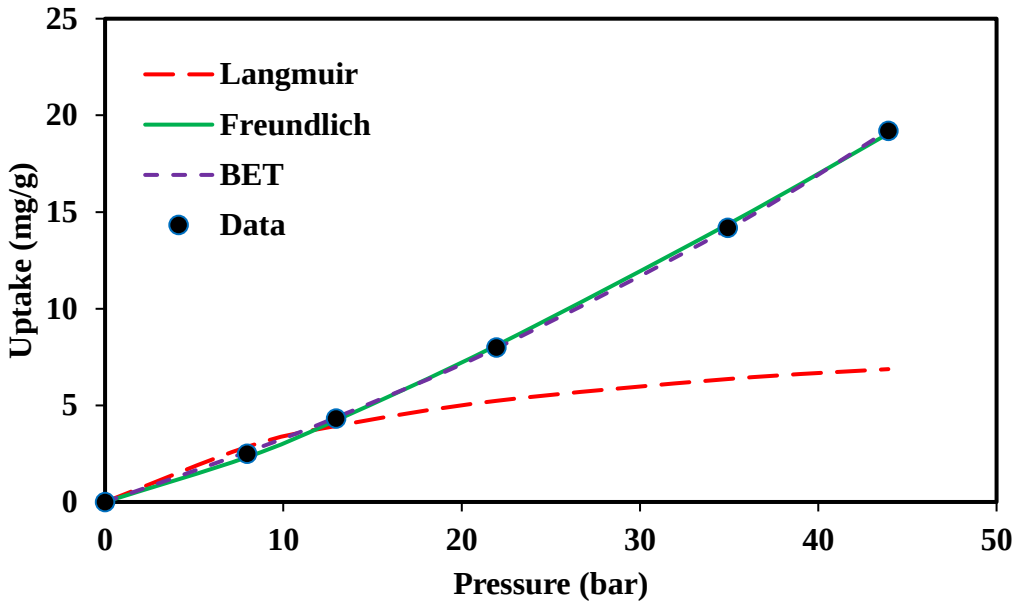

Figure C4 Fitting of CH_4 adsorption on SH1 at 50°C with Langmuir, Freundlich and BET.

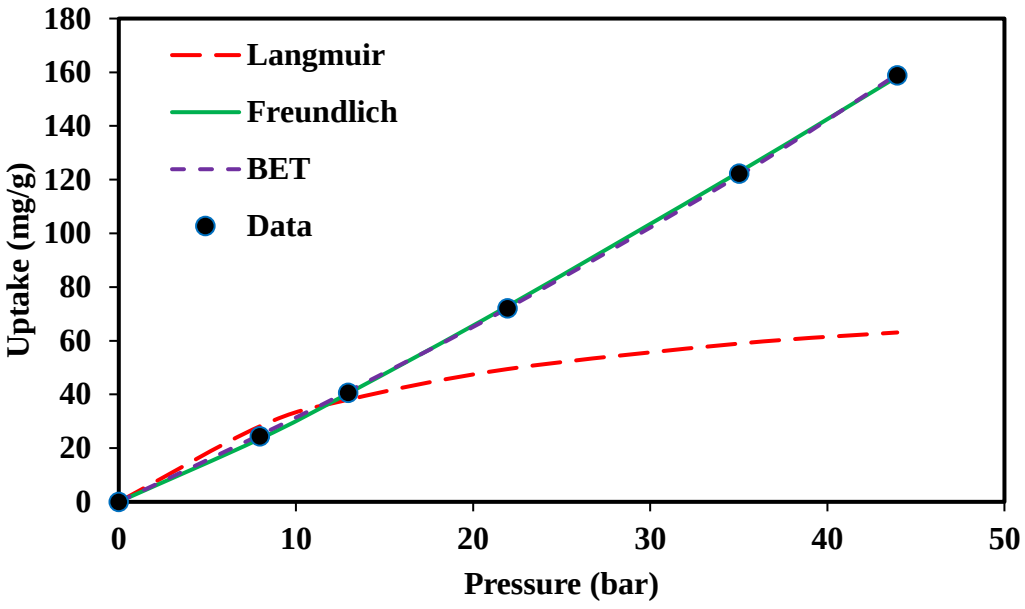

Figure C5 Fitting of CH_4 adsorption on SH1 at 100°C with Langmuir, Freundlich and BET.

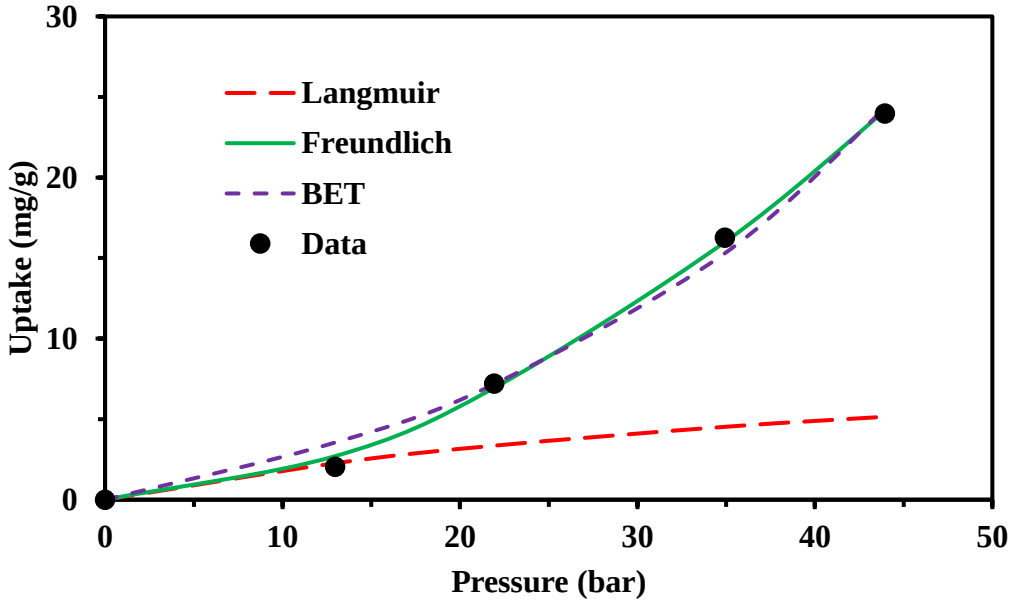

Figure C6 Fitting of 10%CO_2 adsorption on SH1 at 50°C with Langmuir, Freundlich and BET.

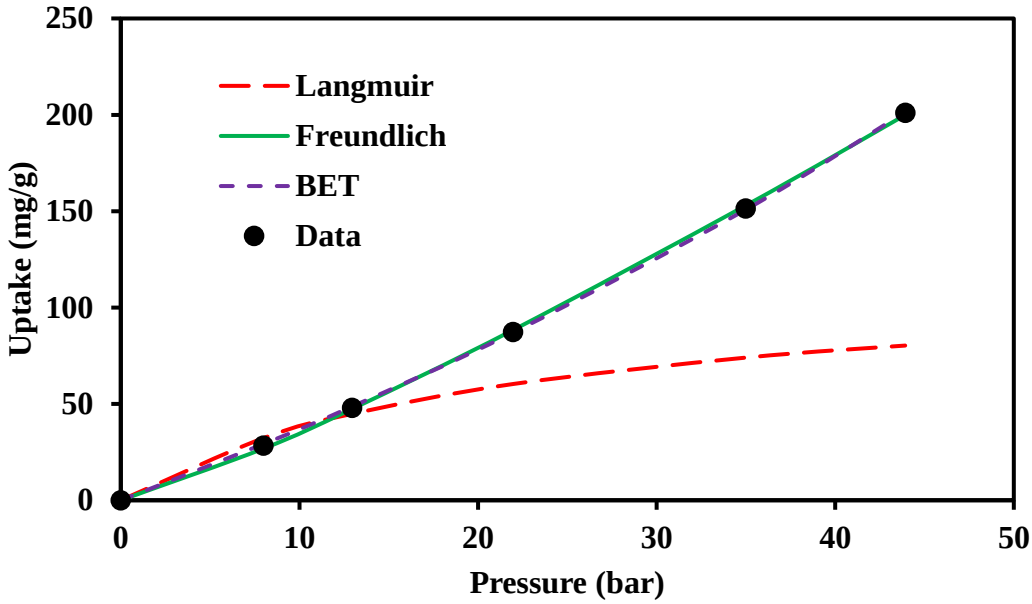

Figure C7 Fitting of 10%CO_2 adsorption on SH1 at 100^{o}C with Langmuir, Freundlich and BET.

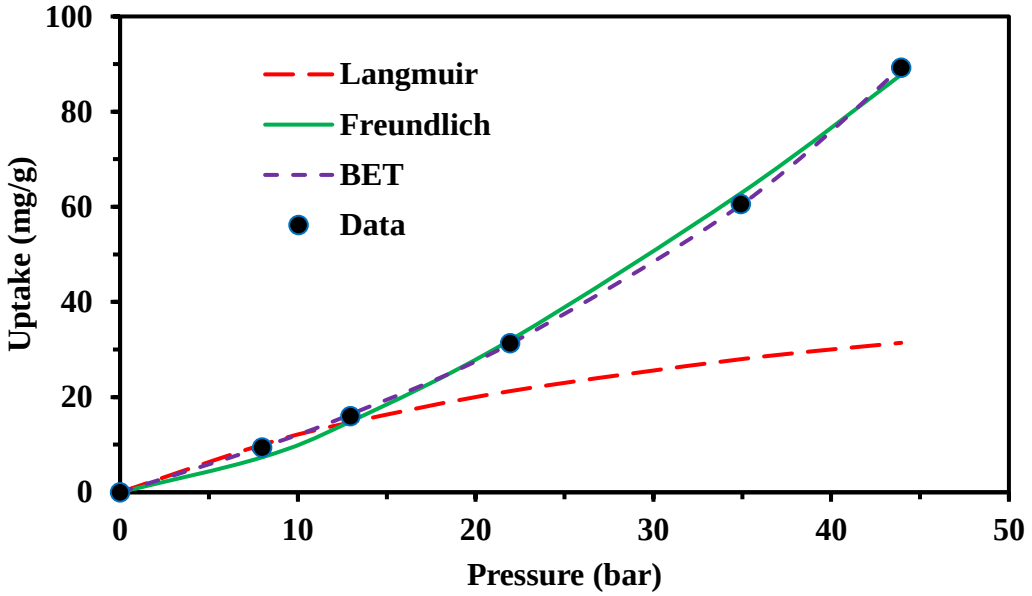

Figure C8 Fitting of CO_2 adsorption on SH1 at 50^{o}C with Langmuir, Freundlich and BET.

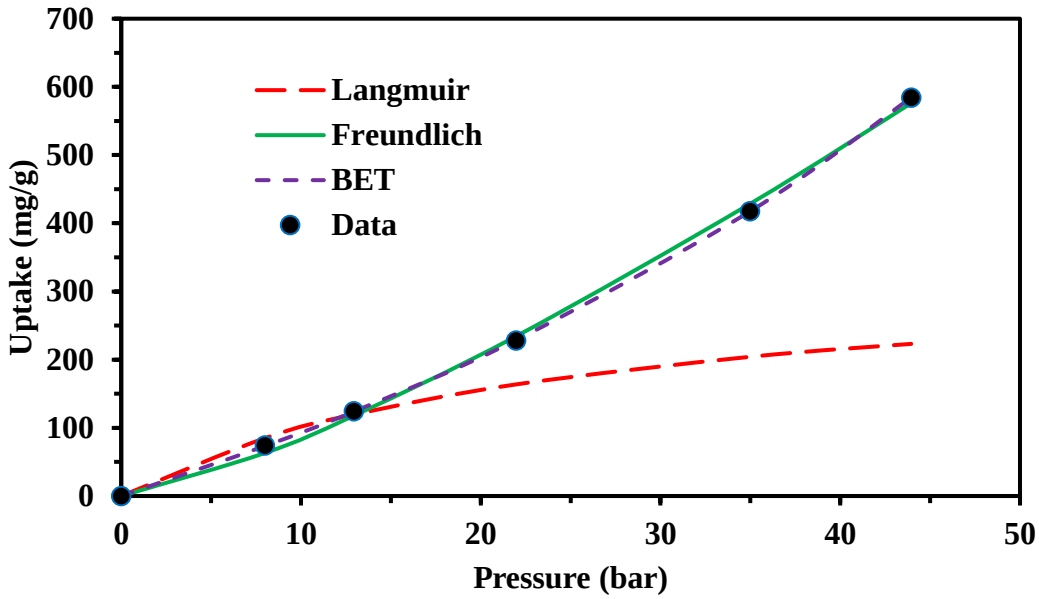

Figure C9 Fitting of CO_2 adsorption on SH1 at 100°C with Langmuir, Freundlich and BET.

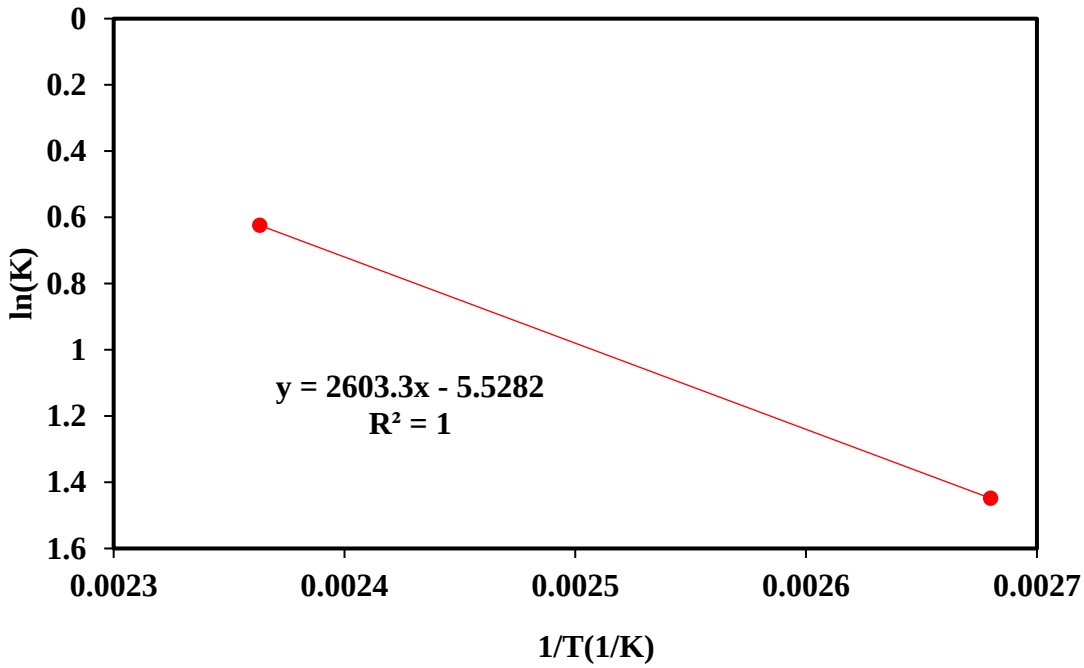

Figure C10 Pure CO_2 heat of adsorption on SH1 Arrhenius plot.

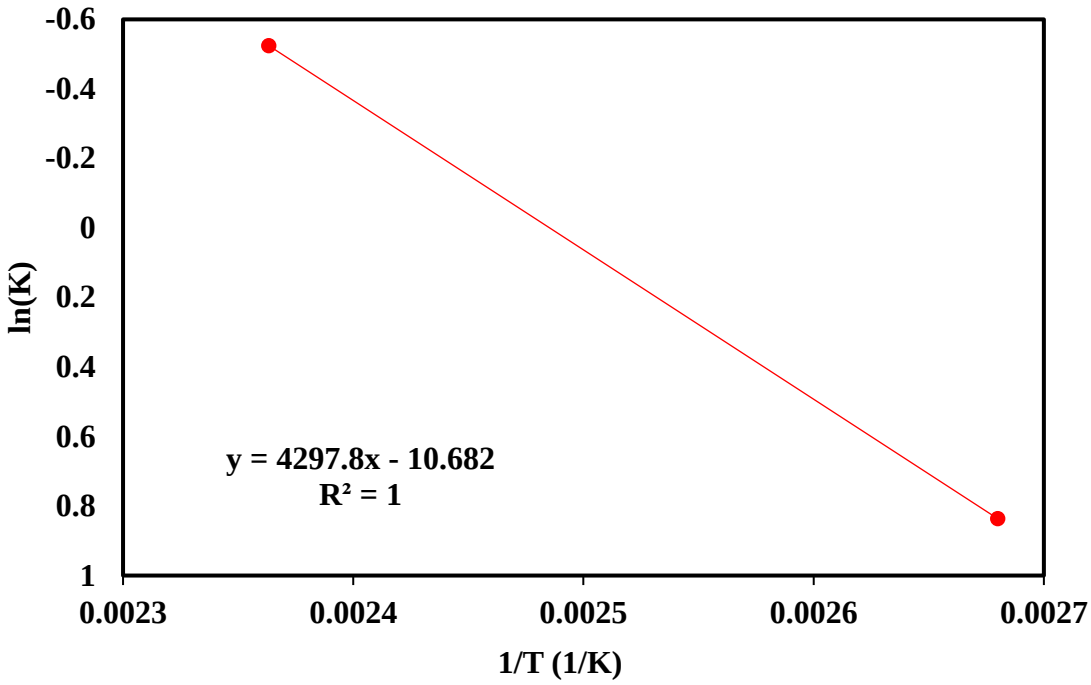

Figure C11 Pure CH_4 heat of adsorption on SH1 Arrhenius plot.

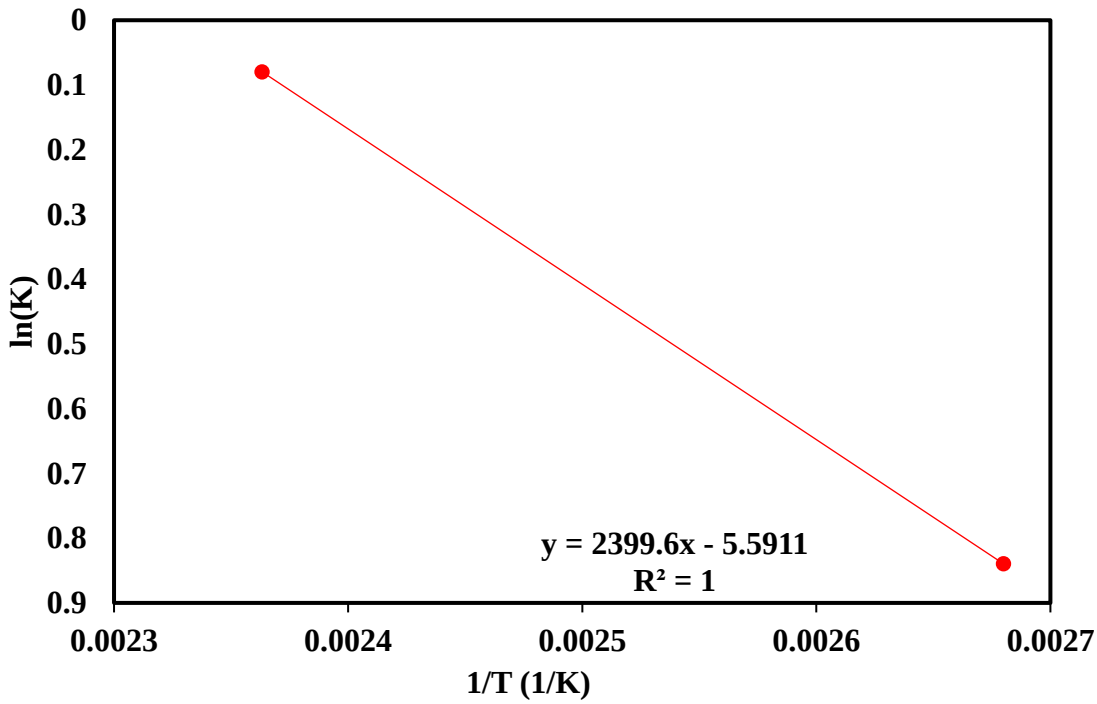

Figure C12 10% CO_2-90% CH_4 heat of adsorption on SH1 Arrhenius plot

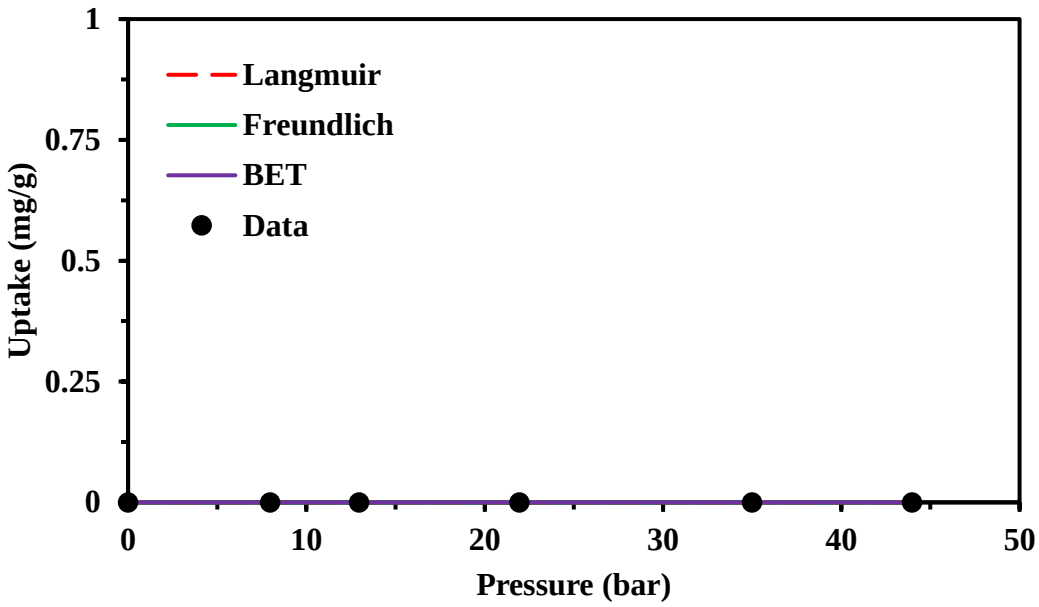

Figure C13 Fitting of CH_4 adsorption on SH2 at 50°C with Langmuir, Freundlich and BET.

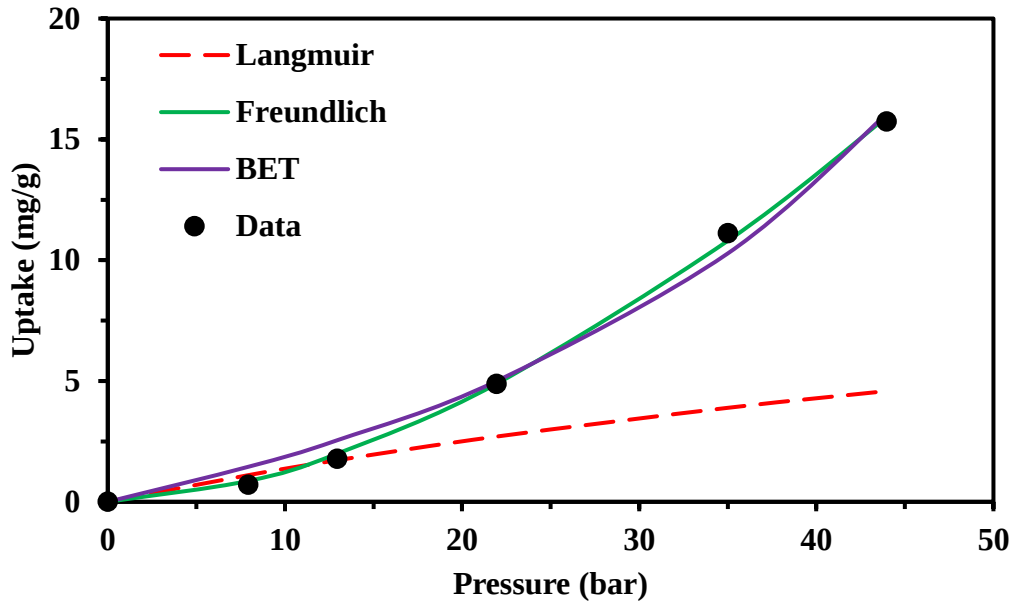

Figure C14 Fitting of CH_4 adsorption on SH2 at 100°C with Langmuir, Freundlich and BET.

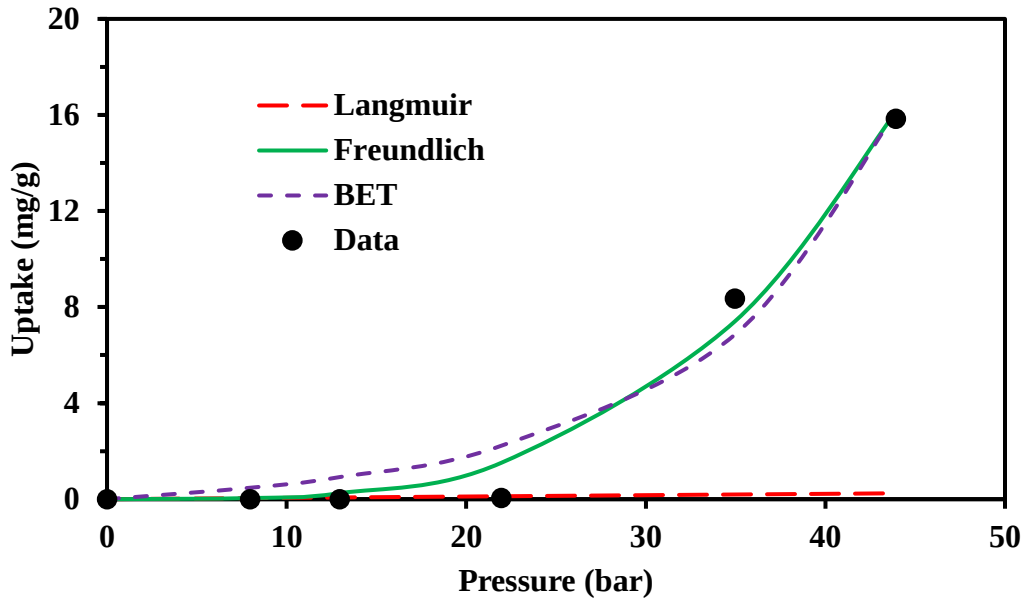

Figure C15 Fitting of 10%CO_2 adsorption on SH2 at 50°C with Langmuir, Freundlich and BET.

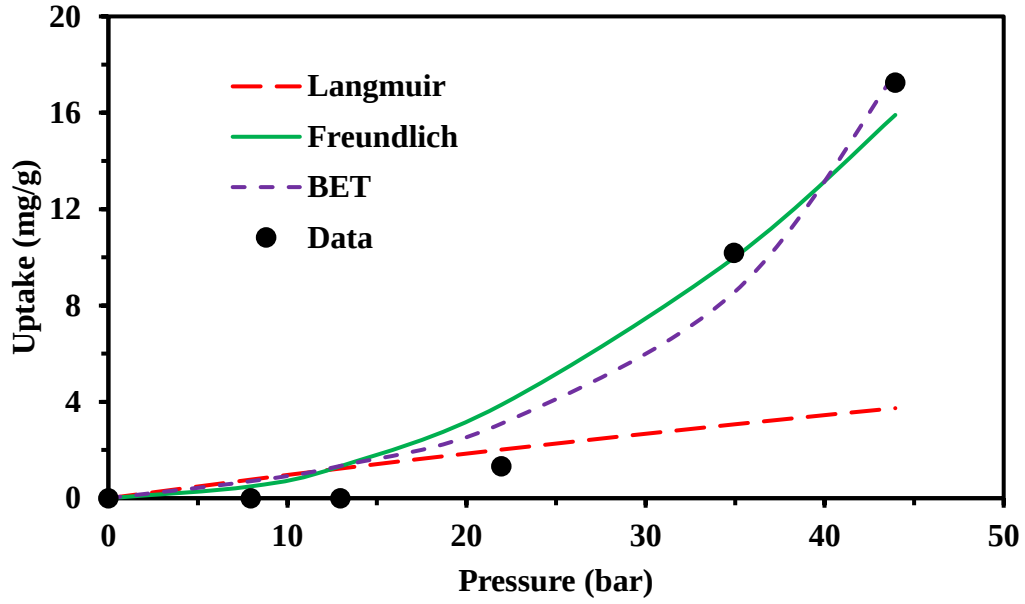

Figure C16 Fitting of 10%CO_2 adsorption on SH2 at 100°C with Langmuir, Freundlich and BET.

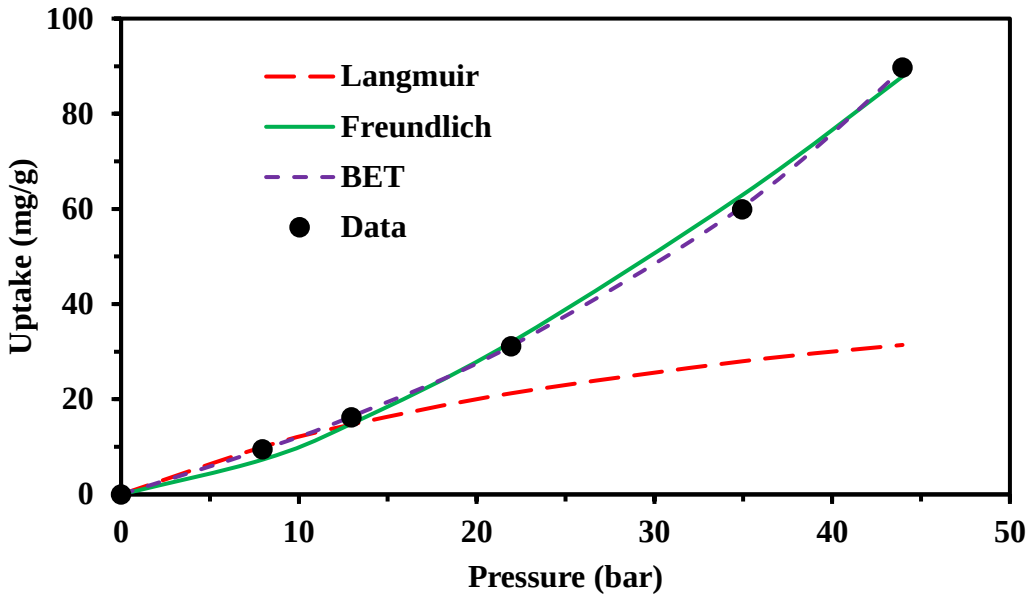

Figure C17 Fitting of CO_2 adsorption on SH2 at 50°C with Langmuir, Freundlich and BET.

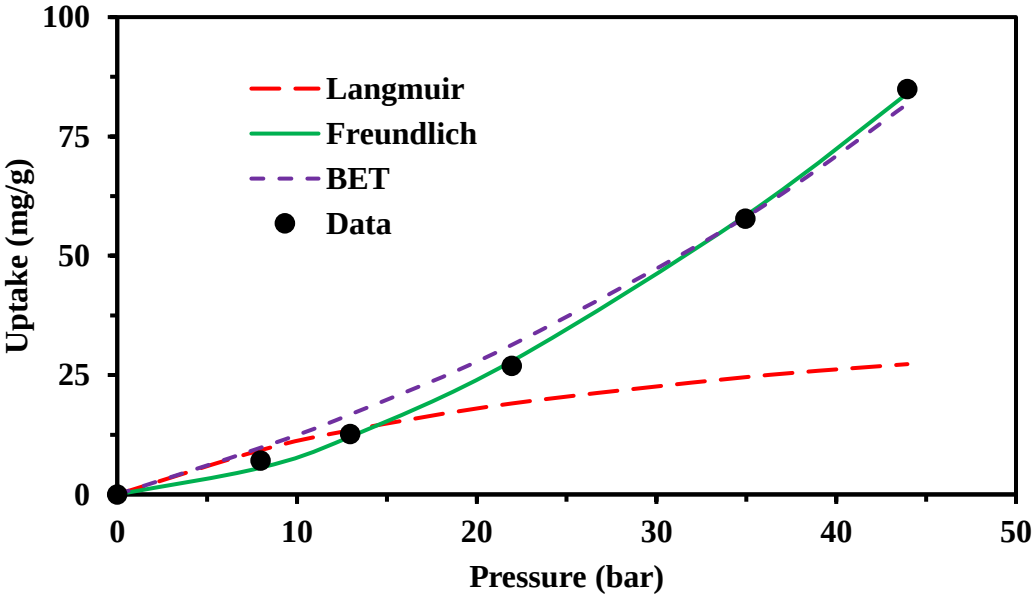

Figure C18 Fitting of CO_2 adsorption on SH2 at 100°C with Langmuir, Freundlich and BET.

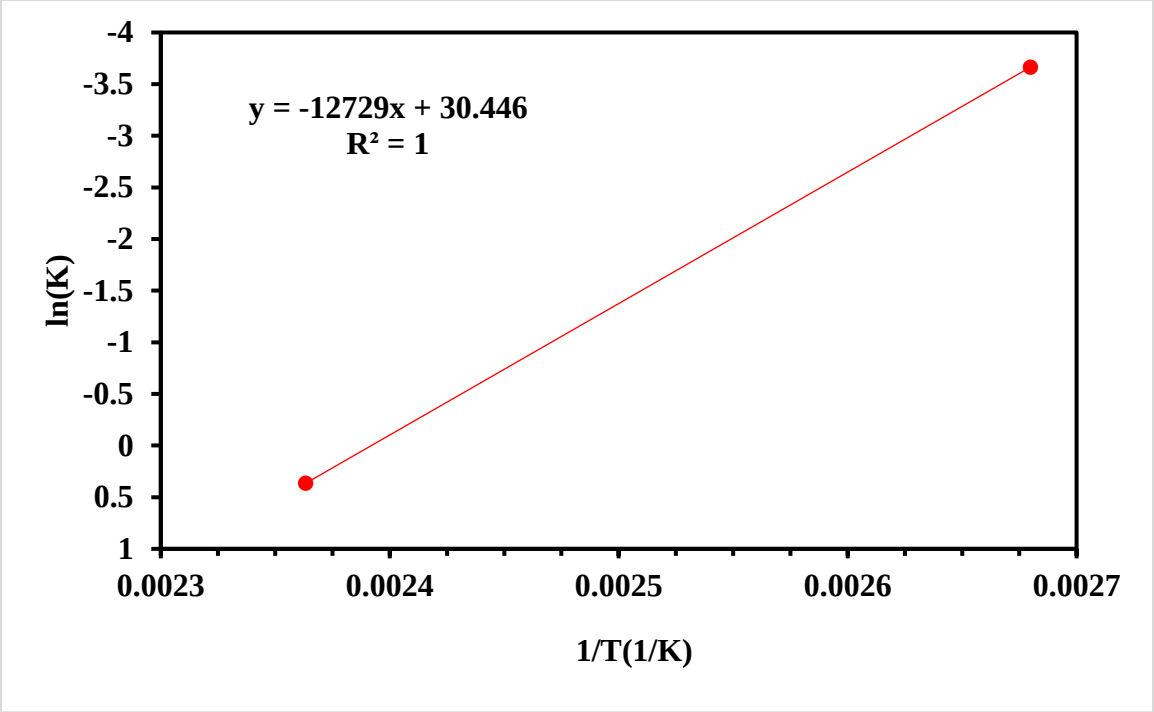

Figure C19 Pure CH_4 heat of adsorption on SH2 Arrhenius plot.

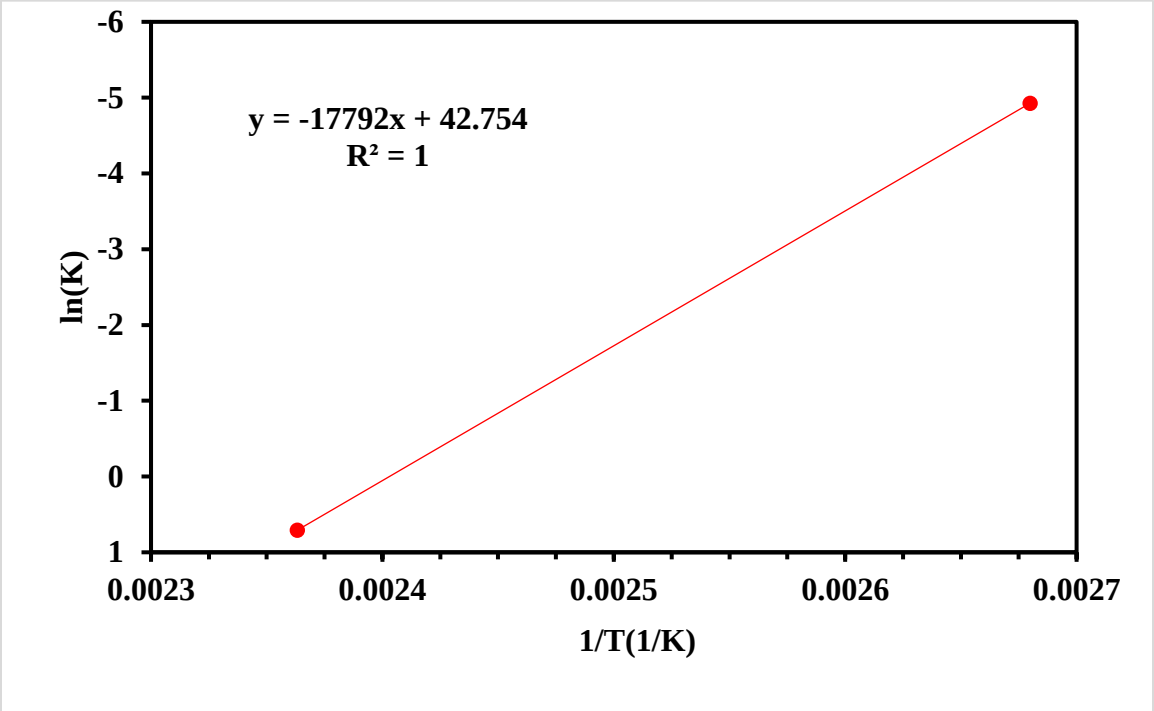

Figure C20 Pure 10%CO_2 heat of adsorption on SH2 Arrhenius plot.

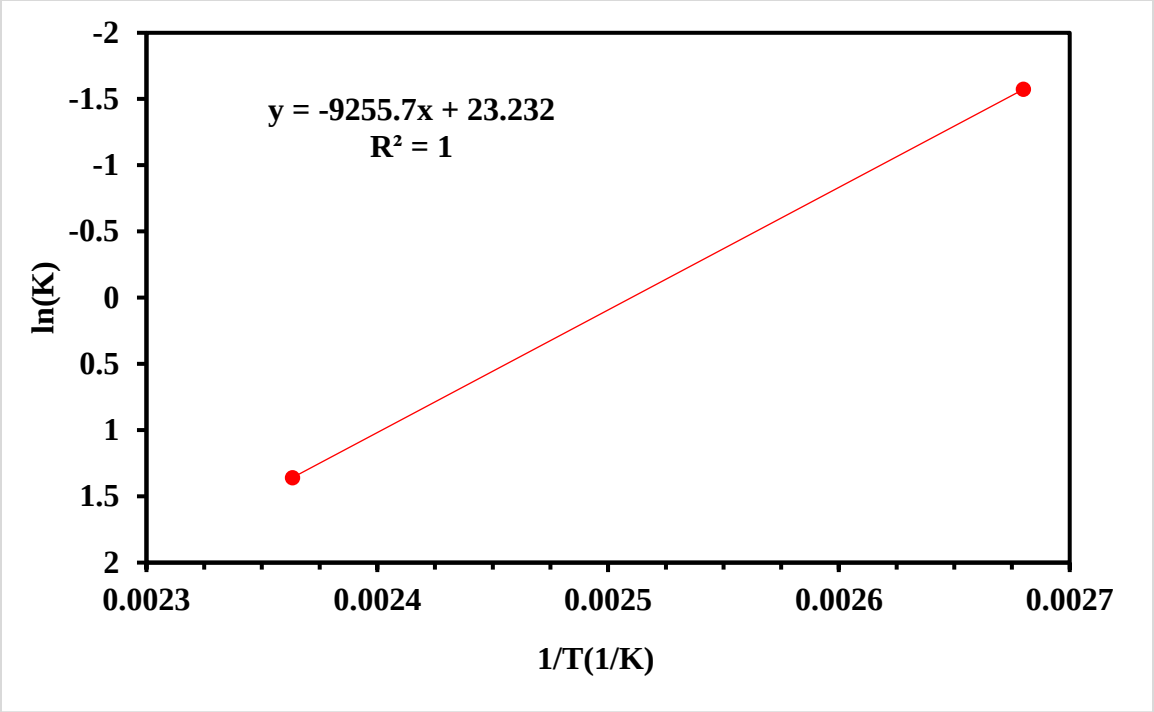

Figure C21 Pure CO_2 heat of adsorption on SH2 Arrhenius plot.

Vitae

Name	:Mohammed Altahir Eliebid Elnaeem
Nationality	:Sudanese
Date of Birth	:7/14/1990
Email	:mohammed.a.eliebid@gmail.com
Address	:Wad Asha, Barakat, Gizera State, Sudan
Academic Background	: **M.Sc. in Petroleum Engineering (December, 2016)** King Fahd University of Petroleum & Minerals Dhahran, Saudi Arabia **B.Sc. in Petroleum Engineering (August, 2011)** University of Khartoum Khartoum, Sudan
Research Interests	: Gas adsorption/desorption, enhanced gas recovery, reservoir simulation, CO_2 sequestration, adsorption thermodynamics, material science and characterization.